NOVEL METHODS FOR THE EFFICACY AND SAFETY IN THE ARTIFICIAL PANCREAS INTENDED FOR DOMICILIARY USE

Charrise Mary Ramkissoon

Universitat de Girona

Doctoral Thesis

Novel Methods for Efficacy and Safety in the Artificial Pancreas Intended for Domiciliary Use

Charrise Mary Ramkissoon

2018

Doctoral Thesis

Novel Methods for Efficacy and Safety in the Artificial Pancreas Intended for Domiciliary Use

Charrise Mary Ramkissoon

2018

Doctoral Programme in Technology

Supervised by: Dr. Josep Vehí

Presented in partial fulfillment of the requirements for a doctoral degree from the University of Girona

Universitat de Girona

DOCTORAL THESIS

NOVEL METHODS FOR EFFICACY AND SAFETY IN THE ARTIFICIAL PANCREAS INTENDED FOR DOMICILIARY USE

A dissertation presented in partial fulfillment of the requirements for a doctoral degree from the University of Girona

By:

Charrise Mary Ramkissoon

Supervisor:

Josep Vehí

To my mother Trot, my father Gilbert,
my brothers Gevan and Christopher,
and to Gabriel, with love.

Acknowledgements

After four years of PhD work, I can say that I have gained a lot not only in the scientific field but also on a personal level. Now, I would like to reflect on the people you have been involved directly and indirectly in this final work.

Firstly, I would like to graciously thank my supervisor Prof. Josep Vehí, whose experience, expertise, and motivation has provided me with the tools that were required to complete this work.

Secondly, I would like to thank Pantelis Georgiou who facilitated my two month stay at Imperial College, London along with all the other students at Imperial College that made me feel welcomed. During this stay, Pau Herrero was my advisor and I would like to acknowledge the large role he played in the beginning stages of my PhD. It was with his aid that I developed that detection algorithms' foundation. I would also like to thank Jorge Bondia who was also present during my stay at Imperial College and facilitated the continued development of both algorithms presented in this thesis. He has also played a large role in the editing of many of the publications that I have presented from this thesis.

I would like to thank Andrea Fachinetti, Yenny Leal, and my colleague Lyvia Biagi who all contributed to an article that was published during the four years of my PhD (although it is not presented in this dissertation). Andrea Fachinetti provided Lyvia and I with a great measure of assistance and expertise during the process of research, article writing, and publication.

I would like to thank Anna Comas, who not only provided technical support in our laboratory, but was there to help with any issue that I had and who welcomed me into Girona when I first arrived. I would also like to thank my colleagues Arthur Bertachi and Aleix Beneyto who collaborated with me during the development of the exercise-induced hypoglycemia reduction algorithm and I would like to thank the medical team associated with our group, Ignacio Conget, Marga Giménez, Carmen Quirós, F. Javier Ampudia, and Paolo Rossetti who have provided insight into type 1 diabetes from a clinical standpoint.

Lastly, I would like to thank the University of Girona, the Spanish Government, and the European Union for the grants BR2014/51, DPI2016-78831-C2-1-R, DPI2016-78831-C2-2-R, and Fondo Europeo de Desarrollo Regional (FEDER) Funds, without which this research would not have been possible.

To everyone, thank you wholeheartedly.

Charrise M. Ramkissoon
Girona, Spain
September 2018

List of Publications

Journals

1. **C. M. Ramkissoon**, A. Bertachi, A. Beneyto, J.Bondia, J. Vehí. "Detection and Control of Unannounced Exercise in the Artificial Pancreas without Additional Physiological Signals: A feasibility study." Submitted to IEEE J Biomed Health Inform. Submitted: September 18, 2018.
2. **C. M. Ramkissoon**, P. Herrero, J. Bondia, J. Vehí. "Unannounced Meals in the Artificial Pancreas: Detection Using Continuous Glucose Monitoring" Sensors 18(3): 884 (**2018**).
3. A. Bertachi, A. Beneyto, **C. M. Ramkissoon**, J. Vehi. "Assessment of mitigation methods to deal with announced exercise to reduce the risk of hypoglycemia in a uni-hormonal artificial pancreas." Diabetes Technol. Ther. 20(4): 1-11 (**2018**).
4. A. Bertachi, **C. M. Ramkissoon**, J. Bondia, J. Vehi. "Automated blood glucose control in type 1 diabetes: A review of progress and challenges." Endocrinología, Diabetes y Nutrición. (**2017**).
5. **C. M. Ramkissoon**, B. Aufderheide, B.W. Bequette, J. Vehí. "A review of safety and hazards associated with the artificial Pancreas." IEEE Rev. Biomed. Eng. 10(1): 1-19 (**2017**).
6. L. Biagi, **C. M. Ramkissoon**, A. Facchinetti, Y. Leal, J. Vehí. "Modeling the error of the medtronic paradigm veo enlite glucose sensor." Sensors. 17(6): 1361 (**2017**).

Conferences

1. **C. M. Ramkissoon**, A. Bertachi, A. Beneyto, J. Vehí. "Insulin-Only Blood Glucose Control during Unannounced Aerobic Exercise." Presented at the 18th Annual Diabetes Technology Meeting, Diabetes Technology Society. Bethesda, MD, November 8-10, 2018.
2. **C. M. Ramkissoon**, P. Herrero, J. Bondia, J. Vehí. "Strategies for Blood Glucose Control During Unannounced Meals." J. Diabetes Sci. Technol. 12(2), A68 (**2017**) [Abstract]. Presented at the 17th Annual Diabetes Technology Meeting, Diabetes Technology Society. Bethesda, MD, November 2-4, 2017.
3. **C. M. Ramkissoon**, P. Herrero, J. Bondia, J. Vehí. "Meal Detection in the Artificial Pancreas: Implications During Exercise." IFAC-PapersOnLine, 50(1): 5462-7 (**2017**). Presented at the 20th World Congress of the International Federation of Automatic Control. Toulouse, FR, July 9-14, 2017.
4. **C. M. Ramkissoon**, P. Herrero, J. Bondia, J. Vehí. "A novel meal detection algorithm for an artificial pancreas." Diabetes Technol. Ther. 19(S1): A71-2, 173 (**2017**) [Abstract]. Presented at the 10th International Conference on Advanced Technologies and Treatment for Diabetes. Paris, FR, February 15-18, 2017.
5. **C. M. Ramkissoon**, P. Herrero, J. Bondia, P. Greorgiou, N. Oliver, J. Vehí. "Automatic detection on exercise in people with type 1 diabetes using an unscented kalman filter." Diabetes Technol. Ther. 18(S1): A56, 135 (**2016**) [Abstract]. Presented at the 9th International Conference on Advanced Technologies and Treatment for Diabetes. Milan, IT, February 3-6, 2016.

6. **C. M. Ramkissoon**, J. Vehí. "Emotions and diabetes." IWBBIO 2015, Part II, LNCS 9044 pp. 720-727 (**2015**). Presented at the 3rd International Work-Conference on Bioinformatics and Biomedical Engineering. Granada, ES, April 15-17, 2015.
7. **C.M. Ramkissoon**, J Vehí. B. Aufderheide, B. W. Bequette, C. C. Palerm. "A Taxonomy of safety issues to be overcome in the artificial pancreas." Diabetes Technol. Ther. 17(S1): A172 (**2015**) [Poster]. Presented at the 8th International Conference on Advanced Technologies and Treatment for Diabetes. Paris, FR, February 18-21, 2015.

NOMENCLATURE

The following acronyms, abbreviations, and variables can be found in this thesis.

Acronyms and abbreviations

AP	Artificial Pancreas
BG	Blood Glucose
CGM	Continuous Glucose Monitor
CHO	Carbohydrates
CLC	Closed-Loop Control
CSII	Continuous Subcutaneous Insulin Infusion
CVGA	Control Variability Grid Analysis
D	Disturbance
DCCT	Diabetes Control and Complications Trial
DKA	Diabetic Ketoacidosis
DM	Diabetes Mellitus
EHRA	Exercise-induced Hypoglycemia Reduction Algorithm
FIR	Finite Impulse Response
FL	Fuzzy Logic
FN	False Negative
FP	False Positive
FP2ase	Fructose 1,6-biphosphatase
G6Pase	Glucose 6-Phospohatase
GIP	Gastric Inhibitory Peptide
GLP-1	Glucagon-Like Peptide 1
GPC	Generalized Predictive Control
HbA1c	Glycated Hemoglobin
HRM	Heart Rate Monitor
HRR	Heart Rate Reserve
IDF	International Diabetes Federation
IFB	Insulin Feedback
IOB	Insulin-on-Board
LGS	Low Glucose Suspend
MARD	Mean Absolute Relative Difference
MDI	Multiple Daily Injections
OL	Open Loop
PD	Proportional-Derivative

PEPCK	Phosphoenol Pyruvate Carboxylase
PID	Proportional-Integral-Derivative
PLGM	Predictive Low Glucose Management
PHRA	Postprandial Hyperglycemia Reduction Algorithm
RMSE	Root Mean Squared Error
Ra	Rate of Glucose Appearance
SMRC	Sliding Mode Reference Conditioning
T1D	Type 1 Diabetes
T2D	Type 2 Diabetes
TP	True Positive
UKF	Unscented Kalman Filter
UKPDS	UK Prospective Diabetes Study
UVA	University of Virginia
$\mathbf{VO_{2max}}$	Maximal Oxygen Consumption Capacity

List of Tables

Table **Page**

List of Figures

Figure **Page**

Table of Contents

Resum

La diabetis tipus 1 (T1D) és una malaltia autoimmunitària que afecta a les cèl•lules β del pàncrees que són responsables de l'excreció de la insulina i que resulta en nivells crònicament elevats de glucosa en sang (BG). Globalment, s'estima que el nombre de nens i adolescents (< 20 anys) amb T1D és 1,1 milions, amb un augment de 132.600 casos nous cada any, i en països de renda elevada, la majoria de nens que són diagnosticats amb diabetis tenen T1D. La T1D resulta en moltes complicacions agudes i cròniques que redueixen la qualitat de la vida, augmenten la càrrega econòmica i augmenten el risc de mortalitat.

Han sorgit eines millorades per a la gestió de la T1D incloent-hi monitors de glucosa contínua (CGM) i bombes d'insulina cada cop més sofisticades, amb millores en les formulacions d'insulina també. Això ha promogut el desenvolupament del pàncrees artificial, que consisteix d'un CGM, una bomba d'insulina i un algoritme de control que té el potencial de reduir les complicacions associades amb la T1D prestant una regulació estricta de BG en pacients. S'han explorat diversos algoritmes de control i s'ha obtingut un control millorat de BG; no obstant això, aquests són sistemes híbrids que requereixen l'anunci de menjars i exercici, i sovint resulten en un rendiment subòptim. Per tant, el desenvolupament d'estratègies innovadores que no requereixen l'anunci de menjars ni exercici són necessaris per millorar el control de BG i reduir els problemes actuals d'optimització, tal com la desestimació de menjars, bolus de menjar perduts i hipoglucèmia induïda per exercici.

En aquesta investigació es desenvolupen estratègies de control en llaç tancat (CLC) encaminades a reduir la hiperglucèmia postprandial i la hipoglucèmia postexercici. Es desenvolupa una nova metodologia per la detecció de pertorbacions que implica l'estimació d'un estat de pertorbació, D, d'un model mínim augmentat calculat amb un filtre de Unscented Kalman. L'algoritme de la reducció d'hiperglucèmia postprandial (PHRA) i l'algoritme de la reducció d'hipoglucèmia postexercici (EHRA) inclouen un algoritme de detecció que provoca accions automàtiques de rebuig de pertorbacions per mitigar de manera segura i efectiva la hiperglucèmia postprandial i la hipoglucèmia postexercici, respectivament. El PHRA és capaç de millorar el control de BG quan es compara amb un controlador de CLC amb bolus de menjar perduts i és capaç de millorar el control de BG durant els menjars d'absorció lenta quan es compara amb un controlador de CLC amb àpats anunciats; malgrat això, no pot prevenir hiperglucèmia durant menjars d'absorció ràpida degut als retards en la detecció d'àpats i l'acció pic d'insulina. El EHRA detecta exercici sense utilitzar senyals fisiològics addicionals i és capaç de superar les estratègies d'exercici aeròbic no anunciat i anunciat en un controlador de CLC evitant hipoglucèmia severa (<54 mg/dl) sense provocar hiperglucèmia addicional a causa dels suggeriments de carbohidrats.

Els sistemes desenvolupats estan destinats a ser millorats, extensivament avaluats in silico i després validats en futurs assajos clínics.

Resumen

La diabetes tipo uno (T1D) es una enfermedad autoinmune que afecta a las células β del páncreas que son responsables de la excreción de la insulina y que resulta en niveles crónicamente elevados de glucosa en sangre (BG). Globalmente, se estima que el número de niños y adolescentes (<20 años) con T1D es 1,1 millones, con un aumento de 132.600 casos nuevos cada año, y en países de altos ingresos, la mayoría de niños que son diagnosticados con diabetes tienen T1D. La T1D resulta en muchas complicaciones agudas y crónicas que reducen la calidad de la vida, aumentan la carga económica y aumentan el riesgo de mortalidad.

Han surgido herramientas mejoradas para la gestión de la T1D incluyendo monitores de glucosa continuos (CGM) y bombas de insulina cada vez más sofisticadas, con mejoras en las formulaciones de insulina también. Esto ha promovido el desarrollo del páncreas artificial, que consiste de un CGM, una bomba de insulina y un algoritmo de control que tiene el potencial de reducir las complicaciones asociadas con la T1D prestando una regulación estricta de BG en pacientes. Han sido explorados varios algoritmos de control y se ha obtenido un control mejorado de BG; sin embargo, estos son sistemas híbridos que requieren el anuncio de comidas y ejercicio y a menudo resultan en un rendimiento subóptimo. Por consiguiente, el desarrollo de estrategias innovadoras que no requieren el anuncio de comidas ni ejercicio son necesarios para mejorar el control de BG y reducir los problemas actuales de optimización, tal como la desestimación de comidas, bolos de comida perdidos e hipoglucemia inducida por ejercicio.

En esta investigación, se desarrollan estrategias de control en lazo cerrado (CLC) encaminadas a reducir la hiperglucemia postprandial y la hipoglucemia postejercicio. Se desarrolla una nueva metodología para la detección de perturbaciones que involucra la estimación de un estado de perturbación, D, de un modelo mínimo modificado calculado con un filtro de Unscented Kalman. El algoritmo de la reducción de hiperglucemia postprandial (PHRA) y el algoritmo de la reducción de hipoglucemia postejercicio (EHRA) incluyen un algoritmo de detección que provoca acciones automáticas de rechazo de perturbaciones para mitigar de manera segura y efectiva la hiperglucemia postprandial y la hipoglucemia postejecicio, respectivamente. El PHRA es capaz de mejorar el control de BG cuando se compara con un controlador de CLC con bolos de comida perdidos y es capaz de mejorar el control de BG durante comidas de absorción lenta cuando se compara con un controlador de CLC con las comidas anunciadas; sin embargo, aún no puede prevenir hiperglucemia durante comidas de absorción rápida por retrasos en la detección de comidas y la acción pico de insulina. El EHRA detecta ejercicio sin usar señales fisiológicas adicionales y es capaz de superar las estrategias de ejercicio aeróbico no anunciado y anunciado en un controlador al impedir hipoglucemia severa (<54 mg/dl) sin provocar hiperglucemia adicional debido a las sugerencias de carbohidratos.

Los sistemas desarrollados están destinados a ser mejorados, extensivamente evaluados in silico y después validados en futuros ensayos clínicos.

Abstract

Type 1 diabetes (T1D) is an autoimmune disease that targets the insulin producing β-cells in the pancreas that results in chronically elevated blood glucose (BG) levels and requires lifelong insulin-replacement therapy. Globally, there is an estimated 1.1 million children and adolescents (<20 years) with T1D, with an increase of 132,600 new cases per year and in most high income countries, the majority of children that are diagnosed with diabetes have T1D. T1D results in many acute and chronic complications that reduce life quality, increase economic burden, and increase the risk of mortality.

Improved tools for the management of T1D have emerged including increasingly sophisticated continuous glucose monitors (CGM) and insulin pumps, with improvements in insulin formulations as well. This has led to the development of the artificial pancreas (AP), which is composed of a CGM, an insulin pump, and a control algorithm that has the potential to reduce the complications associated with T1D by providing tight BG regulation in patients. Several control algorithms have been explored and improved BG control has been obtained; however, these are hybrid systems that require the announcement of meals and exercise and often lead to suboptimal performance. Therefore, the development of innovative strategies that do not require the announcement of meals and exercise are necessary to improve BG control and remove current optimization problems such as meal misestimation, missed meal boluses, and exercise-induced hypoglycemia.

In the work presented in this dissertation, closed-loop control (CLC) strategies to reduce postprandial hyperglycemia and postexercise hypoglycemia were developed. A new methodology for the detection of disturbances, which involves the estimation of a disturbance state, D of an augmented minimal model determined using an Unscented Kalman Filter has been developed. The postprandial hyperglycemia reduction algorithm (PHRA) and the exercise-induced hypoglycemia reduction algorithm (EHRA) developed in this thesis include detection algorithms that trigger automatic disturbance rejection actions to safely and effectively mitigate postprandial hyerglycemia and hypoglycemia induced by aerobic exercise, respectively. The PHRA is able to improve BG control when compared to a CLC controller with missed meal boluses and is able to improve BG control during slow absorption meals when compared to a CLC controller with announced meals; however, it is still unable to prevent hyperglycemia during fast absorption meals due to the delays in meal detection and insulin peak action. The EHRA detects exercise without the use of additional physiological signals and is able to outperform both unannounced and announced aerobic exercise strategies in a CLC controller by preventing severe hypoglycemia (<54 mg/dl) without causing excess hyperglycemia due to carbohydrate suggestions.

The systems developed in this thesis are intended to be improved, extensively evaluated in silico, and then validated in future clinical trials.

CHAPTER 1

INTRODUCTION

Diabetes mellitus (DM) affects over 425 million people worldwide [1]. It is a group of chronic metabolic disorders, which result in hyperglycemia and are associated with many complications that lessen the quality of life for patients. This study offers a way to improve the quality of life of people with type 1 diabetes (T1D) by removing the announcement of meals and exercise that current hybrid closed-loop control (CLC) systems require. This introductory chapter of the thesis begins with an overview of the dissertation and the motivations of the research and then, the challenges and objectives are presented. The chapter is concluded with a description of the structure and content of the thesis.

1.1 Motivation

DM is a group of metabolic disorders characterized by elevated blood glucose (BG) levels, or hyperglycemia, over a prolonged period of time, which is associated with chronic complications such as retinopathy, nephropathy, neuropathy, and cardiovascular disease. DM can be classified into three categories, T1D, type 2 diabetes (T2D), and gestational diabetes although, less common types of DM also exist, including monogenic diabetes and secondary diabetes. This work is focused on T1D, which originates from a deficiency in insulin producing β-cells in the islets of the pancreas gland. T2D is the result of inadequate β-cell function leading to insulin resistance of peripheral tissues and gestational diabetes arises during pregnancy due to hormone production by the placenta that increases insulin resistance.

DM is currently one of the most common chronic conditions and has a significant impact on European public health and economy. The International Diabetes Federation (IDF) [1] estimates that more than 8.8% of the European population in the age range of 20–79, that is, approximately 58 million European citizens, including 22 million undiagnosed cases, currently suffer from

DM; and this number is expected to increase to 66.7 million by the year 2045. The economic consequences of diabetes in Europe, with annual costs of 142.7 billion EUR in 2017, are profound. Europe has the highest number and incidence rate of children and adolescents (0-19 years) with T1D at 286,000 cases and 28,200 new cases per year, respectively [1].

Progress can be seen in many areas of diabetes treatment. Glucometers, which enable on-demand determinations of BG throughout the day, have evolved into continuous glucose monitors (CGM) that are currently less accurate than glucometers. Continuous glucose monitoring provides a clearer picture of overall BG control by providing glucose readings every 5 to 10 minutes throughout the day, some with alarms for hyper- and hypoglycemia. Traditionally, multiple daily injections (MDI) of insulin have been used to treat T1D, which require a basal injection of slow-acting insulin once daily and boluses of fast-acting insulin to cover meals. Now, continuous subcutaneous insulin infusion (CSII) treatment using an insulin pump is available, which can be manually programmed to deliver both basal and bolus insulin according to patient needs.

In the last two decades, these technological advances have fueled research on CLC systems intended for BG control in T1D patients, i.e. artificial pancreas (AP) systems, which regulate BG levels using a CGM informed controller that adjusts insulin infusion via an insulin pump. Although satisfactory clinical results have been reported for overnight BG control [2, 3], several challenges for effectively realizing optimal daytime CLC of BG are evident. The need for meal and aerobic exercise announcement due to lack of physiological control of BG in T1D, carbohydrate (CHO) counting, missed meal boluses, the multifaceted nature of exercise, the effect of meal composition on postprandial glucose, inter- and intra-variability in patients, delays in the subcutaneous route of insulin infusion and glucose sensing, and the lack of accuracy for existing CGMs in the hypoglycemic range, during times of high rate of change, and during aerobic exercise have been identified as limiting factors in the development of an AP for domiciliary use. Current hybrid CLC systems perform optimally with the announcement of both meals and exercise, which are the most frequent and persistent disturbances on BG control. The removal of these announcements are the first natural step towards the realization of the AP as a fully CLC system. Several meal detection algorithms have been developed [4–13]; however, these algorithms have been unable to prevent postprandial hyperglycemia and often lead to hypoglycemic events [14, 15]. Additionally, previous exercise detection studies have been developed for aerobic exercise [16–21]; however, these approaches increase the system complexity, increase the burden to the patient, are prone to failure, and are unable to distinguish between aerobic and anaerobic exercise.

Despite the existing control strategies for unannounced meals and exercise, satisfactory BG control remains a significant challenge for CLC algorithms. Therefore, innovative strategies are needed for effective and safe postprandial and postexercise BG control. Improvements in detection algorithms and associated mitigation actions will deliver the required performance and safety for automated postprandial and postexercise BG control in CLC systems intended for the treatment of T1D.

1.2 Problems and Challenges

A list of the primary challenges for the development of AP systems during meals and aerobic exercise are outlined as follows:

- **Physiological control system of meals in T1D**: In healthy subjects, hypo- and hyperglycemia are counteracted by a physiological control system that includes pancreatic hormones such as insulin and glucagon [22]. In T1D, insulin is virtually absent due to autoimmune destruction of β-cells. Additionally, after a meal, T1D patients exhibit a paradoxical postprandial hyperglucagonemia in which endogenous glucagon levels remain elevated in the portal circulation. Administration of exogenous insulin alone does not normalize the portal glucagon:insulin ratio and the liver continues to release glucose, which enters the circulatory system by exogenous and endogenous means, resulting in further hyperglycemia [23]. Therefore, in T1D, the physiological control system responsible for mediating glucose is lacking, which is especially evident after a meal when a profound postprandial increase in BG is experienced.

- **Physiological control system of aerobic exercise in T1D**: Aerobic exercise is characterized as prolonged physical exertion of submaximal intensity (approximately 50-60% of maximal oxygen consumption capacity (VO_{2max}))[24], which produces an increased rate of glucose disposal in the bloodstream as a result of increased glucose uptake in the skeletal muscle [25]. In T1D, control of BG during aerobic exercise is challenging because, unlike healthy subjects, insulin levels are unable to change rapidly in response to exercise. Insulin in the subcutaneous space is more rapidly absorbed into the bloodstream and excess insulin in the bloodstream promotes amplified glucose uptake in the skeletal muscle and suppresses the production of endogenous glucose. Additionally, it is not uncommon for T1D patients to experience late-onset postexercise hypoglycemia that can occur 6-15 hr after exercise due to factors such as impaired counterregulation in response to hypoglycemia in T1D, the increase in glucose uptake by skeletal muscles for the replenishment of muscle glucose stores, and a rise in insulin sensitivity after exercise [26]. The cumulative effect of these responses results in an increased probability of a hypoglycemic event after aerobic exercise in T1D subjects [27].

- **The burden of current meal announcement strategies**: AP systems are still dependent on feed-forward actions such as meal announcements to achieve effective control. Announcing a meal requires patients to estimate the amount of CHO they are about to consume. This not only increases the burden to the patient but also introduces error into the system as some boluses will be overestimated, underestimated, or missed [28–30]. An overestimated bolus may also occur when the user delivers a bolus but does not consume the entire meal. Overestimation of the meal bolus amount leads to an increased risk of hy-

poglycemia. Additionally, several studies have reported a link between glycated hemoglobin (HbA1c) levels and missed meal boluses [31–33]. These increases in HbA1c lead to an increased risk of long-term complications. Furthermore, this type of meal announcement does not take into account meals of differing compositions that require different types of insulin administration.

- **The burden of current exercise announcement strategies**: The announcement of exercise is even more burdensome to the patient as current aerobic exercise recommendations for T1D patients include decreasing basal insulin before aerboic exercise and ingesting a predetermined amount of CHO before and during aerobic exercise [34]. Due to the complexity of BG control before and during aerobic exercise, T1D patients either abstain from exercise altogether or are unable to maintain BG within acceptable levels leading to poor BG control. Additionally, similar to missed meal boluses, there is a high likelihood of a patient forgetting to announce exercise or announcing exercise late.

- **The downfalls of current strategies for unannounced meals**: As of now, strategies for unannounced meals focus on estimating the CHO content of meals and do not take into account dietary fat and protein, which greatly effect how rapidly glucose appears in the plasma, acute postprandial BG control, and prandial insulin dosing strategies [35]. Additional factors such as rate of glucose appearance (Ra) should be regarded as important for dosing strategies during unannounced meals.

- **The downfalls of current strategies for unannounced exercise**: There is an added complexity with the current approach to aerobic exercise detection, which includes the addition of external physiological sensors, i.e. heart rate monitor (HRM), accelerometers, etc. [16–21]. The addition of devices increases the burden to the patient, which must now wear and maintain these devices in addition to the base components of the AP. The addition of devices increases the probability of failure of individual devices and these physiological sensors have been found to be prone to producing false positives [21]. Additionally, these types of detection schemes are typically unable to differentiate between aerobic and anaerobic exercise, which produce distinct changes to BG.

- **Inter- and intra-patient variability**: Due to the large inter-subject variability of glucose regulation, which requires tuning of the system, an AP system must be patient-specific and address intra-patient variability. Factors affecting inter-patient variability include hormonal changes, stress, illness, and activity levels [36–40]. There exists a wide variability in glucose profiles before, during, and after exercise that can be attributed to a multitude of factors such as the amount of insulin-on-board (IOB), starting glucose, total muscle mass, body mass index, age, duration of T1D, progression of T1D, stress level, insulin sensitivity, rate of glucose uptake, etc. [34]. An AP must consider variations in insulin sensitivity

produced by circadian rhythms, changes in insulin and meal absorption, and variability in the glycemic response to aerobic exercise.

- **Extensive physiological delays in the subcutaneous route**: In healthy people, insulin is delivered from the β-cells in the pancreas to the portal circulation. In this case, the delay in insulin action is approximately 30 minutes [41]. When the subcutaneous route is used to deliver insulin, there is a delay in time-to-peak plasma insulin concentration of 66 ± 22 minutes [42] from the time of infusion, even when rapid-acting insulin analogues are used. An additional delay of 5-15 minutes is attributable to glucose sensing in the subcutaneous route due to the transport of glucose from blood to the interstitial fluid [43, 44]. These delays slow down both the detection of meals and exercise and postprandial hyperglycemia control. Also, due to the IOB, the glucose-lowering effect of insulin that has been delivered, but not yet taken effect, will persist during aerobic exercise although insulin delivery has been shut off.
- **The accuracy and reliability of existing CGM systems**: CGM systems have now achieved a mean absolute relative difference (MARD) of $\pm 10\%$ [45–47]. However, accuracy decreases in the hypoglycemic range [48], with an increasing rate of change [49], and it has been shown that there is a tendency for the MARD to increase during periods of aerobic exercise [50–53]. Several factors have been attributed to this degradation in CGM accuracy during aerobic exercise including microcirculation perturbation, variations of the oxygen concentration in the blood, increase in body temperature, rapid BG changes in the plasma caused by exercise, and mechanical forces on the sensor during aerobic exercise.

1.3 Objectives

The general objective of this research is to develop effective and safe CLC strategies for BG control during unannounced meals and aerobic exercise in T1D patients. To achieve this objective, the study addressed the following specific issues:

1. To implement a state estimator able to use the available data to gain information about system disturbances. This state estimator will be used in meal and exercise detection algorithms.
2. To build and analyze a meal detection algorithm with several tunings in the context of an AP system in a way that it can be used to trigger automatic disturbance rejection actions that safely and effectively mitigate postprandial hyperglycemia. The meal detection algorithm and its tunings will be evaluated using standard detection metrics such as sensitivity, change in glucose, detection time, true positive, false positive, false negative, and false positives per day. Additionally, a sensitivity analysis will be performed to determine which meals can be detected with the most efficacy.

3. To derive postprandial glucose control strategies to be used after meal detection to safely and effectively mitigate postprandial hyperglycemia during meals of various sizes and compositions without the additional risk of postprandial hypoglycemia.

4. To build an exercise detection algorithm that detects aerobic exercise without the use of additional physiological signals at various exercise intensities.

5. To derive aerobic exercise control strategies to be used after detection to safely and effectively reduce hypoglycemia induced by aerobic exercise during exercise sessions of various intensities. This will include disturbance rejection actions such as calculating and suggesting a quantity of fast absorption CHO to be consumed and modifying controller dependent and independent variables.

1.4 Thesis Structure

This dissertation is organized as follows:

- Chapter 1: **Introduction** introduces the motivation for this research, outlines the main challenges of the development of the AP and presents the research objectives.

- Chapter 2: **Type 1 Diabetes** presents an overview of T1D, its prevalence, mortality rate, economic impact, and its associated complications. It the describes glucose control in humans and current T1D treatment.

- Chapter 3: **The Artificial Pancreas** describes the AP, the major advances in the field, and the shortcomings of the current systems. The simulator and closed-loop controller used in this thesis are also described breifly.

- Chapter 4: **State Estimation** is dedicated to the state estimator that employs a minimal model and Unscented Kalman Filter (UKF) to estimate states of the system that are in turn used in the detection of meals and exercise.

- Chapter 5: **Unannounced Meal Detection and Control** details the unannounced meal detection and postprandial CLC strategies. First, the detection algorithm is detailed along with the results and a discussion, then the postprandial disturbance rejection actions triggered by the detection algorithm are described along with the results and a discussion.

- Chapter 6: **Unannounced Aerobic Exercise and Control** describes the aerobic exercise detection algorithm and the postexercise CLC strategies employed after detection. First the detection algorithm is detailed along with results and then the postexercise disturbance rejection actions triggered by the detection algorithm are described along with the results and a discussion.

- Chapter 7: **Conclusion** outlines the conclusions and contributions of this research and future studies.
- Appendix A: **The University of Virginia/Padova Mixed Meal Simulation Model** describes the T1D simulator used in this thesis.
- Appendix B: **Closed-loop Controller** describes the principal controller used in this thesis and outlines the various clinical trials in which it has been tested.

CHAPTER 2

TYPE 1 DIABETES

T1D, formerly called juvenile or childhood-onset diabetes because of its classically early onset, is an autoimmune disease targeting the insulin producing β-cells in the pancreatic islets of Langerhans [54]. The hormone insulin is secreted in response to elevated BG levels. This hormone promotes the transformation of glucose into glycogen and glucose uptake into the muscles and other tissues, which ultimately decrease BG levels [55, 56]. T1D reflects a loss of tolerance to tissue self-antigens caused by defects in both central tolerance, which aims at eliminating potentially autoreactive lymphocytes developing in the thymus, and peripheral tolerance, which normally controls autoreactive T-cells that escape the thymus. Like in other autoimmune diseases, the mechanisms leading to T1D are multi-factorial and depend on a complex combination of genetic, epigenetic, molecular, and cellular elements that result in the breakdown of immunological tolerance [57]. Previously, people affected with T1D died from a diabetic coma; however, since the discovery of insulin in 1921, T1D has been transformed from a uniformly fatal condition into a chronic condition requiring lifelong insulin-replacement therapy [58].

2.1 Prevalence, Mortality, and Economic Impact

DM is one of the most common chronic diseases worldwide with an increasing socio-economic impact. In 2017, there were an estimated 425 million people (20-79 years) living with DM throughout the world, T1D accounts for about 7-12% of this population in high income countries. Globally, there is an estimated 1.1 million of children and adolescents (<20 years) with T1D, with an increase of 132, 600 new cases per year. In most high income countries, the majority of children and adolescents who develop DM have T1D [1]. Figure 2.1 shows the global incidence rate of T1D in children and adolescents (<20 years).

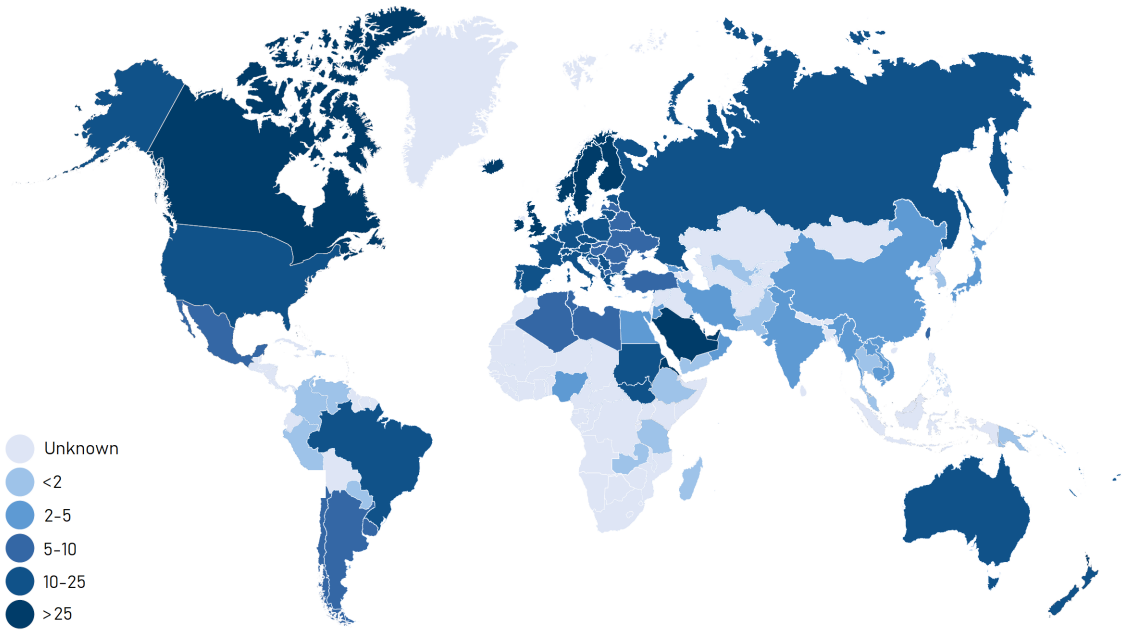

Figure 2.1: Estimated number of children and adolescents (0-19 years) with T1D per 100,000. Data obtained from International Diabetes Federation [1].

Europe has the highest number of children with T1D compared with the other IDF regions and the region also has one of the highest incidence rates of T1D in children. The Russian Federation has the highest number of children and adolescents with T1D– approximately 43,100. The European countries making the largest contribution to the overall numbers in T1D in children are the Russian Federation, the United Kingdom, and Germany [1].

Individuals with T1D have been found to have an increased age-adjusted risk of all cause mortality compared to the general population as a result of the development of chronic complications. One study performed a registry-based observational study from 1998 to 2011 in Sweden and found the mortality rate of patients with T1D to be higher at 8%, as compared to those without diabetes at 2.9% [59]. Additionally, it has been found that women with T1D have approximately 40% greater excess risk of all cause mortality and double the excess risk of fatal and nonfatal vascular events, when compared with men with T1D [60].

Despite the human burden characterized by premature mortality and lower quality of life due to T1D-related complications, T1D also imposes an economic impact for countries, health-care systems, and above all, for individuals with T1D and their families. In the United States, between 1999 and 2005, annual medical and non-health related costs for T1D accounted for an estimated USD 14.4 billion [61]. In Brazil, between 2008 and 2010, an estimated USD 4.2 million was spent annually on the treatment of T1D [62]. In the United Kingdom, an estimated USD 1.3 billion and USD 1.2 billion were spent on medical and non-health related costs in 2010, respectively [63]. Finally, in Spain, the average annual cost of T1D in 2014 was USD 31,107 per patient [64].

2.2 Complications

T1D complications may be disabling or even life-threatening and can be categorized as either acute or chronic complications.

2.2.1 Acute Complications

Short-term complications are the day-to-day problems that can appear without warning. Hypo– and hyperglycemia are considered short-term complications, and the symptoms vary depending on the severity of hypo– or hyperglycemia.

Short-term complications of T1D related to hypoglycemia include:

- High blood pressure
- Headaches
- Weakness or shakiness
- Hunger
- Nervousness
- Nausea
- Dilated pupils
- Palpitations
- Pallor
- Seizures
- Loss of Consciousness
- Coma

Ultimately, after a significant period of time in coma or out of consciousness from hypoglycemia, death can occur.

Short-term complications of T1D related to hyperglycemia include:

- Increased thirst
- Blurred vision
- Fatigue
- Headaches
- Frequent urination
- Unexplained weight loss

The omission of insulin can promote diabetic ketoacidosis (DKA), which is caused by high levels of ketones in the blood and urine. Ketones are a byproduct of the breakdown of muscle and fat that occurs with insufficient insulin in circulation leading to a buildup of acids in the bloodstream. DKA requires immediate medical care as it can cause cerebral edema, acute respiratory distress, thromboembolism, coma, and death [65].

2.2.2 Chronic Complications

HbA1c is the "gold standard" in the management of T1D and is commonly used to assess long-term BG control. The normal range for the HbA1c level is 4–6% for healthy human subjects. Above this range, the higher the HbA1c value, the greater the risk of long-term complications. Chronically elevated BG and HbA1c levels eventually results in long-term clinical complications, including retinopathy, neuropathy, nephropathy, and heart disease.

Retinopathy: Retinopathy associated with DM is caused by vascular damage of the microvasculature in the retina and has been recognized as one of the most common causes of visual impairment and blindess [66]. In people with T1D, retinopathy is usually not evident until five or more years after onset, but after 20 years of T1D, almost all T1D patients show signs of retinopathy [67]. Retinopathy is associated with a decreased quality of life [68] and in the United Kingdom, an estimated USD 7.4 million was spent on the treatment of retinopathy in T1D patients in 2010 [63]. Although the incidence of diabetes associated retinopathy is high, evidence suggests that the prevalence of retinopathy might be decreasing in developed countries [69].

Neuropathy: Neuropathy is the most frequent chronic complication of DM, is currently considered an irreversible end-organ damage complication, and has been found to be correlated with a lower quality of life [70]. Peripheral neuropathy is a particularly debilitating complication of DM and accounts for significant morbidity by predisposing the foot to ulceration and lower extremity amputation [71]. In one study, it was found that 7% of youth with T1D had peripheral neuropathy [72]. In 2001, the range of costs of peripheral neuropathy in T1D patients in the United States was USD 0.3-1.0 billion [73]. In 2010, in T1D patients, the United Kingdom spent USD 55.4 million on the treatment of neuropathy and USD 143.8 million on the treatment of foot ulcers and amputations [63].

Nephropathy: Nephropathy is the leading cause of mortality in T1D [74–76] and has been shown to decrease quality of life in patients [77]. Approximately, 20-30% of patients with T1D develop evidence of nephropathy, with a higher percentage of T1D patients progressing to end-stage renal disease [78]. In 2010, the United Kingdom spent USD 174 million and USD 66.4 million on the treatment of nephropathy and on other renal costs in T1D patients, respectively. [63].

Cardiovascular Complications: A decrease in mortality and a remarkable improvement in life expectancy occurred during the past decades in patients with T1D due to improved prevention and care towards cardiovascular complications. The comparison of two subcohorts of the Pittsburgh Epidemiology of Diabetes Complications study based on the period of diabetes diagnosis (1950–1964 vs. 1965–1980) found an increase in life expectancy by approximately 14 years [79]. Nevertheless, the overall risk of CVD for people with T1D compared to people without diabetes is increased two- to threefold in men, and three- to fivefold in women. A

significant increase in CVD mortality related to increasing HbA1c levels has been reported in T1D [80]. In 2010, the United Kingdom spent USD 65.7 million, USD 37.7 million, USD 39.7 million, and USD 213.2 million on ischemic heart disease, myocardial infarction, heart failure, and other cardiovascular disease treatments of T1D, respectively.

2.3 Glucose Control System

Glucose concentration is tightly regulated in healthy individuals by a complex neuro-hormonal control system. It is currently known that at least ten hormones participate closely in glucose regulation, with several more controlling related functions such as satiety, digestion, and growth. The central nervous system also plays an important role by modulating the responses of endocrine and other tissues according to a variety of inputs, including the circadian rhythm [81]. It is also important to bear in mind that our knowledge of these complex mechanisms is still expanding.

In the healthy human subject, glucose is maintained at a midnormal range of 88–96 mg/dl (4.9–5.3 mmol/L) [82]. Upon ingestion of a meal, incretins help prepare the pancreas for the imminent surge of BG. The incretins glucagon-like peptide 1 (GLP-1) and gastric inhibitory peptide (GIP), secreted by specialized cells in the gastrointestinal tract, promote the first phase secretion of insulin in proportion to the glucose content of the meal even before its appearance in the bloodstream [83]. This constitutes an anticipatory or feed-forward control loop. Insulin promotes the uptake of glucose primarily in skeletal muscle, adipose tissues, the liver, and of proteins in various tissues. Insulin also suppresses lipolysis, the breakdown of lipids. Amylin is co-secreted with insulin by β-cells in the pancreas. Amylin, in combination with GLP-1 and GIP, helps reduce the total insulin demand by slowing gastric emptying and promoting satiety [84]. Insulin and amylin also seem to suppress the release of glucagon, further attenuating the postprandial glucose peak. Incretins also influence the late phase of insulin secretion [83].

During prolonged exercise increased demand for glucose by contracting muscle causes increased glucose uptake to working skeletal muscles due to an increase in the translocation of insulin, contraction of sensitive glucose transporter-4 proteins to the plasma membrane, and activation of the glycolytic and oxidative pathways responsible for glucose disposal. During exercise, glucose production is derived mainly from liver glycogenolysis, which occurs following the activation of glycogen phosphorylase and simultaneous inactivation of glycogen synthase through a series of phosphorylation reactions initiated by hormones such as glucagon and norepinephrine [25]. Liver gluconeogenesis accounts for 10-20% of glucose production during exercise; however, with increasing exercise duration, the contribution of gluconeogenesis rises to about 50% of the total liver glucose production. Gluconeogensis is important for the conversion of glycerol, lactate, and amino acids into glucose in order to delay depletion of liver and muscle glycogen. The rate of gluconeogenesis is mainly controlled by the activities of the unidirectional enzymes, phosphoenol pyruvate carboxylase (PEPCK), fructose 1,6-bisphosphatase (FP2ase), and glucose

6-phosphatase (G6Pase) [85]. The gene transcription of these gluconeogenic enzymes is controlled by hormones, mainly insulin, glucagon, and glucocorticoids. While insulin inhibits gluconeogenesis by suppressing the expression of PEPCK and G6Pase, glucagon and glucocorticoids stimulate gluconeogenesis, thereby hepatic glucose production by expressing these genes [85]. Exercise increases the sensitivity of skeletal muscle to the action of insulin, which together with increased insulin flow due to enhanced muscle flow, may overcome a reduction in plasma insulin levels. Furthermore, insulin affects muscle glucose uptake via its inhibitory effects on adipose tissue lipolysis and muscle glycogenolysis [86].

During hypoglycemia, the healthy human subject has numerous systems in place to maintain an adequate supply of glucose to the brain. As glucose drops below ~80 mg/dl, insulin secretion ceases, allowing renal and hepatic glucose production to be favored. If levels keep falling to ~70 mg/dl, glucagon and catecholamine (epinephrine and norepinephrine) secretions are activated in the pancreas and adrenal glands, respectively. These hormones activate multiple pathways that counteract hypoglycemia. Glucagon stimulates hepatocytes to produce glucose from stored glycogen (glycogenolysis), glycerol, lactate, and amino acids (gluconeogenesis). Catecholamines increase the effect of glucagon directly by stimulating hepatic glucose production and indirectly by mobilizing gluconeogenic substrates. Falling insulin levels trigger the release of lipids through sensitive lipolytic pathways. Prolonged hypoglycemia over several hours promtes the secretion of growth hormone (<65 mg/dl) and cortisol (<60 mg/dl) to help recruit alternative fuels (via lipolysis, proteinolysis, and ketogenesis) and reduce insulin sensitivity in the peripheral tissues, which reduces the uptake of glucose by non-essential organs and tissues. Finally, at lower glucose levels, brain functions become impaired [87].

In healthy subjects, the glucose control system is finely tuned to maintain glucose homeostasis. However, in T1D, insulin-producing β-cells are destroyed due to an autoimmune response in the body and exogenous insulin must be provided to regulate BG levels. Although T1D patients are able to survive using insulin-replacement therapy, other hormones related to glucose control are also disrupted leading to increased difficulty in the control of glucose homeostasis during activities such as eating and exercise.

2.4 Type 1 Diabetes Treatment

T1D became treatable after the discovery and isolation of insulin in 1921 [57]. Due to the proteolysis of the insulin hormone by gut enzymes, parenteral administration of insulin is mandatory. Insulin injections using the subcutaneous route have represented the usual means to deliver insulin; additives to the insulin solute such as protamine or zinc have been used to prolong insulin action, especially for basal coverage. Over the past twenty years or so, the development of bioengineering has allowed the synthesis of insulin analogues characterized by modifications of the insulin primary sequence. These analogues keep the biological action of insulin while they either accelerate or slow down its absorption after a subcutaneous injection.

MDI, which is the combination of a slow-acting analogue for basal coverage, taken once or twice a day to keep BG levels consistent and a fast-acting analogue at meal times, to control BG levels after eating, allows a better mimicry of physiological insulin secretion than previously used combinations (illustrated in Figure 2.2) [88]. Although other hormones, such as glucagon, amylin, glucocorticoids, etc., are used in the physiological control of BG, they are seldom used therapeutically. Glucagon is only available as an emergency treatment for hypoglycemia and other hormones are either not available or are not used for the treatment of T1D.

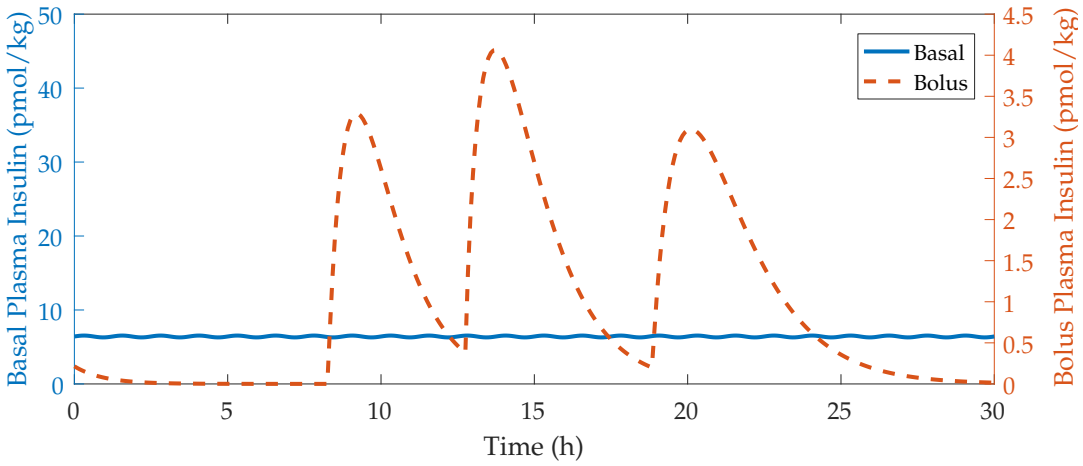

Figure 2.2: Illustration of the basal/bolus concept. Basal insulin is a slow-acting insulin analogue that appears in the plasma throughout the day. Bolus insulin is a fast-acting insulin analogue given at meal times to control BG after eating.

The need for tight glucose control in the long term, aiming at sustained near-normoglycemia, has been clearly demonstrated by the Diabetes Control and Complications Trial (DCCT) performed in T1D patients [89] that showed that the lower the average HbA1c level for several years, the better were the outcomes in terms of chronic complications. However, only limited subsets of patients are able to reach and maintain tight control, close to defined ideal goals, using MDI [89]. Besides being inefficient, the limitations of MDI include postprandial regulation of glucose levels,

the risk of over delivery (resulting in hypoglycemia), and daily burden [4, 90].

Since early 2000, improved tools for managing T1D have emerged. These include CGMs and increasingly sophisticated insulin pumps. CGMs are able to approximate BG concentration using a glucose-oxidase reaction in the subcutaneous space and are required to be calibrated every 6–12 hours using a glucometer. Although, there are now sensors the do not require calibration, such as the Freestyle Libre (Chicago, IL, USA), which is a 14-day factory calibrated flash glucose monitoring system that has proven to be accurate [91]. CGM systems now boast a MARD of ±10% [45–47] and numerous studies have demonstrated clinical benefits such as improvement in HbA1c levels and/or reduction in the risk of hypoglycemia in multiple patient populations– pediatrics, adolescents, adults, T1D and T2D with various levels of BG control at baseline [92–97]. The Dexcom G5 Mobile sensor and Dexcom G6 CGM (San Diego, CA, USA) have been deemed safe and effective by the FDA for non-adjunctive therapeutic decisions, i.e. insulin dosing [98–100] with other models soon to follow.

Insulin pump therapy, also known as CSII, is primarily used by people with T1D and is an open-loop system designed to mimic physiological delivery of insulin. CSII has been associated with improved glycemic management, clinical outcomes [101–105], and increased cost effectiveness [106] when compared to MDI. Introduced in 1970, CSII pumps now have the ability to infuse rapid-acting insulin at preselected infusion rates with multiple programmable basal profiles, which mimics basal insulin secretion. Many CSII pumps now have dedicated meters for self-monitoring of BG that can automatically send BG readings to the pump and are equipped with algorithms for suggesting bolus doses based on user-estimated grams of CHO, BG level from a BG meter or CGM, insulin sensitivity factors, and IOB [107, 108].

Systems with automation are appearing, such as the Medtronic 530G, 640G, and 670G (Northridge, CA, USA), which consist of a dedicated CGM, a CSII pump, and a control algorithm that include low glucose suspend (LGS), predictive low glucose management (PLGM), or hybrid CLC system, respectively. LGS allows basal insulin infusion to be interrupted for up to two hours if the BG level goes below a preset threshold and the patient does not respond to the hypoglycemia alerts [109, 110], PLGM suspends insulin infusion if hypoglycemia is predicted to occur within 30 minutes and resumes insulin delivery when BG levels begin to rise [111], and the hybrid CLC system automatically adjusts insulin basal infusion based on BG levels and includes a PLGM feature [112].

Although there have been many advancements in the field of T1D treatment, patients still experience a heavy burden when it comes to BG control. This is due to the complexity of BG control during exercise and meals where both hypo- and hyperglycemia still occur. Current hybrid CLC systems require the announcement of both meals and exercise. This feed-forward system is an imperfect one as CHO must be estimated to calculate the required insulin to be administered for meals. Also, basal insulin levels must be lowered and a quantity of CHO must be selected for consumption before and/or during aerobic exercise to prevent hypoglycemia. This

not only introduces the possibility of error to the system but also disregards other important meal and exercise factors that affect BG control such as protein and fat composition of meals and exercise type and intensity. Therefore, to ensure patient safety, increase the effectiveness of T1D treatment, and reduce the burden from the patient, these announcements must be removed.

2.5 Summary

T1D is an autoimmune disease that targets the insulin producing β-cells in the pancreas. Globally, it is estimated that 1.1 million children and adolescents (<20 years) have T1D, with 132,600 new cases per year. T1D results in many acute and chronic complications that reduce life quality and increase the risk of all cause mortality.

BG control in a healthy subjects is a finely tuned control system, maintaining BG levels and ensuring that high and low BG levels are immediately counteracted. However, those with T1D lack this control system. This is especially evident after a meal and after the commencement of exercise, where either a large postprandial increase or a large postexercise decrease in BG is experienced. Current treatment options allow a better mimicry of physiological insulin secretion; however, feed-forward announcements of meals and exercise are still required, which introduce patient error into the system and disregard important meal and exercise factors that affect BG control such as protein and fat composition of meals and type and intensity of exercise. Therefore, to increase the efficacy of current CLC systems, increase patient safety, and decrease the burden to the patient, the removal of meal and exercise announcements is paramount.

CHAPTER 3

THE ARTIFICIAL PANCREAS

The AP is a CLC system with the potential to reduce the complications associated with T1D by providing tight BG regulation in patients. As highlighted by the DCCT [89], tighter BG control leads to lower HbA1c levels, which ultimately leads to better outcomes in terms of diabetes-related complications. The AP is composed of a controller with an embedded algorithm that uses BG values provided by a CGM to modulate the insulin infusion rate of a CSII pump (Figure 3.1).

The components of the AP have made several advances in the recent years. BG meters used for self monitoring of BG (used to calibrate the majority of CGM devices), CGMs, and CSII pumps have all evolved into smaller, more reliable devices when compared to their predecessors. Additionally, there has been substantial progress in the development of the AP and a variety of

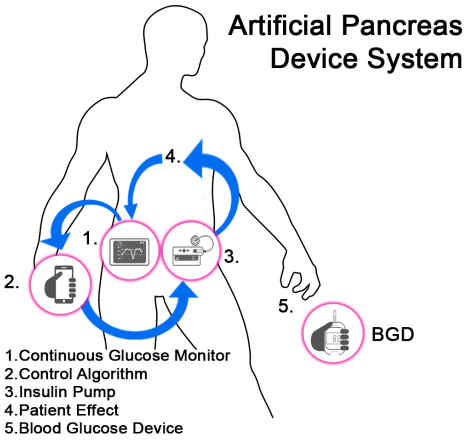

Figure 3.1: Illustration of the basic components in the AP (adapted from [113]).

AP approaches have been investigated. Both insulin only and bihormonal (including glucagon) approaches to the AP have been explored and several control algorithms such as, proportional-integral-derivative (PID) control, model predictive control (MPC), generalized predictive control (GPC), predictive derivative (PD) control, and fuzzy logic (FL) have been employed [114–121]. These systems have been challenged using different scenarios, mostly involving meals and exercise. Furthermore, the number of studies of CLC systems aimed to control BG levels in T1D have increased substantially with upwards of 90 clinical trials completed within the past five years. AP studies have advanced from clinical trials to home studies. The first AP devices have been introduced to the market in the form of the LGS and PLGM devices, with the most recent release of the Medtronic 670G Hybrid Closed Loop System (Northridge, CA, USA), which will be tested in patients aged 12 to 25 years over a six month period to determine its safety and efficacy [122].

3.1 Current State of the Artificial Pancreas

Improved glucose control and quality of life via the use of AP therapy has been found in many studies, with improved time in target (70-180 mg/dl) to ~70–75% and time below target (<70 mg/dl) to <4% [2, 3, 123–126], with one recent study achieving 88% time in the target glucose range [127]. However, these systems are largely hybrid systems that require user announcement of meals and exercise resulting in suboptimal performance due to the lag in insulin, misestimation of CHO, missed meal boluses, the varying effect of meal composition on BG, and different types and intensities of exercise, which have resulted in continued daily hyperglycemia (>180 mg/dl) with the persistent concern of hypoglycemia (<70 mg/dl).

3.1.1 Insulin Lag

Since the discovery of insulin, incremental advances such as highly purified animal-derived insulin, synthetically derived human insulin, rapid acting insulin, and long and ultra long acting insulin [128] have afforded those with T1D more convenience, a higher quality of life, and improvement in overall glycemic control [129]. However, current rapid acting insulin analogues are not absorbed quickly enough to mimic the pattern of physiological insulin secretion and action modulated by the β-cell in response to changes in insulin sensitivity, meal composition, diurnal variations, hormonal changes, and exercise [130].

Subcutaneous exogenous insulin is absorbed into the peripheral rather than the portal circulation. This delivery method leads to a delay in the onset of action (0-15 minutes), peak insulin BG concentration (40-60 minutes), and peak effect (~120 minutes) [101, 131, 132]. Due to this delay, studies have found that the optimum time for prandial insulin dosing is 15–20 minutes before a meal [132]. However as previously noted, these delays do not only apply to the prandial

period, as many other activities including exercise, require insulin levels in the plasma to be quickly adjusted.

New insulin formulations such as faster-acting insulin aspart (insulin aspart in a new fomulation) have been found when compared to insulin aspart to have a faster absorption and a onset of action of 5 min. Faster-acting insulin aspart was found to have an earlier insulin exposure and early glucose-lowering effect of 1.5-to-2 fold larger when compared to insulin aspart [133]. New administration routes such as pulmonary insulin delivery found in Technosphere Inhaled Insulin (Afrezza) has been found to have a faster peak insulin plasma concentration of 8-15 minutes, maximum insulin absorption of ~15 min, and a shorter duration of action of 180-240 minutes [134].

Currently, the lag in insulin is the main culprit of poor BG control during times when insulin BG concentrations are required to change rapidly in response to changing conditions e.g. during meals and aerobic exercise. Until new formulations and administration routes remove this lag, BG control during these disturbances will continue to be a challenge.

3.1.2 Meal Misestimation

CHO counting has been used in diabetes care since the 1920s. The DCCT [89] used CHO counting as one approach to meal planning that resulted in improved glycemic control, a reduction in HbA1c, improved quality of life, and flexibility with food choices. However, it is well-known that patients tend to under- and overestimate CHO quantities leading to higher HbA1c levels and postprandial glucose excursions [135].

One study based on multiple 24-hour food recalls showed that parents tend to overestimate the CHO content of their children's meals by approximately 20% [136]. Another study found an average meal CHO difference, between the patients' estimates and those assessed by a dietitian using a computerized analysis program, of 15.4 ± 7.8 grams or 20.9 ± 9.7% of the total CHO content per meal and 62.7% of the 448 meals analyzed were underestimated [137]. Meade and Rushton [30] found that patients over- and underestimated CHO content by an average of 40% and 12%, respectively. Smart et al. [135] and Kawamura et al. [138] found that CHO tended to be underestimated for larger meals and overestimated for foods containing relatively small amounts of CHO. Additionally, accurate estimation of the CHO in food containing a large amount of rice was particularly difficult and the CHO contents of high-calorie foods such as meats, fried foods, and desserts tended to be overestimated [138]. In addition, one study found that one of five participants who learned CHO counting did not use it to estimate their meal boluses, which suggests that this method may be difficult to implement for a non-negligible proportion of patients with T1D [139].

An additional note to consider is that CHO counting does not take into account dietary fat and protein, which affect the overall meal excursion, the duration of postprandial hyperglycemia, and prandial BG control [35]. Dietary fat modifies postprandial glycemia by delaying gastric

emptying resulting in a later postprandial peak [140–143] and sustained late postprandial hyperglycemia [142, 144]. Protein affects BG concentrations in the late postprandial period but behaves differently when consumed with and without CHO. For protein loads ≥75 grams without CHO, BG levels began to rise after 100 minutes [145], for meals with both protein and CHO, increased BG levels were noted after 3-4 hours [142, 143, 146].

Due to the error incurred by current meal size estimation practices, a new methodology of determining meal bolus quantity is required to optimize BG control.

3.1.3 Missed Meal Boluses

Missed meal boluses increases HbA1c levels, which can lead to an increased risk of long-term complications [31–33]. Burdick et al. [31] reported that out of 49 adolescent patients, 17 patients (35%) missed <1 mealtime bolus per week, while 31 patients (65%) missed ≥1 mealtime bolus per week and showed an average increase in HbA1c of 4 mmol/mol (0.3%) during a 2-week period due to missed meal boluses [31].

A few studies have used unannounced meals simply as a challenge to see how well their controller works when a premeal bolus is not given [147, 148] and have found that their controller is able to overcome small unannounced meals but have difficulty with larger meals [148]. This is largely due to the delay in insulin action that lags behind the rise in BG preventing a sufficient decrease in the glucose excursion. Larger unannounced meals therefore require meal detection systems that are able to quickly detect meals and implement strategies to combat postprandial hyperglycemia.

Dassau et al. [4] designed a meal detection system that uses binary detection that is triggered by a voting scheme. This system was trained with a MiniMed CGMS Gold (Northridge, CA, USA) dataset and tested in clinic using Freestyle Navigator CGM (Chicago, IL, USA) readings. Lee and Bequette [5] detected a meal based on certain logical conditions of first and second derivatives of glucose levels, and then a finite impulse response (FIR) filter was applied to estimate the meal size. Then, Lee et al. [6] refined the logical conditions and generated a series of meal impulses, a moderately sized bolus was then given according to the meal impulses. Cameron et al. [7] developed a probabilistic detection algorithm based on a set of meal shapes with the meal start time and postprandial glucose appearance estimated at the same time. Later on, Cameron and Niemeyer [8] came up with a multi-model method to detect and estimate unannounced meals. The method is also probabilistic based but assumes a constant meal absorption shape. Chen et al. [9] and Weimer et al. [10] are able to detect meals utilizing a bin-counting heuristic that counts the number of decisions generated using a dual parameter-invariant statistics leveraged from a linearized physiological model. Xie and Wang [11] use a multi-model approach to detect meals, meal start time, and meals size using a Variable State Dimension method, which uses a switching criteria to switch between models with different state dimensions. Turksoy et al. [12] propose a method for meal detection and bolus estimation based on an estimated rate of glucose

appearance (Ra). Finally, Mahmoudi et al. [13] use an adaptive Unscented Kalman Filter (UKF) and two redundant CGM sensors to detect meals based on glucose predicted by a model and CGM values. A meal is detected when CGM values of both sensors fall outside the 95% confidence interval of the predicted model.

Lee et al. [6] and Cameron et al. [7] have achieved remarkable in silico results in an adult cohort in terms of postprandial hyperglycemia mitigation with a time in range (70-180 mg/dL) of 90% and 89%, respectively. However, these results have not been translated into a clinical setting where detection modules are still unable to prevent a large majority of postprandial hyperglycemia and in turn result in many hypoglycemic events as seen in Turksoy et al. [14] and Cameron et al. [15]. Therefore, a means to improve outcomes due to unannounced meals and provide an improved methodology for overcoming meal excursions is required.

3.1.4 Exercise

Although, evidence suggests that regular physical activity can lower mortality and morbidity and improve cardiovascular health, lipid profiles, and physiological wellbeing in patients with T1D [149–151], those with T1D are reluctant to participate in exercise due to fear of exercise-induced hypoglycemia.

Current aerobic exercise recommendations for T1D patients include decreasing basal insulin and ingesting a predetermined amount of CHO before and during aerobic exercise [34]. A study by Schiavon et al. [152] found that the optimum adjustment of basal insulin in an in silico population was a reduction of 50% 90 minutes before exercise, with a reduction of 30% during exercise. However, patients should be aware of increased risk of DKA due to insulin reduction/omission over an extended period of time [34]. The amount of CHO required by each patient differs based on intensity and duration of exercise, as well as internal metabolic factors, e.g. rate of glucose uptake, insulin sensitivity, etc.

Due to the multifaceted nature of aerobic exercise, T1D patients either abstain from exercise altogether or are unable to maintain BG within acceptable levels leading to poor BG control. Additionally, similar to missed meal boluses [32, 153], there is a high likelihood of a patient forgetting to perform the manual adjustments before exercise required of current hybrid systems or performing these actions late. Therefore, a methodology to reduce the likelihood of exercise-induced hypoglycemia and remove the burden from the patient is required to improve outcomes due to aerobic exercise, specifically unannounced aerobic exercise.

Stenerson et al. [16] showed that insulin suspension based on accelerometery input alone was successful in preventing exercise-induced hypoglycemia in silico, but not successful in preventing hypoglycemia in children with T1D playing soccer [17]. Turksoy et al. [18] did a study that used a multisensor called SensWear Pro3 (BodyMedia Inc, Pittsburgh, PA) that used accelerometer and skin impedance data as inputs to their single-hormone AP to reduce the delivery of insulin during unannounced exercise; CHO were also suggested if glucose was dropping sharply or

dropping too low. In a study by Breton et al. [21] the addition of a hear rate monitor (HRM) as an input to modify dosing of a control-to-range single-hormone AP system was able to reduce exercise-induced hypoglycemia. Dasanayake et al. [19] used both an accelerometer and HRM to detect both the start and end of exercise using principal component analysis. Finally, Jacobs et al. [20] used an accelerometer and heart rate monitor as inputs into a validated regression model to detect exercise during a 22-hour overnight inpatient study with 13 T1D subjects.

Although previous exercise detection studies have been able to detect aerobic exercise in a short period of time and improve outcomes due to aerobic exercise [16–21], there is an added complexity with the current approach to exercise detection, which includes the addition of external physiological sensors, i.e. heart rate monitor (HRM), accelerometer, etc. The addition of devices increases the probability of failure of individual devices as seen in Dasanayake et al. [19], where dropouts were experienced in both the HRM and accelerometer for significant periods of time. It was also found that both heart rate and accelerometry data are prone to producing false positives, as heart rate can be increased in the presence of stress or a fever and accelerometer data can be increased during activities such as horseback riding [21]. Furthermore, due to the additional burden, patients are likely to resist the use of additional devices that are required to be worn and maintained in conjunction with their existing devices.

Furthermore, this type of detection is not able to distinguish between aerobic and anaerboic exercise. Anaerobic exercise, in contrast to aerobic exercise, can lead to a dramatic increase in BG due to a feed-forward mechanism that causes hepatic glucose production to exceed muscle glucose utilization. Therefore, it is also necessary to distinguish between aerobic and anaerobic exercise during detection. Thus far, there has been one study using additional physiological signals to develop a classification system [154]; however, it has not been implemented into a CLC system and its usefulness has not been determined. Therefore, a new methodology is required for the control of BG during exercise that does not include announcement and is proven safe to the patient.

3.2 The Type 1 Diabetes Simulator

A modified T1D simulator based on the University of Virgina/Padova (UVA/Padova) T1D Simulator [155] was used in this thesis to build different types of scenarios to test the detection and control of meals and aerobic exercise. The simulator is a mixed meal simulation model of a glucose-insulin-glucagon system and further information about the model and its equations can be found in Appendix A. Various insulin pump and CGM models are implemented into the simulator.

The T1D Simulator uses the patient population from the S2008 version of the UVA/Padova T1D Simulator [156] that includes a cohort of ten adults, ten adolescents, and ten children. Although, the newer versions of the UVA/Padova include 100 subjects for each of the three patient

populations, the ten subjects used in our studies give insight into the interpatient variability of key metabolic parameters found in the general population of individuals with T1D [156].

The T1D Simulator has been modified to include a meal library, which consists of 31 fast absorption meals (over 60% of the ingested CHO are absorbed within the first two hours after meal time), 15 medium absorption meals (less than 60% of the ingested CHO absorbed within the first two hours after meal time and more than 80% of the ingested CHO are absorbed within the first four hours after meal time), and three slow absorption meals (less than 80% of the ingested CHO are absorbed within the first four hours after meal time) [157, 158]. An exercise model [159] has also been added to the simulator and fitted using clinical data (previously described in Bertachi et al. [160]) to be used for testing the detection and disturbance rejection of aerobic exercise. Circadian insulin sensitivity variation (sinusoidal type with 24-hour period) was also implemented with random amplitude according to a uniform distribution of ±30% and random phase.

3.3 Closed-Loop Controller

The algorithms presented in this thesis were built around a base closed-loop controller. This closed-loop controller is a PD controller with sliding mode reference conditioning (SMRC) and insulin feedback (IFB) [161–163]. Figure 3.2 is a block diagram of the closed-loop controller which is composed of two loops. The inner control loop is a PD controller with IFB designed to drive the measured glucose to a target value. The outer loop is a safety supervisory loop that uses SMRC to modulate the glucose target value based on the estimated IOB, which reduces the

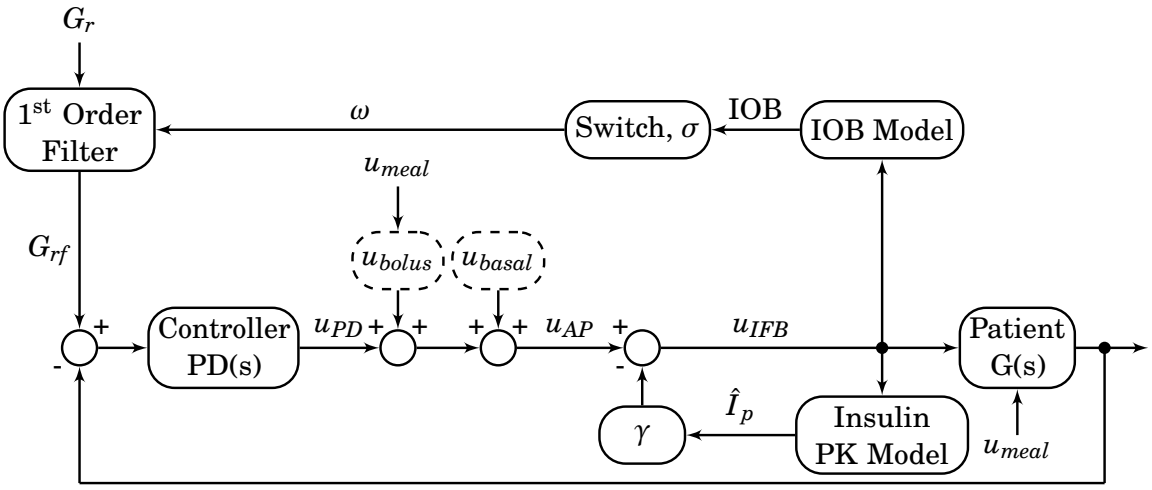

Figure 3.2: Closed-loop controller composed of an inner control loop that contains a PD controller with IFB designed to drive the measured glucose value (G) to a target value (G_r) and an outer loop that acts as a safety supervisory loop and uses SMRC)to modulate G_r to G_{rf} based on the estimated IOB.

risk of hypoglycemia due to controller overcorrection. Further information about the closed-loop controller can be found in Appendix B.

3.4 Summary

The AP is composed of a CGM, an insulin pump, and a control algorithm that has the potential to reduce the complications associated with T1D by providing tight BG regulation in patients. Several control algorithms have been explored such as PID, MPC, GPC, PD, and FL and improved BG control has been obtained; however, these are hybrid systems that require the announcement of meals and exercise and often lead to suboptimal performance.

Innovative strategies that do not require the announcement of meals and exercise are necessary to improve BG control and remove current optimization problems such as meal misestimation, missed meal boluses, and exercise-induced hypoglycemia. However, the lag introduced by the subcutaneous administration of insulin further complicates the control of these events and this limitation must also be taken into account.

The methodologies presented in this thesis will be created, tested, and incorporated into a closed-loop controller using a T1D Simulator, which is a powerful tool for testing the efficacy of CLC strategies on a T1D population.

CHAPTER 4

STATE ESTIMATION

At the core of the strategies proposed in this thesis to better handle unannounced meals and exercise is a state estimator. The derivation of said estimator is presented here with its application/incorporation into the control strategies presented in later chapters. State estimates were performed using an UKF that employs a minimal model. This chapter first presents the minimal model with all of its equations and then elaborates on the UKF.

4.1 Minimal Model

The equations of the minimal model (Figure 4.1) are provided in the following subsections.

4.1.1 Glucose Subsystem

The model is comprised of the Bergman equations (see [164]):

$$\dot{G}_p(t) = -\big(p_1 + X(t)\big)G_p(t) + p_1 G_b + \frac{D(t)}{V_G}, \tag{4.1}$$

$$\dot{X}(t) = -p_2 X(t) + p_2 S_I I(t), \tag{4.2}$$

where G_p is plasma glucose concentration, X is proportional to insulin in the remote compartment, and G_b is basal glucose. p_1 represents the rate at which glucose is removed from the plasma space independent of the influence of insulin. V_G is the distribution volume, p_2 is the rate of disappearance of remote insulin from the remote insulin compartment, and $S_I = p_3/p_2$ is the insulin sensitivity. D, identified using an UKF (Equation (4.9)), is a lumped signal used to describe plasma glucose variations due to meals, exercise, and other disturbances that are not described by the other parameters of the model.

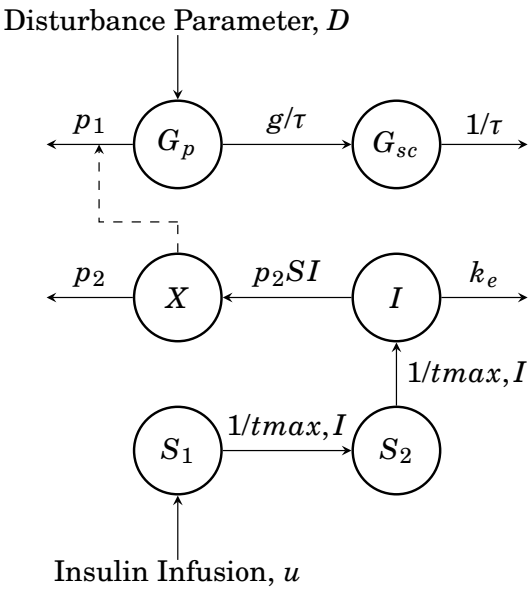

Figure 4.1: Compartmental model of glucose-insulin system. G_p and G_{sc} represent glucose concentrations in the accessible (plasma) and non-accessible (subcutaneous) compartments, I represents plasma insulin, and X represents a remote insulin compartment that accelerates glucose disappearance [164].

The blood-to-interstitial glucose dynamics are described as a first-order linear system [165]:

$$\dot{G}_{sc}(t) = -\frac{1}{\tau}G_{sc}(t) + \frac{g}{\tau}G_p(t), \tag{4.3}$$

where G_{sc} represents subcutaneous glucose, τ represents the time constant of the system and g is the static gain of the system.

4.1.2 Insulin Subsystem

Insulin absorption [166] is described as:

$$\dot{S}_1(t) = u(t) - \frac{S_1(t)}{t_{max,I}}, \tag{4.4}$$

$$\dot{S}_2(t) = \frac{S_1(t) - S_2(t)}{t_{max,I}}. \tag{4.5}$$

S_1 and S_2 are a two compartment chain representing the subcutaneous absorption of rapid-acting (e.g., Lispro) insulin and $u(t)$ (μU/kg/min) represents administration (bolus and infusion) of insulin.

The plasma insulin concentration [166] is given by:

$$\dot{I}(t) = -k_e I(t) + \frac{1}{V_I} \cdot \frac{S_2(t)}{t_{max,I}}, \tag{4.6}$$

where k_e is the fractional elimination rate, V_I is the distribution volume, and $t_{max,I}$ is the time-to-maximum insulin absorption.

The T1D subject model was discretised using a first forward difference derivative approximation (1 min step size) [167]. The mean population values found in Table 4.1 are utilized in this model.

Table 4.1: Mean population parameter values

Symbol	Quantity	Value	Units	Reference
p_1	Glucose removal rate from the plasma space independent of the influence of insulin	0.035	1/min	[168]
p_2	Disappearance rate of remote insulin from the remote insulin compartment	0.05	1/min	[168]
p_3	Appearance rate of remote insulin into the remote insulin compartment	0.000028	mL/μU· min^2	[168]
G_b	Basal plasma glucose	100	mg/dL	[164]
V_G	Volume distribution of glucose compartment	1.6	dL/kg	[166]
V_I	Volume distribution of insulin compartment	120	mL/kg	[166]
k_e	First-order decay rate of insulin in plasma	0.138	1/min	[166]
$t_{max,I}$	Time-to-maximum insulin absorption	55	min	[166]
τ	Time constant of the system	8.2237	min	[165]
g	Static gain of the system	1	unitless	[165]

4.2 Unscented Kalman Filter

The Unscented Kalman Filter (UKF) proposed by [169] is a powerful technique used in nonlinear estimation and machine learning applications. Its foundation lies in the intuition that it is easier to approximate a probability distribution than it is to approximate an arbitrary nonlinear function or transformation [170]. Using the discretized model of Equations (4.1)–(4.6) and the inputs of glucose and insulin infusion rate obtained from a CGM and an insulin pump, respectively, a nonlinear state space model is derived:

$$x(k+1) = f(x(k), u(k)) + w(k), \tag{4.7}$$

$$y(k) = g(x(k)) + v(k), \tag{4.8}$$

where $x(k)$ is the state vector, which has been augmented by $D(t)$, with state equation:

$$\dot{D}(k) = 0. \tag{4.9}$$

$u(k)$ is the input and $w(k)$ and $v(k)$ are defined to be process and measurement noises, respectively. The nonlinear functions $f(\cdot)$ and $g(\cdot)$ are defined from Equations (4.1)–(4.6).

The nonlinear function, $y = f(x)$ of variable x (dimension L) is applied to each point, in turn, to yield a cloud of transformed sigma points, X_i in the form of matrix X (dimension $2L+1$)

according to the following:

$$X_0(k-1) = \hat{x}(k-1), \tag{4.10}$$

$$X_i(k-1) = \hat{x}(k-1) + \left(\sqrt{(L+\lambda)P(k-1)}\right)_i \qquad i = 1,\ldots,L, \tag{4.11}$$

$$X_i(k-1) = \hat{x}(k-1) - \left(\sqrt{(L+\lambda)P(k-1)}\right)_{i-L} \qquad i = L+1,\ldots,2L, \tag{4.12}$$

with scalar weights W_i defined as:

$$W_0^m = \frac{\lambda}{L+\lambda}, \tag{4.13}$$

$$W_0^c = \frac{\lambda}{L+\lambda} + (1-\alpha^2+\beta), \tag{4.14}$$

$$W_i^m = W_i^c = \frac{1}{2(L+\lambda)} \qquad i = 1,\ldots,2L, \tag{4.15}$$

where $\lambda = \alpha^2(L+\kappa) - L$ is a scaling parameter, α determines the spread of the sigma points around $\hat{x}$, κ is a secondary scaling parameter, and β is used to incorporate prior knowledge of the distribution of x. $P(k-1)$ is the covariance matrix and $\left(\sqrt{(L+\lambda)P(k-1)}\right)_i$ is the ith column of the matrix square root, i.e., lower triangle Cholesky factorization.

The sigma vectors, $X_i(k-1)$ are then propagated through the nonlinear function, $f(\cdot)$ as follows:

$$X_i^-(k) = f[X_i(k-1), u(k)] \qquad i = 0,\ldots,2L. \tag{4.16}$$

The statistics of the transformed points can then be calculated to form an estimate of the nonlinearly transformed mean ($\hat{x}$) and covariance ($P(k)$):

$$\hat{x}^-(k) = \sum_{i=0}^{2L} W_i^m \hat{X}_i^-(k-1), \tag{4.17}$$

$$P^-(k) = \sum_{i=0}^{2L} W_i^c (X_i^-(k-1) - \hat{x}^-(k))(X_i^-(k-1) - \hat{x}^-(k))^T + Q_p, \tag{4.18}$$

where Q_p is the covariance matrix of the process noise. The sigma points X_i^- are propagated through the nonlinear function $g(\cdot)$ for the calculation of Y_i^-:

$$Y_i^-(k) = g[X_i^-(k), u(k)] \qquad i = 0,\ldots,2L. \tag{4.19}$$

The measurement estimations are obtained from X_i^- as:

$$\hat{y}^-(k) = \sum_{i=0}^{2L} W_i^m Y_i^-(k). \tag{4.20}$$

The innovation and cross-covariance matrices are then calculated as:

$$P_{yy}(k) = \sum_{i=0}^{2L} W_i^c [Y_i^-(k) - \hat{y}^-(k)][Y_i^-(k) - \hat{y}^-(k)]^T + Q_m, \tag{4.21}$$

$$P_{xy}(k) = \sum_{i=0}^{2L} W_i^c [X_i^-(k) - \hat{x}^-(k)][Y_i^-(k) - \hat{y}^-(k)]^T, \tag{4.22}$$

where Q_m represents the covariance of measurement noise. Lastly, the Kalman filter gain and the updated state vector estimation and covariance matrix are calculated:

$$K(k) = P_{xy}(k)(P_{yy}(k))^{-1}, \tag{4.23}$$

$$\hat{x}(k) = \hat{x}^{-}(k) + K(k)(y(k) - \hat{y}^{-}(k)), \tag{4.24}$$

$$P(k) = P^{-}(k) - K(k)P_{yy}(k)(K(k))^{T}. \tag{4.25}$$

The UKF requires the definition of initial conditions and tuning parameters, which in our case were selected as:

$$\hat{x}(0) = \begin{bmatrix} G_p(0) \\ X(0) \\ I(0) \\ S_1(0) \\ S_2(0) \\ G_{sc}(0) \\ D(0) \end{bmatrix} = \begin{bmatrix} BG(0) \\ 0 \\ 0 \\ \mathrm{u}(0) \\ 0 \\ BG(0) \\ 0 \end{bmatrix},$$

$$q = 0.6103 \quad r = 8.9614,$$

$$Q_p = diag\left[q^2\ 0\ 0\ 0\ 0\ q^2\ q^2\right],$$

$$P(0) = I_{7\times 7} \quad Q_m = r^2,$$

$$\alpha = 10^{-3} \quad \kappa = 0 \quad \beta = 2,$$

where $G_{sc}(0)$ is the first measured glucose value from a CGM, q is the standard deviation of the process noise, and r is the standard deviation of the measurement noise.

4.3 Unscented Kalman Filter State Estimations

The in silico state estimations of an augmented minimal model using an UKF were compared to the model states of the T1D Simulator and the populational values are shown in Figure 4.2. The scenario used for this comparison included: three meals per day with varying CHO content and meal time following a normal distribution with mean 30 grams at 8:30h (breakfast), 60 grams at 13:00h (lunch), and 50 grams at 19:00h (dinner). Coefficient of variance for the meal size was ±20%, and the standard deviation for meal time was ±10 minutes. For each meal, a meal absorption profile was selected randomly from a meal library of eleven meals, which are the meals of the ten adults and the average adult provided by the T1D Simulator.

The root mean squared error (RMSE) between the T1D Simulator and the UKF was calculated for each of the states over a 14-day period. The RMSE values of the mean populational values for G_p, G_{sc}, I_p, X, S_1, S_2, and Ra were found as 5.8 mg/dl, 0 mg/dl, 3.7 pmol/l, 25.6 pmol/l, 43.2 pmol/l, 60.1 pmol/l, and 2.8 mg/dl/min, respectively. The percentage error of the mean

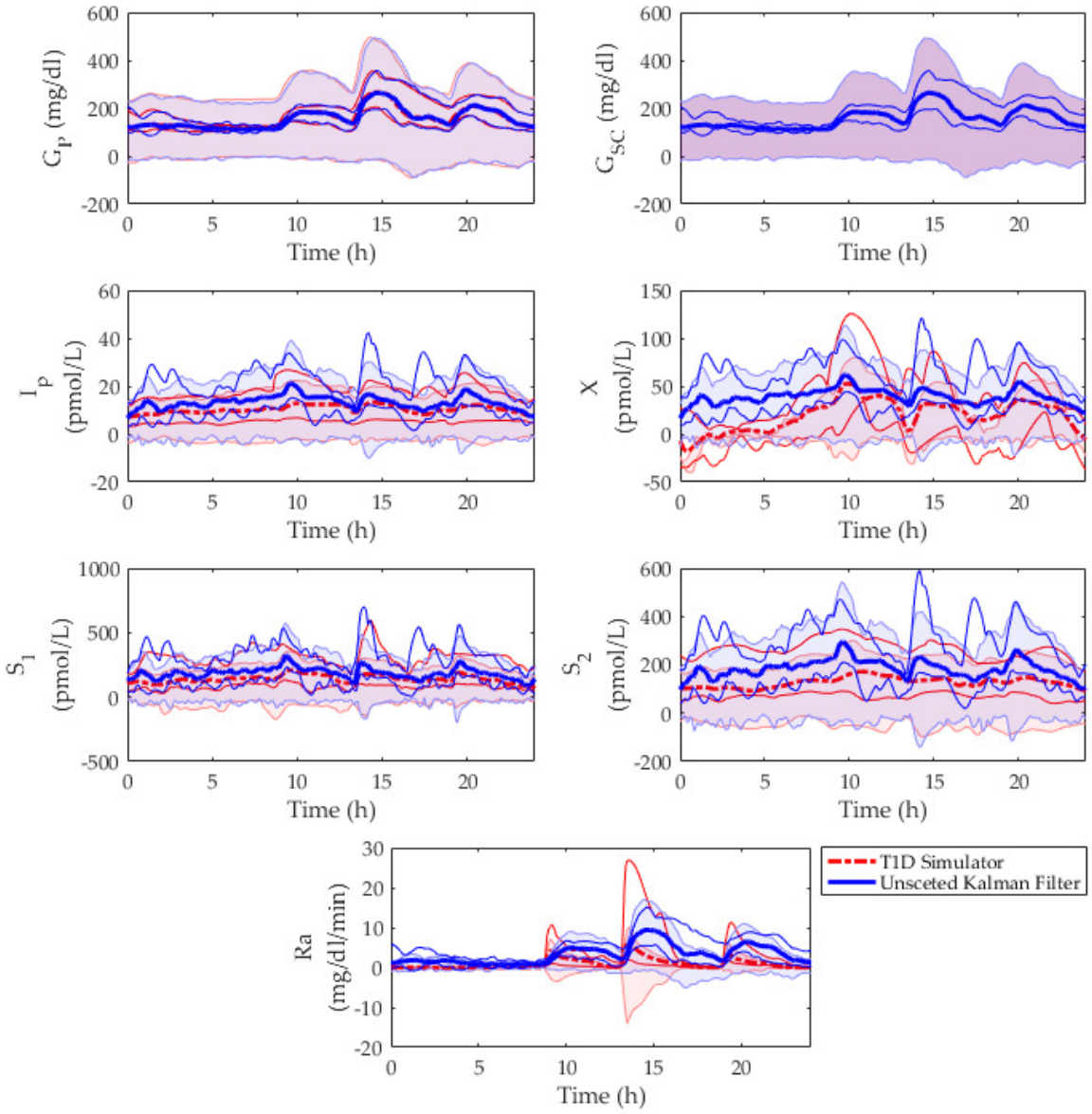

Figure 4.2: Population state estimations of the T1D Simulator versus the UKF over a 24-hour period in silico. States shown are plasma glucose (G_P), subcutaneous glucose (G_{SC}), plasma insulin (I_p), remote insulin (X), insulin in the first subcutaneous compartment (S_1), insulin in the second subcutaneous compartment (S_2), and rate of glucose appearance (Ra) equated to the disturbance parameter, D. Graph reported as median (bold lines) and 25 percentile and 75 percentile (lightly shaded area), minimum (thin lower line), and maximum values (thin upper line).

population values for G_p, G_{sc}, I_p, X, S_1, S_2, and Ra were found as 1%, 0%, 31%, 49%, 23%, 37%, and 28%, respectively. These findings suggest that the states were estimated with reasonable precision. The states of S_1 and S_2 have been found to have higher RMSE values, although both UKF estimated states seem to follow a similar trend to that of the T1D Simulator model states. The X state has been found to have a higher percentage error value, where large deviations in

the median value can be seen in Figure 4.2. The Ra between the T1D Simulator and the UKF was found to have a relatively low RMSE and percentage error however, the peak time and absorption dynamics appear to be quite different and these differences must be taken into account if using this state to aid in bolus decisions.

4.4 Summary

The states of an augmented minimal models are estimated using a UKF with the inputs of glucose and insulin infusion rate values from the T1D Simulator. The UKF is able to estimate the states of the T1D Simulator with reasonable precision and are a viable option for the use in meal and exercise detection.

CHAPTER 5

Unannounced Meal Detection and Postprandial Glycemic Control

In AP systems, postprandial control remains one of the biggest challenges. This is due to the lag in insulin action that occurs in current insulin formulations administered subcutaneously. This means that insulin must be administered preemptively in order to prevent postprandial hyperglycemia. Postprandial control is further complicated by current hybrid CLC systems that calculate meal boluses using a user-estimated CHO quantity and an insulin-to-carbohydrate ratio. This requires T1D patients to estimate the CHO content of a meal prior to ingestion, which can lead to CHO misestimation and missed meal boluses due to lack of user compliance. CHO underestimation can lead to postprandial hyperglycemia, CHO overestimation carries a serious risk of hypoglycemia due to insulin overdosing, and missed meal boluses can lead to severe postprandial hyperlgycemia. CHO estimation also tends to neglect the effect of dietary fat and protein, which have a profound effect on postprandial outcomes. Additionally, it has been found that a subset of patients tend to opt-out of CHO estimation entirely. These downfalls in postprandial control generally produce an increase in HbA1c levels that leads to the development of diabetes-related complications.

The idea behind this work was to build a postprandial hyperglycemia reduction algorithm (PHRA) in the context of an AP system that includes a meal detection algorithm, which triggers automatic disturbance rejection actions to safely and effectively mitigate postprandial hyperglycemia.

5.1 Meal Detection

The meal detection algorithm presented in this thesis was tuned and validated using a 14-day in silico simulation. A sensitivity analysis is also presented for meals over a 500-day period in ten adult subjects. The algorithm collects glucose and insulin infusion rate values and computes a disturbance parameter from an augmented minimal model using an UKF (as described in Chapter 4). The cross-covariance between the glucose data and the forward difference of computed disturbance parameter is then calculated over three different sliding windows. A threshold is then applied, different for each sliding window. One threshold is applied to obtain a detection that has a high true positive (TP) value, the second is a trade-off tuning, which has both a high TP value and a low false positive (FP) value, and the third tuning has a very low FP value.

5.1.1 Meal Detection Algorithm

After the states in Equations (4.1)–(4.6) are estimated using the UKF, the values of $G_{sc}(k)$ from the CGM simulated data and $D_{diff}(k)$, which is the forward difference of $D(k)$, are scaled between -1 and 1 using minimum and maximum values determined a priori through simulation. Then, the biased estimate of the cross-covariance between the two sequences is calculated during windows of a specified length.

The true cross-covariance sequence of two jointly stationary random processes, G_{sc_n} and D_{diff_n}, is the cross-correlation of mean-removed sequences [171],

$$\Phi_{G_{sc},D}(m) = E\{(G_{sc}(n+m) - \mu_{G_{sc}})(D_{diff}(n) - \mu_{D_{diff}})^*)\}, \tag{5.1}$$

where $\mu_{G_{sc}}$ and $\mu_{D_{diff}}$ are the mean values of the two stationary random processes and E is the expected value operator. The asterisk denotes complex conjugation.

The raw cross-covariances are computed as:

$$c_{G_{sc},D_{diff}}(m) = \begin{cases} \sum_{n=0}^{N-m-1} \left(G_{sc}(n+m) - \frac{1}{N}\sum_{i=0}^{N-1} G_{sc}(i)\right)\left(D^*_{diff}(n) - \frac{1}{N}\sum_{i=0}^{N-1} D^*_{diff}(n)\right) & \text{m } \geq 0, \\ \\ c^*_{D_{diff},G_{sc}}(-m), & \text{m } < 0, \end{cases} \tag{5.2}$$

where $G_{sc}(n)$ and $D^*_{diff}(n)$ are indexed from 0 to $N-1$, and $c_{G_{sc},D_{diff}}(m)$ from $-(N-1)$ to $N-1$, where N is the number of samples.

A meal is then detected as follows:

$$Meal = \begin{cases} True, & if \;\; c_{G_{sc},D_{diff}}(m) \geq threshold, \\ & \quad and \; D_{diff}(k) > 0, \\ & \quad and \; G_{sc}(k) - G_{sc}(k-3) > 0, \\ False, & otherwise. \end{cases} \tag{5.3}$$

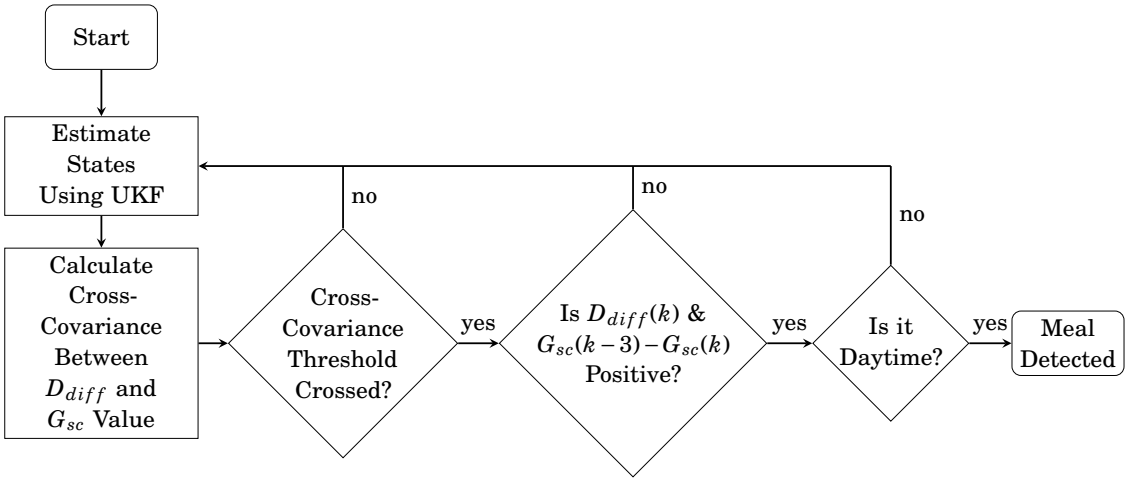

Figure 5.1: Flow chart of the meal detection algorithm. First, the states of a minimal model are estimated using an UKF and then the cross-covariance is found between the state estimation for the forward difference of the disturbance parameter (D_{diff}) and the glucose value G_{sc} obtained from a CGM. A threshold is applied to the cross-covariance, and, once crossed, the last unscaled value of D_{diff} and the slope with respect to the measurement 15 minutes ago (3 samples) of G_{sc} are checked, if both are positive and it is daytime, a meal is detected.

A meal was assumed to have been consumed if the cross-covariance between the $G_{sc}(n)$ and $D_{diff}(n)$ signals exceeded a pre-specified threshold and the last unscaled value of D_{diff} and the slope of G_{sc} with respect to the measurement 15 minutes ago (three samples) were positive (see Figures 5.1 and 5.2). It should be noted that meals are not detected during the nighttime period (23:00h–6:00h) as a safety precaution.

5.1.2 Performance Metrics

Seven performance metrics were used: sensitivity, TP, FP, false negative (FN), FP per day, detection time, and Δ glucose. True negatives (TN) and specificity cannot determined in this framework due to the fact that one TP can span multiple time points depending on meal duration; however, a TN can be counted for each time sample that a negative occurrence is correctly identified. This skews the specificity to the higher end of the spectrum. Therefore, sensitivity and FP were used as measures of performance. Sensitivity measures the percentage of positive results that are correctly identified. Correct detection (a TP) is when the algorithm has detected a meal from the beginning of the meal to 120 minutes after the time of the commencement of the meal. An FP is when detection is positive without a meal. Negative detection or an FN is when a meal has not been detected up to 120 minutes after ingestion. To compare the FP values between the two scenarios, the FP/day is used. Detection time reflects the time at which a TP is detected with respect to meal time and Δ glucose reflects the change in glucose from the start of the meal to the time when the meal was detected. All values are reported as mean $\pm$ standard deviation and median (5th percentile, 95th percentile).

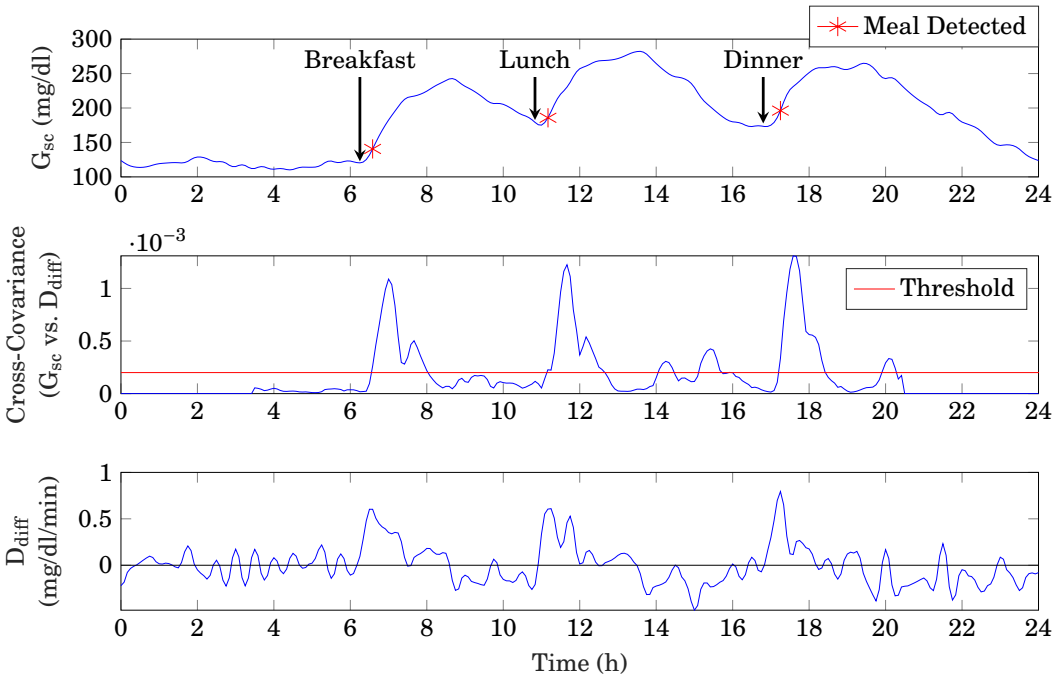

Figure 5.2: Illustration of the meal detection algorithm showing subcutaneous glucose (G_{sc}) values from a CGM values (top graph), cross-covariance (middle graph) and the forward difference of the disturbance parameter, D_{diff} (bottom graph).

5.1.3 Diabetes Simulation Scenario

The T1D Simulator (Chapter 3.2) was used to build two different types of scenarios: (1) a meal detection tuning and validation scenario and (2) a meal detection sensitivity analysis scenario. Meal absorption rate and subcutaneous insulin absorption rate were varied at each meal according to a uniform distribution of ±10% and ±30%, respectively. Circadian insulin sensitivity variation (sinusoidal type with 24-hour period) was implemented with random amplitude according to a uniform distribution of ±30% and random phase. Finally, CGM error was according to the default model available in the T1D simulator.

Meal Detection Tuning and Validation Scenario

Two challenging 14-day scenarios were built: one scenario was used for tuning and the other was used for validation. These scenarios included: three meals per day with varying CHO content and meal time following a normal distribution with a mean of 30 grams at 8:30h (breakfast), 60 grams at 13:00h (lunch), and 50 grams at 19:00h (dinner). Coefficient of variance for the meal size was ±20%, and the standard deviation for meal time was ±10 min. For each meal, a meal absorption profile was selected randomly from a meal library of eleven meals, which are the meals of the ten adults and the average adult provided by the T1D Simulator. There were 420 meals in total for all ten subjects over the 14-day period.

Meal Detection Sensitivity Analysis Scenario

A 500-day scenario with ten adult subjects was built for a sensitivity analysis of the meal detection algorithm. Meals were uniformly distributed and ranged from 20 to 120 grams of CHO with meal time following a normal distribution with a standard deviation of ±10 minutes at 8:30h (breakfast), 13:00h (lunch), and 19:00h. (dinner). For each meal, a meal absorption profile was selected randomly from a meal library of 49 meals. The meal library consisted of 31 fast absorption meals, 15 medium absorption meals, and three slow absorption meals. There were 15,000 meals in total for all ten subjects over the 500-day period.

5.1.4 Results

Three different tunings of the same detection algorithm were analyzed, one had the highest sensitivity, the second had a trade-off between the number of TP and FP, and the third had the lowest number of FP. These tunings were used to decipher the usefulness of the detection algorithms for the purpose of postprandial hyperglycemia mitigation during unannounced meals. Here, the results for the scenarios where the algorithms were first tuned and validated, and then a sensitivity analysis scenario where the algorithm is analyzed in depth to determine factors that affect detection performance are presented.

Meal Detection Algorithm: Tuning

The tuning of the algorithm was done both by window size and threshold on the cross-covariance between D_{diff} and the current CGM value. The window sizes and thresholds were empirically derived based on the sensitivity and the FP number, which were used as indicators of performance. In general, smaller window sizes and lower thresholds result in a higher sensitivity in the meal detection algorithm as seen in Table 5.1. The amount of CHO consumed per meal by the ten adult subjects in the tuning and validation scenarios had a mean of 47 ± 16 grams and 47 ± 13 grams and a median of 45 (23, 74) grams and 46 (28, 69) grams, respectively. These scenarios reflect CHO consumption on a typical day for an average patient. Table 5.1 reports the mean, standard deviation, median, 5th percentile, and 95th percentile values for the sensitivity, Δ glucose, detection time, TP, FP, FN, and FP/day of each meal detection tuning. Typically, a higher sensitivity reflects lower Δ glucose, detection time, and FN values with increased TP, FP, and FP/day values. The high sensitivity tuning for both the tuning and validation scenarios had a mean sensitivity of 99 ± 1% and 99 ± 2% and a median of 99 (95, 100)% and 98 (90, 100)% and FP of mean 18 ± 6 and 20 ± 6 and median of 19 (9, 25) and 20 (11, 26). The trade-off tuning for both the tuning and validation scenarios had a mean sensitivity of 93 ± 5% and 94 ± 5% and median of 93 (86, 100)% and 94 (83, 100)% and FP of mean 4 ± 4 and 4 ± 3 and median 3 (0, 7) and 4 (1, 9). Finally, the low FP tuning for both the tuning and validation scenarios had a mean sensitivity of 47 ± 10% and 47 ± 16% and median of 50 (26, 64)% and 45 (29, 71)% and mean FP of 0 ± 0 and 0.2 ± 0.4 and median of 0 (0, 0) and 0 (0, 1).

Table 5.1: Population performance metrics of meal detection algorithm in tuning scenario. Total number of meals per patient was 42.

	Sensitivity (%)	**Δ Glucose (mg/dL)**	**Detection Time (min)**	**TP**	**FP**	**FN**	**FP/day**
Highest Sensitivity (window = 15 min; threshold = 0.000039)							
Tuning	99 ± 2 99 (95, 100)	7 ± 7 6 (−1, 17)	28 ± 10 25 (15, 45)	41 ± 1 42 (40, 42)	17 ± 5 19 (9, 25)	1 ± 1 1 (0, 2)	1 ± 1 1 (0, 3)
Validation	98 ± 4 98 (90, 100)	6 ± 8 5 (−2, 13)	28 ± 9 25 (15, 40)	41 ± 2 42 (38, 42)	18 ± 5 20 (11, 26)	1 ± 2 0 (0, 4)	1 ± 1 1 (0, 3)
Trade-Off (window = 45 min; threshold = 0.00019)							
Tuning	93 ± 5 93 (86, 100)	19 ± 5 19 (11, 28)	37 ± 9 35 (25, 55)	39 ± 2 39 (36, 42)	3 ± 2 3 (0, 7)	3 ± 2 3 (0, 6)	0.2 ± 0.5 0 (0, 1)
Validation	93 ± 6 94 (83, 100)	19 ± 5 18.43 (11, 26)	37 ± 83 35 (25, 50)	39 ± 3 40 (35, 42)	3 ± 3 4 (1, 9)	3 ± 3 3 (0, 7)	0 ± 0 0 (0, 0)
Lowest False Positive (window = 60; threshold = 0.00082)							
Tuning	47 ± 12 50 (26, 64)	45 ± 7 45 (36, 54)	46 ± 8 45 (35, 60)	20± 5 21 (11, 27)	0 ± 0 0 (0, 0)	22 ± 5 21 (15, 31)	0 ± 0 0 (0, 0)
Validation	46 ± 16 45 (29, 71)	43 ± 7 45 (35, 56)	48 ± 8 50 (35, 60)	19 ± 7 19 (12, 30)	0.2 ± 0.4 0 (0, 1)	23 ± 7 23 (12, 30)	0.01 ± 0.1 0 (0, 0)

Values reported as mean ± standard deviation and median (5th percentile, 95th percentile).

Meal Detection Algorithm: Sensitivity Analysis

A 500-day simulated scenario was used to perform a sensitivity analysis. The amount of CHO consumed per meal by the ten adult subjects had a mean of 70 ± 29 grams and a median of 70 (25, 116) grams. The population performance metrics can be found in Table 5.2, which, when compared to the three-meal algorithm tunings in the previous section (Chapter 5.1.4), shows a decrease in sensitivity for both the high sensitivity and trade-off tunings with mean values of 92 ± 3% and 82 ± 4% and median values of 92 (87, 96)% and 83 (76, 87)%, respectively. The low FP tuning, however, showed an increase in sensitivity with a mean value of 54 ± 9% and median value of 52 (44, 71)%. The FP/day between scenarios are roughly the same. The FP/day of the high sensitivity scenario for the tuning and validation scenarios and the sensitivity all shared a mean of 1 ± 1 and a median of 1 (0, 3). The FP/day in the trade-off scenario also had a similar value for the sensitivity analysis with a mean 0.2 ± 0.5 and median 0 (0, 1) versus mean 0.2 ± 0.5 and 0 ± 0 and median 0 (0, 1) and 0 (0, 0) of the tuning and validation scenarios. The FP/day in the low FP scenario was only slightly higher with a mean value of 0.02 ± 0.2 and median 0 (0, 0) versus mean 0 ± 0 and 0.01 ± 0.1 and median 0 (0, 0) and 0 (0, 0) in the tuning and validation scenarios. Figure 5.3 illustrates the cumulative detection rates over change in time and Δ glucose from the onset of meals for the three meal algorithm tunings and further emphasizes that algorithms with higher sensitivities have a shorter detection time and lower Δ glucose at detection.

Table 5.2: Population performance metrics of meal detection algorithm in sensitivity analysis scenario. Total number of meals per patient was 1500.

Sensitivity (%)	Δ Glucose (mg/dL)	Detection Time (min)	TP	FP	FN	FP/day
Highest Sensitivity (window = 15 min; threshold = 0.000039)						
92 ± 3 92 (87, 96)	6 ± 13 5 (−8, 17)	31 ± 16 25 (10, 60)	1375 ± 38 1374 (1306, 1433)	719 ± 111 716 (561, 897)	126 ± 38 126 (67, 194)	1 ± 1 1 (0, 3)
Trade-Off (window = 45 min; threshold = 0.00019)						
82 ± 4 83 (76, 87)	19 ± 9 19 (6, 31)	38 ± 14 35 (25, 65)	1232 ± 56 1242 (1139, 1310)	100 ± 23 96 (72, 154)	268 ± 56 259 (190, 361)	0.2 ± 0.5 0 (0, 1)
Low False Positive (window = 60 min; threshold = 0.00082)						
54 ± 9 52 (44, 71)	42 ± 18 45 (10, 56)	43 ± 11 40 (30, 65)	813 ± 130 776 (663, 1060)	11 ± 9 10 (5, 34)	687 ± 130 724 (440, 837)	0.02 ± 0.2 0 (0, 0)

Values reported as mean ± standard deviation and median (5th percentile, 95th percentile).

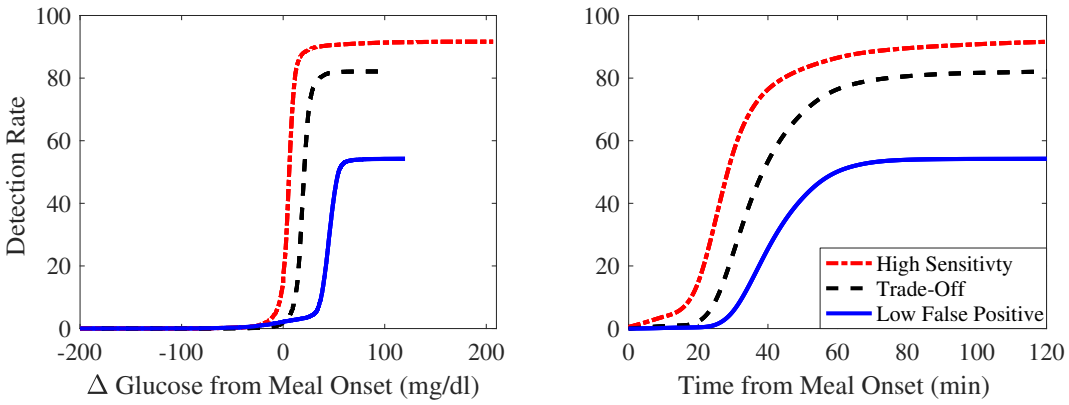

Figure 5.3: Cumulative detection rates over change in Δ glucose and time from the onset of meals for the meal algorithm tunings of high sensitivity, trade-off, and low false positive in the sensitivity analysis scenario.

An analysis of the effect of CHO quantity (Table 5.3) on detection performance was performed. CHO quantities of 20–40 grams have the longest detection time followed by 40–80 grams and then 80–120 grams. However, CHO quantities of 20–40 grams had the lowest Δ glucose at detection followed by 40–80 grams and then 80–120 grams. The meal detection sensitivity increased with increasing amounts of CHO. The sensitivity for the highest sensitivity tuning was mean 74 ± 6% and median 72 (67, 87)% for 20–40 grams of CHO, mean 93 ± 3% and median 94 (87, 96)% for 40–80 grams of CHO, and mean 99 ± 1% and median 99 (97, 100)% for 80–120 grams of CHO. The sensitivity for the trade-off tuning was mean 49 ± 9% and median 47 (39, 64)% for 20–40 grams of CHO, mean 84 ± 4% and median 86 (76, 89)% for 40–80 grams of CHO, and mean 96 ± 2% and median 97 (94, 98)% for 80–120 grams of CHO. The sensitivity for the lowest FP

Table 5.3: Analysis of the effect of carbohydrate quantity on detection time, Δ glucose, and sensitivity.

			Carbohydrates (grams)		
			20–40	**40–80**	**80–120**
High Sensitivity window = 15 min threshold = 0.000039	Detection Time (min)	Mean	39 ± 22	31 ± 16	25 ± 13
		Median	30 (10, 90)	30 (10, 60)	25 (0, 50)
	Δ Glucose (mg/dL)	Mean	5 ± 14	5 ± 10	7 ± 15
		Median	5 (−13, 23)	5 (−7, 16)	6 (−6, 15)
	Sensitivity (%)	Mean	74 ± 6	93 ± 3	99 ± 1
		Median	72 (67, 87)	94 (87,96)	99 (97, 100)
Trade-Off window = 45 min threshold = 0.00019	Detection Time (min)	Mean	46 ± 18	40 ± 16	32± 15
		Median	45 (25, 80)	35 (25, 65)	30 (0, 55)
	Δ Glucose (mg/dL)	Mean	18 ± 11	17 ± 9	20 ± 9
		Median	19 (0, 32)	18 (0, 28)	20 (8, 32)
	Sensitivity (%)	Mean	49 ± 9	84 ± 4	96 ± 2
		Median	47 (39, 64)	86 (76, 89)	97 (94, 98)
Low False Positive window = 60 min threshold = 0.00082	Detection Time (min)	Mean	45 ± 11	44 ± 8	41 ± 11
		Median	50 (14, 71)	45 (30, 65)	40 (30, 60)
	Δ Glucose (mg/dL)	Mean	29 ± 42	42 ± 18	42 ± 16
		Median	43 (−46, 57)	45 (12, 57)	44 (16, 56)
	Sensitivity (%)	Mean	8 ± 7	49 ± 12	83 ± 7
		Median	6 (2, 26)	45 (36, 71)	82 (73, 93)

Values reported as mean ± standard deviation and median (5th percentile, 95th percentile).

tuning was mean 8 ± 7% and median 6 (2, 26)% for 20–40 grams of CHO, mean 49 ± 12% and median 45 (36, 71)% for 40–80 grams of CHO, and mean 83 ± 7% and median 82 (73, 93)% for 80–120 grams of CHO.

The effect of Ra on meal detection performance was also analyzed (Table 5.4). Meals with faster Ra values have a shorter detection time but a greater Δ glucose, while meals with slower Ra values take longer to detect but result in a lower Δ glucose before detection. The meal detection sensitivity increased with faster Ra values. The sensitivity for the highest sensitivity tuning was mean 77 ± 9% and median 77 (62, 92)% for meals with slow Ra values, mean 87 ± 4% and median 88 (81, 95)% for meals with medium Ra values, and mean 95 ± 1% and median 95 (92, 97)% for meals with fast Ra values. The sensitivity for the trade-off tuning was mean 54 ± 10% and median 57 (38, 71)% for meals with slow Ra values, mean 73 ± 6% and median 73 (65, 81)% for meals with medium Ra values, and mean 89 ± 3% and median 89 (84, 92)% for meals with fast Ra values. The sensitivity for the lowest FP tuning was mean 10 ± 8% and median 6 (2, 29)% for meals with slow Ra values, mean 33 ± 12% and median 29 (18, 57)% for meals with medium Ra values, and mean 68 ± 7% and median 67 (59, 81)% for meals with fast Ra values.

Table 5.4: Analysis of the effect of rate of glucose appearance on detection time, Δ glucose, and sensitivity.

			Rate of Glucose Appearance		
			Slow	**Medium**	**Fast**
High Sensitivity window = 15 min threshold = 0.000039	Detection Time (min)	Mean	47 ± 22	38 ± 20	27 ± 11
		Median	45 (10, 90)	35 (10, 80)	25 (10, 45)
	Δ Glucose (mg/dL)	Mean	3 ± 15	4 ± 13	6 ± 13
		Median	4 (−22, 25)	4 (−14, 23)	6 (−5, 15)
	Sensitivity (%)	Mean	77 ± 9	87 ± 4	95 ± 1
		Median	77 (62, 92)	88 (81, 95)	95 (92, 97)
Trade-Off window = 45 min threshold = 0.00019	Detection Time (min)	Mean	57 ± 18	47 ± 16	34 ± 10
		Median	55 (35, 90)	45 (30, 80)	30 (25, 50)
	Δ Glucose (mg/dL)	Mean	16 ± 14	18 ± 12	20 ± 7
		Median	18 (−5, 36)	19 (1, 33)	19 (9, 30)
	Sensitivity (%)	Mean	54 ± 10	73 ± 6	89 ± 3
		Median	57 (38, 71)	73 (65, 81)	89 (84, 92)
Low False Positive window = 60 min threshold = 0.00082	Detection Time (min)	Mean	63 ± 14	52 ± 13	40 ± 9
		Median	65 (45, 80)	50 (35, 75)	40 (30, 55)
	Δ Glucose (mg/dL)	Mean	37 ± 44	43 ± 24	41 ± 15
		Median	48 (−39, 72)	47 (−2, 63)	44 (13, 55)
	Sensitivity (%)	Mean	10 ± 8	33 ± 12	68 ± 7
		Median	6 (2, 29)	29 (18, 57)	67 (59, 81)

Values reported as mean ± standard deviation and median (5th percentile, 95th percentile).

5.1.5 Discussion

In this study, three different tunings of the same meal detection algorithm were evaluated in order to determine meal detection performance. This first tuning obtains the highest sensitivity possible as seen in Tables 5.1 and 5.2 where sensitivities of mean 99 ± 2% and median 99 (95, 100)% for the tuning scenario, mean 98 ± 4% and median 98 (90, 100)% for the validation scenario, and mean 92 ± 3% and median 92 (87, 96)% for the sensitivity analysis scenario were achieved. The purpose of this high sensitivity tuning is to allow postprandial hyperglycemia mitigation action to be performed at the earliest possible instant. However, this tuning also contains a high FP value that increases risk of hypoglycemia due to insulin administration without meal ingestion.

The second tuning was a trade-off tuning that has both a high sensitivity with a low FP/day value. It obtained sensitivities of mean 93 ± 5% and median 93 (86, 100)% for the tuning scenario, mean 93 ± 6% and median 94 (83, 100)% for the validation scenario, and mean 82 ± 4% and median 83 (76, 87)% for the sensitivity analysis scenario (see Tables 5.1 and 5.2). The FP/day values were mean 0.2 ± 0.5 and median 0 (0, 1) for the tuning scenario, mean 0 ± 0 and median 0 (0, 0) for the validation scenario, and mean 0.2 ± 0.5 and median 0 (0, 1) for the sensitivity analysis scenario. This tuning serves as a detection that is more reliable with less FP/day but

has a longer detection time than that of the high sensitivity tuning, which entails a greater delay in insulin delivery and action.

The final tuning was a low FP tuning, originally the fixed FP value was evaluated during tuning but for the purposes of comparison between scenarios the FP/day values were used. The FP/day values were mean 0 ± 0 and median 0 (0, 0) for the tuning scenario, mean 0.01 ± 0.1 and median 0 (0, 0) for the validation scenario, and mean 0.02 ± 0.2 and median 0 (0, 0) for the sensitivity analysis scenario (see Tables 5.1 and 5.2). This tuning allows postprandial hyperglycemia mitigation with very little risk of hypoglycemia due to FP detections. However, it has the longest detection time of the three tunings and its obtained sensitivities are quite low: mean 47 ± 12% and median 50 (26, 64)% for the tuning scenario, mean 46 ± 16% and median 45 (29, 71)% for the validation scenario, and mean 54 ± 9% and median 52 (44, 71)% for the sensitivity analysis scenario.

Several other meal detection algorithms have been created for use during unannounced meals and their comparable metrics can be found in Table 5.5. Dassau et al. [4] studied 17 patients using clinical data during a breakfast of 56 grams with a range between 22 and 105 grams. However, with only meal detection time, it is difficult to compare the performance between meal detection algorithms. Lee et al. [6] studied an in silico population of 100 patients during 72 hours with an average meal size of 47.5 ± 25 grams. Their meal detection algorithm can be compared to the trade-off tuning of this study when the sensitivity and detection time are compared. Although the sensitivities in this study in the tuning and validation scenarios are higher and comparable for the sensitivity analysis scenario, without an FP/day value, it is not possible to determine which meal detection algorithm outperforms the other. Chen et al. [9] studied 10,000 patients over three days. However, with only the sensitivity value, it is difficult to compare algorithms. Weimer et al. [10] studied 61 patients using clinical data over a period of 17 days. Their algorithm has both a lower sensitivity of 86.9% and high FP/day of 2.01.

Table 5.5: Population performance metrics of meal detection algorithm in other studies.

Reference	Sensitivity (%)	Δ Glucose (mg/dL)	Detection Time (min)	TP	FP	FN	FP/day
Dassau et al. [4]	–	–	30	–	–	–	–
Lee et al. [6]	82	–	31	656	54	144	–
Chen et al. [9]	99.6	–	–	–	–	–	–
Weimer et al. [10]	86.9	–	–	–	–	–	2.01
Xie and Wang [11]	95	–	–	–	–	–	–
Turksoy et al. [12]	97 ± 6	16 ± 9	–	7 ± 2	0.1 ± 0.3	0.2 ± 0.4	–
Mahmoudi et al. [13]	99.5	46.3 ± 21.2	58.4 ± 18.7	–	–	–	–

Values reported as mean ± standard deviation.

Xie and Wang [11] studied 30 patients during two days with an average meal size of 61.7 ± 14.4 grams. However, with only a sensitivity value, it is difficult to compare algorithms. Turksoy et al. [12] studied nine in clinic patients over 32 hours with an average meal size of

44 ± 9.4 grams. This meal detection algorithm has both a high sensitivity of 97 ± 6% and low Δ glucose of 16 ± 9.4 mg/dL and, out of 63 meals and snacks, there was only one FP and two FN. Although their results outperform the results found in this study, the duration of this study was not long enough to truly reflect meal detection capabilities. Finally, Mahmoudi et al. [13] studied ten in silico patients over 50 days. They achieved a high sensitivity of 99.5% however, their detection time was very long at 58.4 ± 18.7 minutes. In addition, additional information about FP or FP/day is not given, making it difficult to compare algorithms.

A sensitivity analysis was done to see the effect of CHO quantity and meal composition on meal detection performance. Meal absorption related parameters of the T1D Simulator were varied in meals in such a way to suggest varying fat percentages, which ultimately affected Ra [172]. Although this is simulated data with a small cohort and meal variability limited to the meals included in the meal library, it gives insight into the effect of CHO quantity and meal composition on detection capabilities. The population performance metrics (Table 5.2) differ from those in the tuning and validation scenario because of the increased amount of meal variability as mentioned in Chapter 5.1.3. In addition, meals in the sensitivity analysis scenario tended towards higher CHO amounts due to the uniform distribution of meals between 20 and 120 grams. It can been seen that there is a decrease in the sensitivities of the highest sensitivity and trade-off tunings with values of mean 92 ± 3% and median 92 (87, 96)% and mean 82 ± 4% and median 83 (76, 87)%, respectively. There is a slight increase in the sensitivity for the low FP tuning to mean 54 ± 9% and median 52 (44, 71)%. Interestingly, the number of FP/day remain very similar between scenarios.

An analysis of the effect of CHO quantity (Table 5.3) on detection performance reveals that larger amounts of CHO have a shorter detection time but a greater Δ glucose, while smaller quantities of CHO take longer to detect but result in a lower glucose increase before detection due to lower amounts of CHO ingestion. The meal detection sensitivity decreased with decreasing amounts of CHO representing that small meals are generally more difficult to detect.

The effect of meal composition and ultimately Ra on meal detection performance was also analyzed (see Table 5.4). A similar trend was found when compared to CHO quantity where just like large meals, meals with faster Ra values take less time to be detected but result in a greater Δ glucose. The meal detection sensitivity increased with faster Ra values representing that meals that are slowly digested or have a higher quantity of fat are generally more difficult to detect. This is consistent with the results reported by Bell et al. [35], which state that, during high fat meals, glucose values have a reduced area under the curve in the first 2-3 hours due to a delayed gastric emptying rate.

This sensitivity analysis reveals that, fortunately, the meals of most interest, i.e., those that require both detection and postprandial hyperglycemia mitigation due to large disturbances in glucose, such as large and rapidly appearing meals, are able to be detected quickly with very little change in glucose at detection. However, meals with slow rates of glucose appearance such

as those high in fat may be more prone to late-onset postprandial hyperglycemia.

5.2 Postprandial Glucose Control

This section describes the three refined tunings for the detection of meals, the identification of fast absorption meals, CHO estimation, and the disturbance rejection actions of the PHRA.

5.2.1 Diabetes Simulation Scenario

Meal type discrimination, CHO estimation, and postprandial disturbance rejection actions were tested using two sets of nine 15-day scenarios, which include large, medium, and small CHO content meals and fast, medium, and slow absorption meals in all combinations using the T1D Simulator (see Chapter 3.2). One set was used for tuning and the other set was used for validation. Each scenario included breakfast at 7:00h, lunch at 14:00h, and dinner at 21:00h. Large, medium, and small meals were uniformly distributed between 80 and 120, 40 and 80, 15 and 40 grams of CHO, respectively. For each meal, a meal absorption profile was selected randomly from a meal library of 31 fast, 15 medium, or 3 slow absorption meals depending on the Ra of the scenario. Circadian insulin sensitivity variation (sinusoidal type with 24-hour period) was implemented with random amplitude according to a uniform distribution of ±30% and random phase. The standard deviation for meal time was ± 20 min. There were 450 meals in total for all ten subjects over the 15-day period.

5.2.2 Refined Meal Detection Tunings

The meal detection tunings found in Chapter 5.1 have been refined using the tuning set of the nine scenarios described above and have been tuned so that each detection is separated by ~5 minutes. To find these tunings, a detection bank was created using window sizes from 5–75 minutes with intervals of 5 minutes. Thresholds for windows sizes 5–25 minutes were tested from 0.00001 to 0.001 with intervals of 0.000005. Thresholds for window sizes 30–75 minutes were tested from 0.001 to 0.0035 with intervals of 0.00001. Outcomes for this detection bank were compared and three combinations of windows and thresholds were chosen based on performance and following the same criteria as Chapter 5.1. The refined tunings were then tested using the validation set of the nine scenarios.

The first detection is called Detection 1 (win = 5 minutes; TH = 0.000045) and is the fastest detection tuning with the highest sensitivity and FP, the second detection is called Detection 2 (win = 10 minutes; TH = 0.00012) and is slower than the previous detection with a lower sensitivity and FP, and the third detection is called Detection 3 (win = 20 minutes; TH = 0.000415) is the slowest detection of all three with the lowest sensitivity and FP. The performance metrics for these three detections can be found in Tables 5.6, 5.7, and 5.8.

Table 5.6: Population performance metrics of the Detection 1 tuning (win=5 minutes; TH=0.000045).

Scenario		Sensitivity (%)	Δ Glucose (mg/dl)	Detection Time (min)	FP/day
Large Fast	**Tuning**	98.9 ± 1.6 100 (95.6, 100)	5.0 ± 7.5 5.1 (-6.3, 16.6)	23.4 ± 3.9 25 (20, 30)	0.4 ± 0.2 0.3 (0.1, 0.7)
	Validation	99.8 ± 0.7 100 (97.8, 100)	5.4 ± 7.5 5.8 (-6.8, 16.5)	23.4 ± 5.1 25 (20, 30)	0.4 ± 0.2 0.4 (0.1, 0.6)
Large Medium	**Tuning**	76.2 ± 8.8 75.6 (62.2, 91.1)	9.1 ± 19.6 5.1 (-11.4, 48)	37.4 ± 17.7 30 (20, 80)	0.5 ± 0.2 0.4 (0.1, 0.7)
	Validation	81.3 ± 10.3 78.9 (62.2, 95.6)	8.2 ± 18.1 5.1 (-11.7, 43.2)	36.2 ± 18 30 (20, 81)	0.4 ± 0.2 0.4 (0.3, 0.7)
Large Small	**Tuning**	40.2 ± 12.5 41.1 (24.4, 57.8)	7.2 ± 17.4 4.8 (-17.6, 40.2)	46.6 ± 20.4 45.0 (10.0, 90.0)	0.7 ± 0.2 0.6 (0.5, 1.0)
	Validation	40.0 ± 12.8 44.4 (22.2, 57.8)	9.1 ± 16.5 7.4 (-12.8, 45.4)	47.9 ± 20.6 45.0 (5.0, 85.0)	0.8 ± 0.2 0.8 (0.5, 1.1)
Medium Fast	**Tuning**	89.1 ± 4.9 88.9 (80.0, 97.8)	8.0 ± 10.0 7.0 (-4.3, 20.4)	27.5 ± 10.4 25.0 (20.0, 35.0)	0.4 ± 0.2 0.4 (0.1, 0.7)
	Validation	88.2 ± 6.2 88.9 (77.8, 100.0)	6.6 ± 8.5 6.3 (-5.5, 19.1)	26.3 ± 6.5 25.0 (20.0, 35.0)	0.4 ± 0.1 0.4 (0.2, 0.7)
Medium Medium	**Tuning**	49.3 ± 10.8 45.6 (33.3, 66.7)	10.9 ± 16.5 7.4 (-7.6, 44.7)	40.7 ± 21.2 35.0 (20.0, 90.0)	0.6 ± 0.2 0.6 (0.2, 0.9)
	Validation	47.6 ± 12.2 46.7 (33.3, 68.9)	11.2 ± 18.0 7.3 (-7.2, 53.6)	41.4 ± 22.1 35.0 (25.0, 95.0)	0.5 ± 0.3 0.4 (0.1, 0.9)
Medium Small	**Tuning**	25.3 ± 11.7 23.3 (11.1, 46.7)	5.9 ± 15.5 5.1 (-16.3, 29.8)	51.8 ± 25.0 50.0 (10.0, 105.0)	0.7 ± 0.2 0.7 (0.5, 1.1)
	Validation	24.0 ± 5.6 24.4 (15.6, 33.3)	9.7 ± 16.8 7.5 (-12.2, 43.4)	47.6 ± 23.9 45.0 (9.5, 95.5)	0.6 ± 0.2 0.6 (0.3, 0.9)
Small Fast	**Tuning**	38.7 ± 11.5 35.6 (24.4, 55.6)	10.5 ± 13.4 8.9 (-3.3, 37.2)	35.2 ± 18.5 30.0 (20.0, 86.0)	0.6 ± 0.2 0.7 (0.3, 1.1)
	Validation	42.2 ± 10.6 42.2 (24.4, 57.8)	9.4 ± 10.1 8.8 (-6.1, 29.0)	33.4 ± 16.0 30.0 (20.0, 75.0)	0.6 ± 0.3 0.6 (0.1, 1.1)
Small Medium	**Tuning**	25.1 ± 11.5 25.6 (8.9, 42.2)	11.8 ± 14.6 10.3 (-6.4, 44.1)	51.1 ± 31.3 40.0 (6.5, 115.0)	0.5 ± 0.2 0.6 (0.1, 0.7)
	Validation	19.3 ± 6.7 16.7 (11.1, 33.3)	13.8 ± 18.4 10.5 (-7.7, 47.6)	54.2 ± 31.4 45.0 (14.3, 115.0)	0.6 ± 0.2 0.6 (0.3, 0.9)
Small Slow	**Tuning**	13.1 ± 4.0 13.3 (6.7, 20.0)	9.4 ± 12.0 8.4 (-8.0, 30.3)	55.9 ± 32.6 50.0 (5.0, 115.0)	0.6 ± 0.2 0.5 (0.3, 0.9)
	Validation	14.4 ± 4.8 15.6 (6.7, 20.0)	7.0 ± 12.1 6.1 (-12.5, 34.2)	57.5 ± 28.3 55.0 (13.8, 116.3)	0.7 ± 0.2 0.7 (0.4, 1.0)

Values reported as mean ± standard deviation and median (5th percentile, 95th percentile).

Table 5.7: Population performance metrics of the Detection 2 tuning (win=10 minutes; TH=0.00012).

Scenario		Sensitivity (%)	Δ Glucose (mg/dl)	Detection Time (min)	FP/day
Large Fast	**Tuning**	98.7 ± 1.9	9.7 ± 9.1	25.9 ± 5.1	0.2 ± 0.1
		100.0 (95.6, 100.0)	9.4 (-2.5, 21.0)	25.0 (20.0, 35.0)	0.1 (0.1, 0.4)
	Validation	99.3 ± 1.5	9.7 ± 7.6	25.5 ± 4.3	0.2 ± 0.1
		100.0 (95.6, 100.0)	9.8 (-3.3, 21.9)	25.0 (20.0, 30.0)	0.2 (0.1, 0.3)
Large Medium	**Tuning**	72.2 ± 10.0	12.4 ± 19.3	39.7 ± 17.2	0.3 ± 0.1
		70.0 (55.6, 86.7)	8.4 (-10.6, 51.9)	35.0 (25.0, 77.5)	0.2 (0.1, 0.5)
	Validation	76.7 ± 12.5	11.9 ± 18.2	38.1 ± 16.6	0.3 ± 0.1
		75.6 (51.1, 95.6)	8.7 (-8.4, 41.5)	35.0 (25.0, 75.0)	0.2 (0.1, 0.6)
Large Small	**Tuning**	33.6 ± 13.6	10.6 ± 17.0	48.0 ± 20.1	0.4 ± 0.2
		35.6 (13.3, 51.1)	9.4 (-13.0, 39.7)	45.0 (10.0, 85.0)	0.3 (0.1, 0.7)
	Validation	33.1 ± 10.9	12.2 ± 16.7	49.7 ± 19.0	0.4 ± 0.2
		34.4 (17.8, 48.9)	11.4 (-8.7, 44.6)	50.0 (10.0, 85.0)	0.5 (0.1, 0.7)
Medium Fast	**Tuning**	86.7 ± 5.6	11.6 ± 10.0	29.7 ± 9.7	0.2 ± 0.1
		86.7 (80.0, 95.6)	11.2 (-1.2, 23.1)	30.0 (25.0, 40.0)	0.2 (0.1, 0.5)
	Validation	87.6 ± 7.0	10.6 ± 8.9	28.7 ± 6.4	0.2 ± 0.1
		88.9 (73.3, 100.0)	10.1 (-2.6, 24.4)	25.0 (25.0, 40.0)	0.2 (0.1, 0.3)
Medium Medium	**Tuning**	40.4 ± 13.7	12.9 ± 15.6	40.4 ± 17.6	0.3 ± 0.2
		36.7 (24.4, 64.4)	11.2 (-6.4, 40.1)	35.0 (25.0, 82.0)	0.2 (0.1, 0.6)
	Validation	39.1 ± 12.0	14.3 ± 17.6	43.2 ± 20.3	0.2 ± 0.1
		36.7 (22.2, 62.2)	9.9 (-3.7, 52.6)	35.0 (25.0, 95.0)	0.2 (0.0, 0.5)
Medium Small	**Tuning**	16.2 ± 8.7	8.9 ± 14.9	51.9 ± 22.2	0.4 ± 0.2
		14.4 (4.4, 33.3)	8.2 (-14.2, 34.8)	50.0 (10.0, 93.5)	0.3 (0.1, 0.7)
	Validation	16.2 ± 6.3	13.5 ± 18.7	50.0 ± 22.9	0.4 ± 0.2
		18.9 (6.7, 24.4)	9.8 (-13.0, 42.4)	50.0 (10.0, 95.0)	0.4 (0.1, 0.7)
Small Fast	**Tuning**	33.6 ± 10.7	13.5 ± 13.6	36.5 ± 17.7	0.4 ± 0.2
		34.4 (17.8, 51.1)	10.7 (-1.1, 40.3)	30.0 (25.0, 79.5)	0.3 (0.1, 0.7)
	Validation	32.2 ± 12.9	12.2 ± 9.7	34.2 ± 14.3	0.3 ± 0.2
		35.6 (15.6, 51.1)	11.9 (-1.7, 25.5)	30.0 (25.0, 60.0)	0.3 (0.1, 0.7)
Small Medium	**Tuning**	16.0 ± 8.2	15.1 ± 16.8	51.4 ± 27.7	0.2 ± 0.2
		16.7 (4.4, 31.1)	13.3 (-4.5, 45.0)	42.5 (20.5, 110.0)	0.3 (0.0, 0.5)
	Validation	12.0 ± 5.2	20.9 ± 20.6	53.2 ± 33.3	0.3 ± 0.2
		12.2 (6.7, 20.0)	13.9 (-4.5, 65.9)	40.0 (6.0, 119.0)	0.3 (0.1, 0.7)
Small Slow	**Tuning**	6.9 ± 2.7	16.6 ± 14.4	62.1 ± 33.7	0.3 ± 0.2
		6.7 (2.2, 11.1)	13.4 (-5.8, 41.8)	50.0 (10.0, 114.5)	0.3 (0.1, 0.7)
	Validation	8.7 ± 4.0	10.5 ± 13.3	60.4 ± 29.8	0.3 ± 0.2
		8.9 (2.2, 15.6)	7.0 (-9.2, 35.1)	60.0 (12.3, 117.7)	0.3 (0.0, 0.7)

Values reported as mean ± standard deviation and median (5th percentile, 95th percentile).

Table 5.8: Population performance metrics of the Detection 3 tuning (win=20 minutes; TH=0.000415).

Scenario		Sensitivity (%)	Δ Glucose (mg/dl)	Detection Time (min)	FP/day
Large Fast	**Tuning**	98.0 ± 2.4 98.9 (93.3, 100.0)	20.6 ± 8.3 20.3 (7.9, 33.3)	30.1 ± 4.7 30.0 (25.0, 40.0)	0.0 ± 0.0 0.0 (0.0, 0.1)
	Validation	98.2 ± 2.9 100.0 (93.3, 100.0)	20.7 ± 8.4 20.5 (6.3, 34.2)	29.9 ± 5.9 30.0 (25.0, 35.0)	0.0 ± 0.1 0.0 (0.0, 0.1)
Large Medium	**Tuning**	51.8 ± 15.0 50.0 (31.1, 73.3)	19.8 ± 17.0 17.0 (-2.1, 48.5)	41.4 ± 11.6 40.0 (30.0, 60.0)	0.1 ± 0.1 0.1 (0.0, 0.1)
	Validation	58.9 ± 14.3 56.7 (35.6, 82.2)	22.0 ± 17.1 18.7 (1.7, 52.8)	41.9 ± 13.1 40.0 (30.0, 66.3)	0.1 ± 0.1 0.0 (0.0, 0.2)
Large Small	**Tuning**	15.8 ± 10.2 13.3 (4.4, 35.6)	18.2 ± 16.6 17.4 (-9.0, 49.1)	52.3 ± 16.0 50.0 (16.0, 74.8)	0.1 ± 0.1 0.0 (0.0, 0.2)
	Validation	12.2 ± 8.5 12.2 (2.2, 26.7)	21.2 ± 16.7 19.5 (-0.6, 44.4)	54.0 ± 15.4 55.0 (21.3, 75.0)	0.1 ± 0.1 0.1 (0.0, 0.3)
Medium Fast	**Tuning**	75.1 ± 10.5 77.8 (57.8, 91.1)	21.7 ± 9.9 21.1 (9.2, 34.0)	33.7 ± 6.8 35.0 (25.0, 40.0)	0.0 ± 0.1 0.0 (0.0, 0.1)
	Validation	76.9 ± 9.9 75.6 (64.4, 95.6)	21.0 ± 8.7 20.9 (7.6, 34.1)	33.4 ± 5.4 32.5 (25.0, 41.0)	0.0 ± 0.1 0.0 (0.0, 0.1)
Medium Medium	**Tuning**	22.4 ± 10.1 20.0 (8.9, 35.6)	23.8 ± 13.4 23.0 (4.6, 49.5)	43.6 ± 12.2 40.0 (30.0, 70.0)	0.1 ± 0.1 0.1 (0.0, 0.2)
	Validation	20.7 ± 10.2 18.9 (8.9, 44.4)	22.8 ± 14.9 20.4 (5.0, 49.2)	43.3 ± 14.1 40.0 (30.0, 69.2)	0.0 ± 0.0 0.0 (0.0, 0.1)
Medium Small	**Tuning**	4.4 ± 5.0 2.2 (0.0, 15.6)	15.7 ± 13.8 16.5 (-12.8, 36.3)	53.0 ± 20.8 55.0 (12.5, 87.5)	0.1 ± 0.1 0.1 (0.0, 0.2)
	Validation	4.4 ± 3.5 4.4 (0.0, 11.1)	26.9 ± 21.7 24.2 (-14.5, 68.8)	55.8 ± 21.1 55.0 (15.0, 97.5)	0.1 ± 0.0 0.1 (0.0, 0.1)
Small Fast	**Tuning**	14.4 ± 7.4 12.2 (6.7, 28.9)	20.9 ± 9.9 19.3 (8.4, 36.1)	37.3 ± 9.2 35.0 (28.8, 52.5)	0.1 ± 0.1 0.1 (0.0, 0.3)
	Validation	16.4 ± 11.0 14.4 (4.4, 37.8)	21.1 ± 9.0 19.3 (6.9, 34.3)	36.1 ± 7.5 35.0 (30.0, 45.0)	0.0 ± 0.0 0.0 (0.0, 0.1)
Small Medium	**Tuning**	3.8 ± 3.6 3.3 (0.0, 11.1)	28.7 ± 16.8 26.7 (11.6, 69.3)	44.7 ± 19.3 40.0 (30.0, 92.2)	0.0 ± 0.0 0.0 (0.0, 0.1)
	Validation	2.0 ± 3.4 1.1 (0.0, 11.1)	27.5 ± 20.3 21.7 (1.1, 57.3)	64.4 ± 34.1 45.0 (25.0, 110.0)	0.1 ± 0.1 0.1 (0.0, 0.2)
Small Slow	**Tuning**	1.3 ± 1.6 1.1 (0.0, 4.4)	26.7 ± 18.6 21.8 (8.6, 50.5)	63.3 ± 48.9 72.5 (5.0, 110.0)	0.1 ± 0.1 0.1 (0.0, 0.3)
	Validation	1.6 ± 1.5 2.2 (0.0, 4.4)	21.1 ± 21.8 16.1 (0.3, 62.7)	71.4 ± 23.8 75.0 (40.0, 105.0)	0.1 ± 0.1 0.1 (0.0, 0.2)

Values reported as mean ± standard deviation and median (5th percentile, 95th percentile).

5.2.3 Meal Type Discrimination

Two additional tunings were identified from the detection bank mentioned in the previously in Chapter 5.2.2. All detections with the difference between detection times equal to zero were compared and their ability to detect rapidly appearing meals was measured. These tunings are called Rapid 1 (win=5 minutes; TH=0.00009) and Rapid 2 (win=5 minutes; TH=0.000125). It was found that when these two detection tunings detect a meal at the same time, the meal detected is more likely to be a meal that rapidly appears in the BG (see Table 5.9).

$$\text{Rapid Meal} = \begin{cases} \text{true} & \text{if Rapid 1} = \text{true} \wedge \text{ Rapid 2} = \text{true}, \\ \text{false} & \text{otherwise.} \end{cases} \tag{5.4}$$

Table 5.9: Identification of fast absorption meals.

		Carbohydrates (grams)			
		15-40	40-80	80-120	15-120
		Tuning			
Sensitivity (%)	Mean	6 ± 4.5	44.9 ± 16	90.4 ± 7.6	47.1 ± 36.5
	Median	4.4 (0, 15.6)	44.4 (17.8, 68.9)	92.2 (77.8, 100)	44.4 (2.2, 100)
Δ Glucose (mg/dl)	Mean	20.9 ± 0	14.4 ± 9.6	13.4 ± 7	25.7 ± 3.1
	Median	20.9 (20.9, 20.9)	12.9 (0.3, 33.5)	11.8 (4.3, 28.7)	25 (20, 30)
Detection Time (min)	Mean	25 ± 0	27 ± 2.9	25 ± 3.1	13.9 ± 7.9
	Median	25 (25, 25)	25 (25, 31.7)	25 (20, 30)	12.2 (3.3, 28.9)
		Validation			
Sensitivity (%)	Mean	6.7 ± 6.1	52.7 ± 14.1	92.2 ± 6	50.5 ± 36.7
	Median	4.4 (0, 17.8)	52.2 (35.6, 80)	90 (84.4, 100)	52.2 (2.2, 100)
Δ Glucose (mg/dl)	Mean	44.2 ± 55.1	14.4 ± 8.4	13.5 ± 7	25.7 ± 6.7
	Median	44.2 (5.2, 83.1)	13.4 (-0.3, 30.7)	13 (3.2, 24.9)	25 (20, 35)
Detection Time (min)	Mean	50 ± 28.3	26.7 ± 4.2	23.9 ± 3.5	14.8 ± 11.2
	Median	50 (30, 70)	25 (20, 35.7)	25 (20, 30)	13.2 (2.9, 30.3)

Values reported as mean ± standard deviation and median (5th percentile, 95th percentile).

This discrimination technique is able to detect 47 ± 37% (44 (2, 100)%) in the tuning set and 51 ± 37% (52 (2, 100%)) in the validation set of all fast absorption meals, with the ability to detect 90 ± 8% (median: 92 (78, 100)%) in the tuning set and 92 ± 6% (median: 90 (84, 100)%) in the validation set of fast absorption meals with >80 grams of CHO, 45 ± 16% (44 (18, 69)%) in the tuning set and 53 ± 14% (52 (36, 82%)) in the validation set of fast absorption meals with between 40–80 grams of CHO, and 6 ±5% (4 (0, 16)%) in the tuning set and 7 ± 6% (4 (0, 18%)) in the validation set of fast absorption meals with <40 grams of CHO.

For medium absorption meals, the technique incorrectly identifies 25 ± 11% (23 (9, 47)%) and 31 ± 11% (29 (18, 53)%) of meals with >80 grams of CHO, 6 ± 6% (4 (0, 20)%) and 6 ± 6% (4 (0, 18)%) of meals with 40–80 grams of CHO, and 2 ± 3% (1 (0, 9)%) and 1 ± 2% (0 (0, 7)%) of meals with <40 grams, for the tuning and validation sets, respectively. For slow absorption meals, 4 ± 5% (2 (0, 11)%) and 4 ± 4% (3 (0, 9)%) of meals with >80 grams of CHO, 1 ± 2% (0 (0, 7)%) and 2 ± 2% (1 (0, 4)%) of meals with 40–80 grams of CHO, and 1 ± 1% (0 (0, 2)%) and 1 ± 2% (0 (0, 4)%) of meals with <40 grams are incorrectly identified for the tuning and validation sets, respectively. Although some medium absorption meals with >80 grams of CHO are detected, these meals are likely to cause a profound increase in BG. This discrimination will be utilized in the next sections to aid in CHO estimation and during postprandial glucose control.

5.2.4 Carbohydrate Estimation

After detection, the CHO of each meal is estimated using the area under the curve of the disturbance parameter, D multiplied by a gain, k_{CHO_i} as follows:

$$u_{meal} = \int_{t-1}^{t} D(\tau)d\tau \cdot k_{CHO_i} \tag{5.5}$$

where

$$k_{CHO_i} = \begin{cases} 25.4 & \text{if Rapid Meal = true } \wedge \text{ Bolus 1 = true,} \\ 16.6 & \text{if Rapid Meal = false } \wedge \text{ Bolus 1 = true,} \\ 22.3 & \text{if Rapid Meal = true } \wedge \text{ Bolus 2 = true,} \\ 15.9 & \text{if Rapid Meal = false } \wedge \text{ Bolus 2 = true.} \end{cases} \tag{5.6}$$

The estimation of error of the estimated CHO quantities in the tuning and validation sets of scenarios (Chapter 5.2.1) can be found in Table 5.10 and Figures 5.4, 5.5, 5.6, and 5.7 contain histograms of the CHO estimation for all meals estimated and also separated by absorption rate and CHO quantity for the tuning and validation sets of the Detection 2 and Detection 3 tunings, respectively.

Here we can see that there is a tendency towards underestimation in the CHO estimation methodology presented. The is no difference between Detection 2 and Detection 3, nor between the tuning and validation sets in terms of accuracy of CHO estimation. However, Figures 5.4 and 5.5 show that the CHO estimation in the Detection 3 tuning tends more towards zero than that of the Detection 2 tuning and the same is true for Figures 5.6 and 5.7. Additionally, the spread of error seen (Table 5.10 and Figures 5.4–5.7) is quite large indicating an overall poor precision. Therefore, the application of CHO estimation for the use in postprandial hyperglycemia mitigation may be limited.

Table 5.10: The root mean squared error of carbohydrate estimation and detected meals.

Scenario			Detection 2		Detection 3	
		CHO (grams)	Estimated CHO (grams)	Estimated Error (%)	Estimated CHO (grams)	Estimated Error (%)
				Tuning		
Large Fast	Mean	98 ± 12	71 ± 51	-27 ± 52	71 ± 52	-27 ± 53
	Median	98 (82, 117)	54 (16, 176)	-44 (-84, 79)	54 (15, 178)	-45 (-84, 79)
Large Medium	Mean	99 ± 12	77 ± 62	-21 ± 65	75 ± 67	-24 ± 70
	Median	100 (81, 117)	58 (18, 189)	-40 (-83, 100)	53 (16, 196)	-46 (-84, 102)
Large Slow	Mean	103 ± 13	92 ± 67	-10 ± 66	92 ± 65	-10 ± 68
	Median	106 (82, 119)	65 (26, 239)	-35 (-76, 121)	65 (28, 230)	-35 (-75, 133)
Medium Fast	Mean	61 ± 12	42 ± 28	-30 ± 47	39 ± 28	-36 ± 43
	Median	61 (41, 78)	36 (9, 91)	-40 (-86, 60)	34 (6, 86)	-43 (-89, 49)
Medium Medium	Mean	61 ± 11	47 ± 41	-20 ± 71	42 ± 37	-32 ± 63
	Median	61 (43, 77)	37 (5, 110)	-42 (-93, 115)	33 (3, 115)	-46 (-94, 81)
Medium Slow	Mean	63 ± 12	55 ± 32	-11 ± 54	56 ± 35	-2 ± 68
	Median	65 (43, 79)	48 (16, 115)	-23 (-74, 102)	41 (17, 119)	-31 (-68, 149)
Small Fast	Mean	31 ± 6	28 ± 23	-5 ± 78	24 ± 29	-27 ± 85
	Median	31 (18, 38)	25 (1, 64)	-15 (-96, 130)	22 (-4, 64)	-34 (-112, 71)
Small Medium	Mean	31 ± 6	31 ± 21	6 ± 72	36 ± 30	12 ± 90
	Median	31 (19, 39)	28 (6, 61)	-11 (-84, 140)	28 (3, 108)	-25 (-90, 191)
Small Slow	Mean	29 ± 7	40 ± 25	48 ± 100	35 ± 35	18 ± 102
	Median	32 (16, 37)	37 (3, 86)	52 (-89, 184)	27 (-15, 82)	23 (-146, 136)
				Validation		
Large Fast	Mean	100 ± 11	69 ± 50	-31 ± 49	69 ± 51	-31 ± 50
	Median	103 (82, 118)	51 (18, 171)	-46 (-80, 75)	51 (18, 174)	-46 (-81, 77)
Large Medium	Mean	105 ± 9	81 ± 60	-22 ± 58	80 ± 61	-24 ± 59
	Median	105 (90, 119)	60 (15, 209)	-43 (-86, 104)	60 (13, 209)	-44 (-88, 104)
Large Slow	Mean	102 ± 11	92 ± 61	-8 ± 63	90 ± 66	-10 ± 71
	Median	103 (84, 119)	74 (21, 215)	-29 (-80, 115)	67 (19, 230)	-37 (-82, 166)
Medium Fast	Mean	61 ± 11	46 ± 33	-24 ± 52	46 ± 35	-26 ± 54
	Median	62 (44, 76)	39 (10, 102)	-35 (-84, 74)	37 (10, 112)	-38 (-86, 73)
Medium Medium	Mean	63 ± 11	49 ± 40	-21 ± 67	44 ± 45	-32 ± 72
	Median	64 (44, 80)	38 (7, 135)	-38 (-89, 111)	28 (4, 137)	-50 (-94, 122)
Medium Slow	Mean	63 ± 13	53 ± 43	-17 ± 60	68 ± 60	0 ± 79
	Median	61 (44, 79)	36 (9, 154)	-38 (-88, 123)	43 (12, 187)	-39 (-82, 150)
Small Fast	Mean	31 ± 6	27 ± 21	-7 ± 77	27 ± 25	-15 ± 82
	Median	33 (19, 38)	24 (4, 60)	-22 (-83, 172)	22 (1, 81)	-28 (-98, 148)
Small Medium	Mean	31 ± 7	41 ± 28	36 ± 94	49 ± 33	73 ± 139
	Median	33 (20, 40)	33 (10, 102)	1 (-64, 209)	56 (-6, 101)	52 (-126, 322)
Small Slow	Mean	27 ± 8	32 ± 25	34 ± 128	45 ± 42	78 ± 185
	Median	28 (15, 39)	31 (-7, 67)	0 (-121, 348)	44 (-13, 122)	68 (-147, 444)

Values reported as mean ± standard deviation and median (5th percentile, 95th percentile).

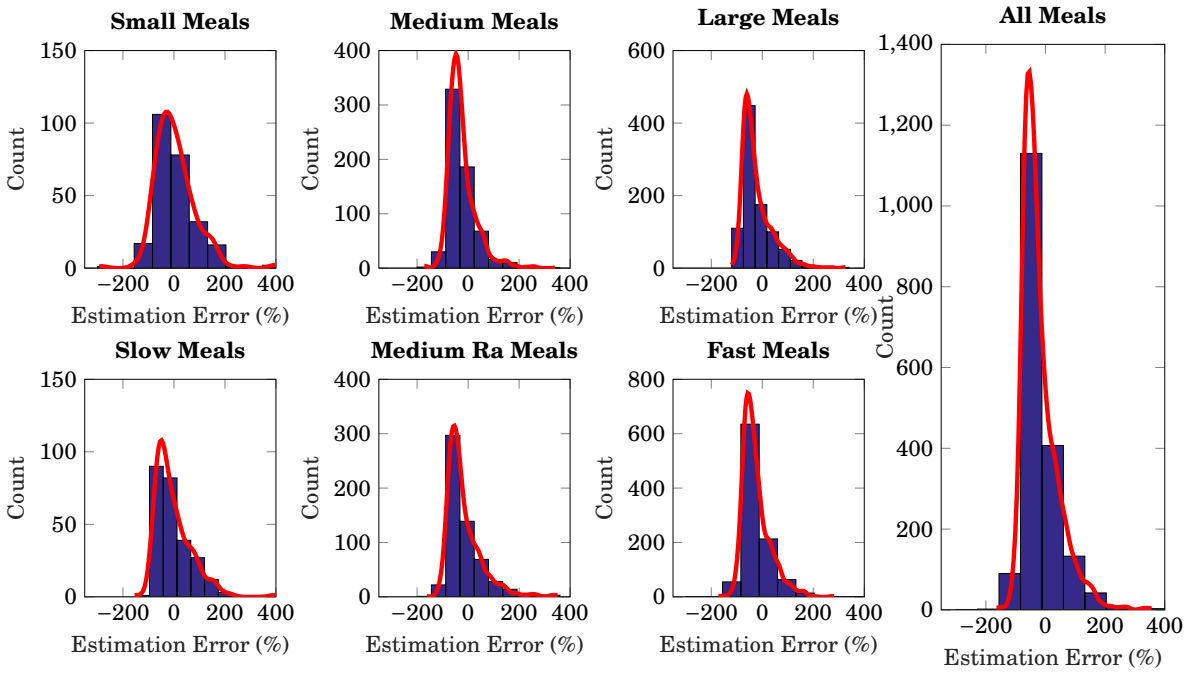

Figure 5.4: Histograms of CHO estimation of the tuning set during the Detection 2 meal detection tuning for all meals, meals of large, medium, and small sizes and fast, medium, and slow absorption meals.

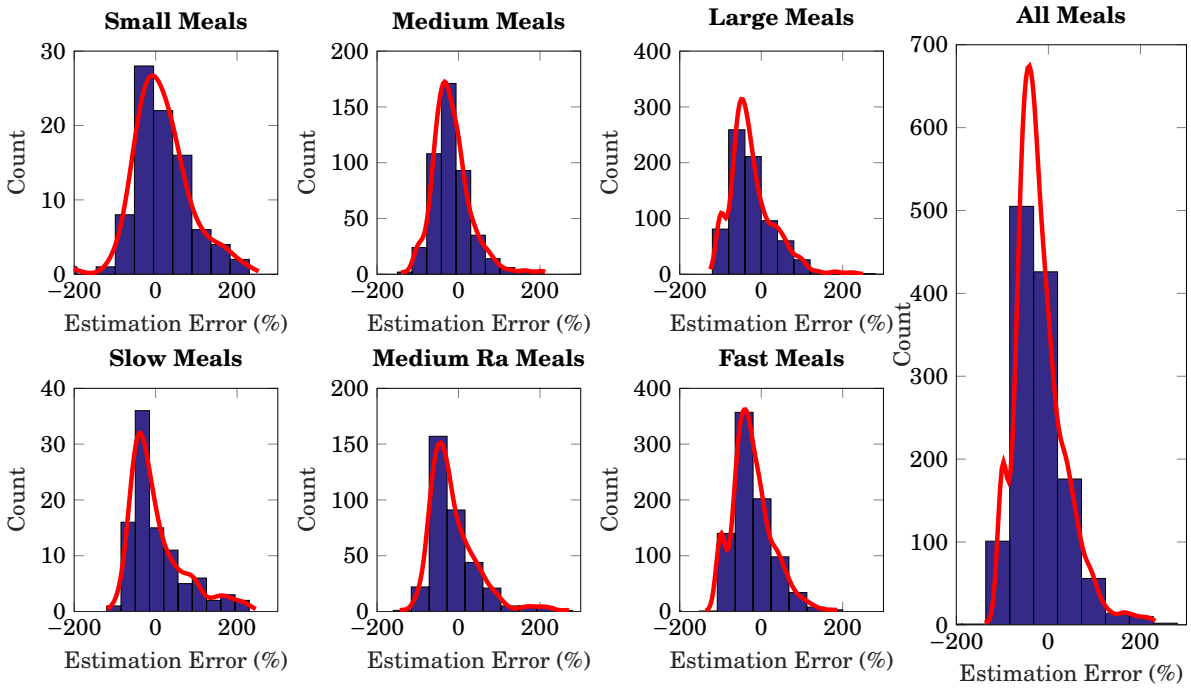

Figure 5.5: Histograms of CHO estimation of the validation set during the Detection 2 meal detection tuning for all meals, meals of large, medium, and small sizes and fast, medium, and slow absorption meals.

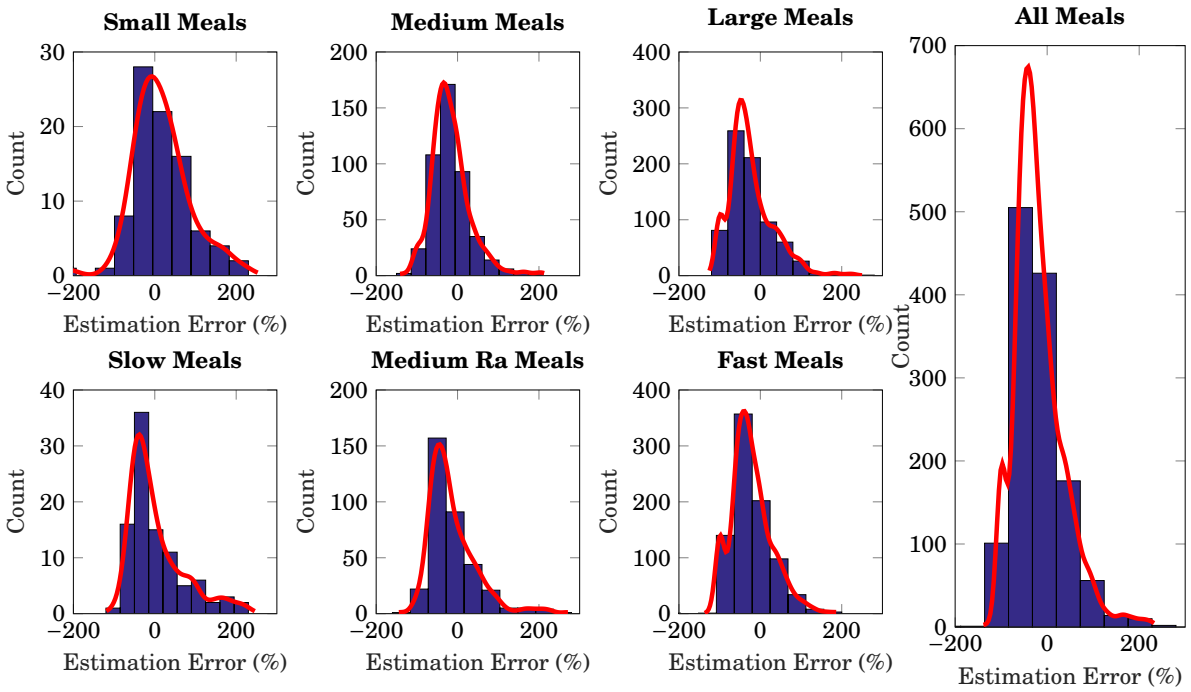

Figure 5.6: Histograms of CHO estimation of the tuning set during the Detection 3 meal detection tuning for all meals, meals of large, medium, and small sizes and fast, medium, and slow absorption meals.

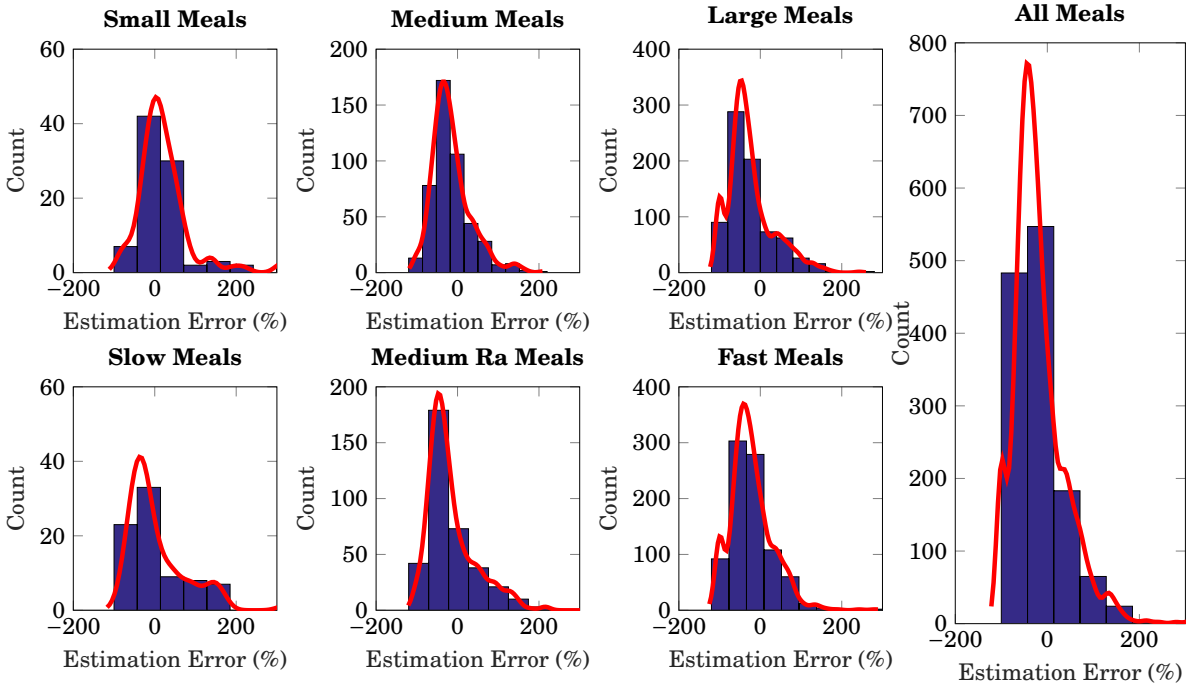

Figure 5.7: Histograms of CHO estimation of the validation set during the Detection 3 meal detection tuning for all meals, meals of large, medium, and small sizes and fast, medium, and slow absorption meals.

5.2.5 The Postprandial Hyperglycemia Reduction Algorithm

The closed-loop controller previously described in Chapter 3 and Appendix B has been modified to include a meal rejection loop as seen in Figure 5.8. The top inner loop is the meal rejection loop that comprises of the PHRA that uses an UKF to estimate the disturbance parameter, D, which is used to detect meals and apply postprandial hyperglycemia mitigation actions.

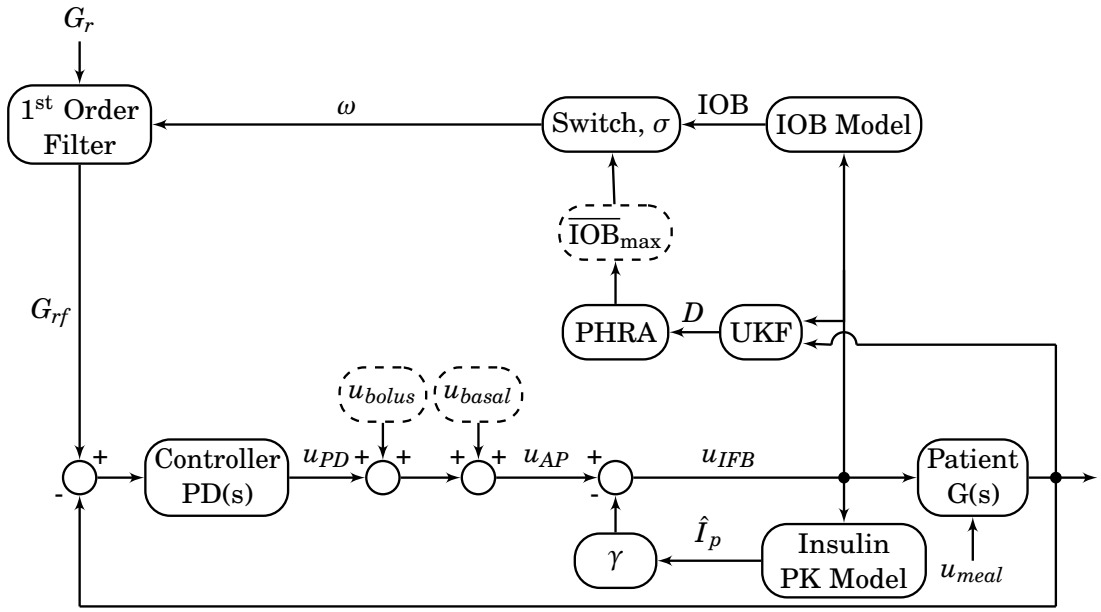

Figure 5.8: Closed-loop controller composed of an inner control loop that contains a PD controller with IFB, a top outer loop that acts as a safety supervisory loop and uses SMRC, and a top inner loop that uses an UKF to estimate the disturbance parameter, D that is then introduced into a PHRA, which when activated applies disturbance rejection actions to reduce postprandial hyperglycemia by modifying $\overline{\text{IOB}}_{\text{max}}$.

Due to the increased risk of hypoglycemia due to late boluses and the lack of precision of the CHO estimation described previously, the PHRA will not utilize the meal type discrimination or the CHO estimation methodologies in the following sections.

The three meal detection tunings, Detection 1, Detection 2, and Detection 3 detect a meal and are triggered in succession. All three meal detections allow changes to the $\overline{\text{IOB}}_{max}$, which increases insulin delivery to the patient as follows:

$$\overline{IOB}_{max}(t) = \begin{cases} \overline{IOB}_{max_n}(t) \cdot k_{IOBadapt} & \text{if } \forall \dot{G}(t-2,...t) > 0 \wedge \overline{IOB}(t-1) >= \frac{\overline{IOB}_{max}(t-1)}{2}, \\ \overline{IOB}_{max}(t-1) & \vee \forall \dot{G}(t-2,...t) > 0, \\ \overline{IOB}_{max_n}(t) & \text{otherwise.} \end{cases} \tag{5.7}$$

where $\overline{\text{IOB}}_{max_n}(t)$, described in Appendix B, is calculated as follows:

$$\overline{IOB}_{max_n}(t) = k_{IOB} \frac{2 \cdot u_{basal}(t)}{60 \cdot k_{DIA}}, \tag{5.8}$$

$\dot{G}$ is the derivative of the measured glucose, and $k_{IOBadapt}$ is a gain on $\overline{\text{IOB}}_{max}(t)$ equal to 1.011.

5.2.6 Performance Metrics

Glucose values are measured as population median glucose (median of the median value for each subject), percentage of time between 70–180 mg/dl, >180 mg/dl, <70 mg/dl, and <54 mg/dl. The number of hypoglycemic events are categorized as either a level 1 or level 2 event defined as BG <70 mg/dl and ≥54 mg/dl and BG <54 mg/dl, respectively [65]. A hypoglycemic event requires a minimum duration of 15 min below/within threshold, with a separation of at least 30 minutes [173]. All values are reported as median (25th percentile, 75th percentile). The Wilcoxon signed-rank test was used to obtain p values where a p value of <0.05 is considered significant. The percentage of time between 70–180 mg/dl, >180 mg/dl, and <70 mg/dl are used as measures of performance, where higher values are desirable for the percentage of time between 70–180 mg/dl and lower values are desirable for the percentage of time >180 mg/dl and <70 mg/dl.

5.2.7 Typical Day Scenario

A challenging 15-day scenario was built that included: three meals per day with varying carbohydrate content and meal time following a normal distribution with mean 30 grams at 8:30h (breakfast), 60 grams at 13:00h (lunch), and 50 grams at 19:00h (dinner). Coefficient of variance for the meal size was ±20%, and the standard deviation for meal time was ±10 min. For each meal, a meal absorption profile was selected randomly from a meal library of 31 fast, 15 medium, or 3 slow absorption meals. There were 450 meals in total for all ten subjects over the 15-day period. Circadian insulin sensitivity variation (sinusoidal type with 24-hour period) was implemented with random amplitude according to a uniform distribution of ±30% and random phase.

5.2.8 Results

Three insulin-only CLC cases of missed meal boluses, announced meals, and unannounced meals were tested using the scenarios previously described. The announced meals controller has been successfully tested in a clinical trial [161] and further information about the controller can be found in Appendix B. The PHRA was tuned using the nine tuning scenarios, validated with the nine validation scenarios (Chapter 5.1.3), and then tested in the context of a real-life typical day (Chapter 5.2.7). The Tables 5.11–5.19 contain the overall outcomes for the tuning and validation scenarios and allow us to compare and contrast the three strategies during meals of varying sizes and absorption rates.

Table 5.11: Overall population outcomes of a 15-day simulation with large (80–120 grams) fast absorption meals for three strategies in closed-loop control: missed meal boluses, announced meals, and unannounced meals with a PHRA. There were 450 meals in total.

	Missed Meal Boluses	Announced	PHRA	p*	p†
		Tuning			
Population Median Glucose (mg/dl)	206.2 (177.3, 272.5)	129.8 (127.7, 135.1)	160.7 (147.0, 188.8)	0.002	0.002
Insulin/day	37.3 (30.2, 42.6)	50.0 (47.1, 59.9)	41.2 (37.4, 44.6)	0.002	0.002
Percentage of time spent in... (mg/dl)					
70-180	40.1 (18.4, 50.9)	87.3 (85.0, 89.5)	55.4 (47.6, 60.1)	0.002	0.002
>180	59.9 (49.1, 81.6)	12.5 (10.3, 15.0)	44.6 (39.9, 52.4)	0.002	0.002
>250	32.7 (24.1, 58.0)	0.3 (0.0, 0.5)	21.4 (17.6, 34.8)	0.002	0.002
<70	0.0 (0.0, 0.0)	0.4 (0.0, 0.5)	0.0 (0.0, 0.0)	1	0.016
Hypoglycemic Events					
Level 1	0	13	0	1	0.063
Level 2	0	4	0	1	0.125
		Validation			
Population Median Glucose (mg/dl)	205.3 (179.2, 260.4)	129.6 (127.8, 135.5)	163.3 (147.6, 174.3)	0.002	0.002
Insulin/day	37.4 (30.4, 42.3)	50.6 (46.6, 60.9)	41.5 (36.5, 44.3)	0.002	0.002
Percentage of time spent in... (mg/dl)					
70-180	38.6 (19.0, 50.2)	88.0 (80.5, 91.0)	55.0 (50.9, 60.9)	0.002	0.002
>180	61.4 (49.8, 80.7)	11.8 (9.0, 18.7)	45.0 (39.1, 48.5)	0.002	0.002
>250	28.4 (23.0, 54.4)	0.2 (0.0, 0.3)	21.4 (15.2, 31.8)	0.002	0.002
<70	0.0 (0.0, 0.0)	0.6 (0.0, 0.8)	0.0 (0.0, 0.0)	1	0.031
Hypoglycemic Events					
Level 1	0	8	1	1	0.25
Level 2	1	10	1	1	0.031

Values reported as median (25th percentile, 75th percentile). *p value between missed meal boluses and PHRA scenarios. †p value between announced and PHRA.

Large sized meals (Tables 5.11–5.13) were the most difficult to control during missed meal boluses, the announced meals strategy, and the PHRA strategy. Missed meal boluses experienced the lowest percentage of time between 70–180 mg/dl with 40 (18, 51)% and 39 (19, 50)%, 33 (6, 46)% and 30 (3, 40)%, and 33 (6, 46)% and 30 (3, 40)% for fast, medium, and slow absorption meals, respectively. The announced meals strategy had the highest percentage of time between 70–180 mg/dl, however, it also experienced the most amount of time <70, which resulted in many hypoglycemic events for the tuning and validation scenarios with 13 and 8, 23 and 23, and 52

Table 5.12: Overall population outcomes of a 15-day simulation with large (80–120 grams) medium absorption meals for three strategies in closed-loop control: missed meal boluses, announced meals, and unannounced meals with a PHRA. There were 450 meals in total.

	Missed Meal Boluses	Announced	PHRA	p*	p†
		Tuning			
Population Median Glucose (mg/dl)	213.4 (188.5, 285.5)	135.0 (130.2, 142.4)	172.3 (153.9, 191.9)	0.002	0.002
Insulin/day	37.2 (29.9, 41.0)	51.0 (47.7, 61.1)	41.4 (37.4, 44.9)	0.002	0.002
Percentage of time spent in... (mg/dl)					
70-180	32.7 (6.1, 45.8)	92.3 (82.8, 94.7)	52.7 (46.1, 62.0)	0.002	0.002
>180	67.3 (54.2, 93.9)	7.7 (4.4, 15.9)	47.3 (38.0, 53.9)	0.002	0.002
>250	24.6 (16.4, 67.5)	0.0 (0.0, 0.2)	13.9 (9.7, 30.7)	0.002	0.002
<70	0.0 (0.0, 0.0)	0.5 (0.2, 1.7)	0.0 (0.0, 0.0)	1	0.008
Hypoglycemic Events					
Level 1	0	23	0	1	0.016
Level 2	0	6	0	1	0.125
		Validation			
Population Median Glucose (mg/dl)	220.2 (203.4, 293.7)	138.6 (133.7, 143.8)	176.5 (164.4, 203.1)	0.002	0.002
Insulin/day	37.5 (29.8, 42.2)	52.5 (49.2, 62.3)	41.9 (37.1, 46.3)	0.002	0.002
Percentage of time spent in... (mg/dl)					
70-180	30.3 (3.4, 39.7)	88.9 (83.6, 93.4)	51.0 (42.9, 55.9)	0.002	0.002
>180	69.7 (60.3, 96.6)	11.1 (5.1, 16.4)	49.0 (44.1, 57.1)	0.002	0.002
>250	30.8 (26.6, 71.5)	0.0 (0.0, 0.0)	18.5 (12.2, 37.0)	0.002	0.002
<70	0.0 (0.0, 0.0)	0.4 (0.0, 1.4)	0.0 (0.0, 0.0)	1	0.016
Hypoglycemic Events					
Level 1	0	23	0	1	0.016
Level 2	0	9	0	1	0.125

Values reported as median (25th percentile, 75th percentile). *p value between missed meal boluses and PHRA scenarios. †p value between announced and PHRA.

and 55 level 1 events and 4 and 10, 6 and 9, and 125 and 116 level 2 events for fast, medium, and slow absorption meals, respectively. The PHRA when compared to the missed meal boluses achieved a significant improvement in time between 70–180 mg/dl without increasing the number of hypoglycemic events during large meals with a time between 70–180 mg/dl for the tuning and validation scenarios of 55 (48, 60)% (p = 0.002) and 55 (51, 61)% (p=0.002), 53 (46, 62)% (p=0.002) and 51 (43, 56)% (p=0.002), and 41 (37, 57)% (p=0.004) and 48 (33, 55)% (p=0.002) for the fast, medium, and slow absorption meals, respectively.

Table 5.13: Overall population outcomes of a 15-day simulation with large (80–120 grams) slow absorption meals for three strategies in closed-loop control: missed meal boluses, announced meals, and unannounced meals with a PHRA. There were 450 meals in total.

	Missed Meal Boluses	Announced	PHRA	p*	p†
			Tuning		
Population Median Glucose (mg/dl)	211.9 (189.1, 288.0)	138.6 (133.6, 147.4)	191.5 (170.6, 201.5)	0.002	0.002
Insulin/day	38.0 (30.0, 41.1)	52.7 (49.8, 64.3)	41.3 (36.0, 45.7)	0.002	0.002
Percentage of time spent in... (mg/dl)					
70-180	23.6 (4.2, 42.3)	76.6 (69.3, 84.5)	41.3 (36.7, 57.0)	0.002	0.004
>180	76.4 (57.7, 95.8)	16.7 (6.1, 24.5)	58.7 (43.0, 63.3)	0.002	0.002
>250	19.8 (9.4, 76.9)	0.0 (0.0, 1.0)	9.5 (2.0, 27.0)	0.002	0.004
<70	0.0 (0.0, 0.0)	5.3 (3.5, 10.2)	0.0 (0.0, 0.0)	1	0.002
Hypoglycemic Events					
Level 1	0	52	0	1	0.002
Level 2	0	125	0	1	0.002
			Validation		
Population Median Glucose (mg/dl)	205.2 (188.5, 282.7)	136.0 (131.2, 142.5)	185.6 (174.7, 213.8)	0.002	0.002
Insulin/day	38.0 (30.0, 41.1)	53.3 (49.6, 63.7)	41.5 (36.0, 46.5)	0.002	0.002
Percentage of time spent in... (mg/dl)					
70-180	26.7 (3.7, 42.5)	77.8 (67.2, 84.5)	44.7 (33.1, 54.7)	0.002	0.002
>180	73.3 (57.5, 96.3)	15.4 (10.6, 24.8)	55.3 (45.3, 66.9)	0.002	0.002
>250	15.8 (8.9, 73.0)	0.0 (0.0, 0.2)	7.4 (3.7, 24.6)	0.002	0.002
<70	0.0 (0.0, 0.0)	4.4 (3.5, 12.2)	0.0 (0.0, 0.0)	1	0.002
Hypoglycemic Events					
Level 1	0	55	0	1	0.002
Level 2	0	116	0	1	0.002

Values reported as median (25th percentile, 75th percentile). *p value between missed meal boluses and PHRA scenarios. †p value between announced and PHRA.

During medium sized meals (Tables 5.14-5.16, the PHRA achieved adequate improvement in glycemic control when compared to missed meal boluses, without provoking additional hypoglycemic events for the tuning and validation scenarios with 76 (65, 78)% (p=0.002) and 74 (66, 79)% (p=0.002), 74 (66, 79)% (p=0.002) and 76 (66, 82)% (p=0.002), and 81 (55, 87)% (p=0.004) and 81 (57, 84)% (p=0.004) of time between 70–180 mg/dl for fast, medium, and slow absorption meals, respectively.

Table 5.14: Overall population outcomes of a 15-day simulation with medium (40–80 grams) fast absorption meals for three strategies in closed-loop control: missed meal boluses, announced meals, and unannounced meals with a (PHRA. There were 450 meals in total.

	Missed Meal Boluses	Announced	PHRA	p*	p†
		Tuning			
Population Median Glucose (mg/dl)	157.4 (148.2, 202.6)	125.4 (123.9, 132.0)	135.1 (130.1, 146.2)	0.002	0.002
Insulin/day	36.5 (28.8, 39.2)	43.4 (37.4, 50.1)	38.2 (32.4, 40.4)	0.002	0.002
Percentage of time spent in... (mg/dl)					
70-180	66.4 (35.6, 69.1)	96.9 (91.2, 98.0)	75.8 (65.1, 78.0)	0.002	0.002
>180	33.6 (30.9, 64.4)	3.1 (2.0, 8.8)	24.2 (22.0, 34.9)	0.002	0.002
>250	3.6 (0.9, 19.4)	0.0 (0.0, 0.0)	2.2 (0.5, 6.4)	0.002	0.004
<70	0.0 (0.0, 0.0)	0.0 (0.0, 0.2)	0.0 (0.0, 0.0)	1	0.25
Hypoglycemic Events					
Level 1	0	6	0	1	0.25
Level 2	0	2	0	1	1
		Validation			
Population Median Glucose (mg/dl)	161.5 (146.5, 208.0)	127.2 (124.3, 129.9)	135.9 (131.7, 148.7)	0.002	0.002
Insulin/day	36.4 (28.8, 39.3)	43.5 (38.2, 50.6)	38.6 (32.9, 40.5)	0.002	0.002
Percentage of time spent in... (mg/dl)					
70-180	64.9 (34.6, 70.8)	96.2 (91.1, 98.0)	74.2 (65.8, 79.1)	0.002	0.002
>180	35.1 (29.2, 65.4)	3.8 (1.9, 8.9)	25.8 (20.9, 34.2)	0.002	0.002
>250	4.2 (0.9, 21.6)	0.0 (0.0, 0.0)	2.7 (0.5, 5.1)	0.002	0.002
<70	0.0 (0.0, 0.0)	0.0 (0.0, 0.0)	0.0 (0.0, 0.0)	1	0.5
Hypoglycemic Events					
Level 1	0	2	0	1	0.5
Level 2	0	3	0	1	1

Values reported as median (25th percentile, 75th percentile). *p value between missed meal boluses and PHRA scenarios. †p value between announced and PHRA.

Generally, small meals (Tables 5.17–5.19) achieved the highest performance during missed meal boluses and during the implementation of the PHRA. During missed meal boluses the tuning and validation scenarios achieved 96 (91, 98) and 97 (90, 98)%, 97 (91, 100) and 98 (94, 100)%, and 100 (97, 100) and 100 (97, 100)% of time between 70–180 mg/dl for small meals of fast, medium, and slow absorption, respectively. The PHRA achieved during the tuning and validation scenarios

Table 5.15: Overall population outcomes of a 15-day simulation with medium (40–80 grams) medium absorption meals for three strategies in closed-loop control: missed meal boluses, announced meals, and unannounced meals with a PHRA. There were 450 meals in total.

	Missed Meal Boluses	Announced	PHRA	p*	p†
		Tuning			
Population Median Glucose (mg/dl)	161.5 (146.5, 208.0)	127.2 (124.3, 129.9)	135.9 (131.7, 148.7)	0.002	0.002
Insulin/day	36.4 (28.8, 39.3)	43.5 (38.2, 50.6)	38.6 (32.9, 40.5)	0.002	0.002
Percentage of time spent in... (mg/dl)					
70-180	64.9 (34.6, 70.8)	96.2 (91.1, 98.0)	74.2 (65.8, 79.1)	0.002	0.002
>180	35.1 (29.2, 65.4)	3.8 (1.9, 8.9)	25.8 (20.9, 34.2)	0.002	0.002
>250	4.2 (0.9, 21.6)	0.0 (0.0, 0.0)	2.7 (0.5, 5.1)	0.002	0.002
<70	0.0 (0.0, 0.0)	0.0 (0.0, 0.0)	0.0 (0.0, 0.0)	1	1
Hypoglycemic Events					
Level 1	0	2	0	1	0.5
Level 2	0	3	0	1	0.5
		Validation			
Population Median Glucose (mg/dl)	157.9 (147.8, 198.1)	128.3 (125.4, 136.1)	147.0 (140.7, 155.6)	0.002	0.002
Insulin/day	36.7 (29.0, 39.7)	43.9 (38.5, 49.5)	37.5 (31.1, 40.2)	0.002	0.002
Percentage of time spent in... (mg/dl)					
70-180	70.8 (38.4, 77.8)	97.6 (96.3, 99.0)	76.0 (66.0, 82.4)	0.002	0.002
>180	29.2 (22.2, 61.6)	2.1 (0.5, 3.5)	24.0 (17.6, 34.0)	0.002	0.002
>250	0.6 (0.0, 12.5)	0.0 (0.0, 0.0)	0.4 (0.0, 6.5)	0.016	0.016
<70	0.0 (0.0, 0.0)	0.1 (0.0, 1.0)	0.0 (0.0, 0.0)	1	0.0625
Hypoglycemic Events					
Level 1	0	13	0	1	0.25
Level 2	0	12	0	1	0.125

Values reported as median (25th percentile, 75th percentile). *p value between missed meal boluses and PHRA scenarios. †p value between announced and PHRA.

97 (94, 99) and 98 (93, 100)%, 98 (94, 100) and 98 (94, 100)%, and 100 (97, 100) and 100 (97, 100)% of time between 70–180 mg/dl for small meals of fast, medium, and slow absorption, respectively. Meanwhile, the announced strategy had a higher propensity for hypoglycemic events during these meals with 4 and 2, 9 and 8, and 18 and 29 level 1 events and 0 and 0, 6 and 7, and 10 and 20 level 2 events for slow, medium, and fast absorption meals, respectively.

Table 5.16: Overall population outcomes of a 15-day simulation with medium (40-80 grams) slow absorption meals for three strategies in closed-loop control: missed meal boluses, announced meals, and unannounced meals with a PHRA. There were 450 meals in total.

	Missed Meal Boluses	Announced	PHRA	p*	p†
		Tuning			
Population Median Glucose (mg/dl)	158.8 (147.0, 200.3)	127.9 (127.0, 134.0)	154.2 (144.0, 175.7)	0.002	0.002
Insulin/day	37.2 (29.3, 40.0)	44.6 (38.8, 51.0)	37.7 (31.2, 40.4)	0.002	0.002
Percentage of time spent in... (mg/dl)					
70-180	77.5 (32.0, 84.6)	93.1 (90.1, 94.2)	80.5 (54.5, 87.4)	0.002	0.004
>180	22.5 (15.4, 68.0)	3.4 (1.8, 5.5)	19.5 (12.6, 45.5)	0.002	0.002
>250	0.2 (0.0, 13.4)	0.0 (0.0, 0.0)	0.0 (0.0, 5.3)	0.125	0.125
<70	0.0 (0.0, 0.0)	3.0 (1.9, 5.4)	0.0 (0.0, 0.0)	1	0.002
Hypoglycemic Events					
Level 1	0	40	0	1	0.004
Level 2	0	71	0	1	0.008
		Validation			
Population Median Glucose (mg/dl)	157.3 (148.4, 203.0)	128.0 (125.4, 133.2)	153.6 (145.1, 169.2)	0.002	0.002
Insulin/day	37.0 (29.4, 40.5)	44.7 (38.6, 50.3)	37.4 (32.0, 40.8)	0.002	0.002
Percentage of time spent in... (mg/dl)					
70-180	76.5 (36.1, 80.6)	93.5 (85.6, 95.8)	80.6 (57.4, 83.5)	0.002	0.004
>180	23.5 (19.4, 63.9)	4.2 (0.9, 11.8)	19.4 (16.5, 42.6)	0.002	0.002
>250	0.5 (0.0, 9.1)	0.0 (0.0, 0.0)	0.3 (0.0, 2.9)	0.031	0.031
<70	0.0 (0.0, 0.0)	3.0 (2.7, 3.4)	0.0 (0.0, 0.0)	1	0.002
Hypoglycemic Events					
Level 1	0	42	0	1	0.002
Level 2	0	74	0	1	0.002

Values reported as median (25th percentile, 75th percentile). *p value between missed meal boluses and PHRA scenarios. †p value between announced and PHRA.

The announced meals strategy performed its best during fast meals (Tables 5.11, 5.14, and 5.17) where it experienced a higher percentage of time between 70–180 mg/dl compared with the PHRA strategy with few hypoglycemic events. The announced meals strategy achieved 87 (85, 90)% (p=0.002) and 88 (81, 91)% (p=0.002), 97 (91, 98) (p=0.002) and 96 (91 98)% (p=0.002), and 100 (99, 100)% (p=0.004) and 100 (99, 100)% (p=0.004) of time between 70–180 mg/dl for large, medium, and small sized meals with fast absorption, respectively.

Table 5.17: Overall population outcomes of a 15-day simulation with small (15—40 grams) fast absorption meals for three strategies in closed-loop control: missed meal boluses, announced meals, and unannounced meals with a PHRA. There were 450 meals in total.

	Missed Meal Boluses	Announced	PHRA	p*	p†
		Tuning			
Population Median Glucose (mg/dl)	124.5 (121.7, 132.4)	119.1 (117.8, 121.4)	123.0 (120.9, 125.3)	0.002	0.002
Insulin/day	35.2 (27.7, 38.4)	37.2 (30.0, 39.7)	35.4 (28.0, 38.5)	0.002	0.002
Percentage of time spent in... (mg/dl)					
70-180	96.4 (91.2, 98.4)	99.8 (99.4, 100.0)	97.3 (93.5, 98.9)	0.002	0.004
>180	3.6 (1.6, 8.8)	0.1 (0.0, 0.5)	2.7 (1.1, 6.5)	0.002	0.004
>250	0.0 (0.0, 0.0)	0.0 (0.0, 0.0)	0.0 (0.0, 0.0)	1	1
<70	0.0 (0.0, 0.0)	0.0 (0.0, 0.1)	0.0 (0.0, 0.0)	1	0.25
Hypoglycemic Events					
Level 1	0	4	0	1	0.25
Level 2	0	0	0	1	1
		Validation			
Population Median Glucose (mg/dl)	125.8 (122.2, 132.9)	120.7 (118.7, 122.1)	124.0 (121.2, 126.6)	0.004	0.002
Insulin/day	35.2 (27.9, 39.0)	37.4 (30.3, 40.2)	35.4 (28.1, 39.1)	0.002	0.002
Percentage of time spent in... (mg/dl)					
70-180	97.0 (89.8, 99.7)	100.0 (99.4, 100.0)	97.7 (92.5, 99.8)	0.016	0.004
>180	3.0 (0.3, 10.2)	0.0 (0.0, 0.6)	2.3 (0.2, 7.5)	0.016	0.004
>250	0.0 (0.0, 0.0)	0.0 (0.0, 0.0)	0.0 (0.0, 0.0)	1	1
<70	0.0 (0.0, 0.0)	0.0 (0.0, 0.0)	0.0 (0.0, 0.0)	1	0.5
Hypoglycemic Events					
Level 1	0	2	0	1	0.5
Level 2	0	0	0	1	1

Values reported as median (25th percentile, 75th percentile). *p value between missed meal boluses and PHRA scenarios. †p value between announced and PHRA.

During medium absorption meals (Tables 5.12, 5.15, and 5.18), the announced meals strategy also experienced a high performance in terms of time between 70–180 mg/dl, however, many hypoglycemic events occurred during this meal type. The percentage of time between 70–180 mg/dl for the announced meals strategy for the tuning and validation scenarios were 92 (83, 95)% and 90 (84, 93)%, 96 (91, 98)% and 98 (96, 99)%, and 99 (99, 100)% and 100 (99, 100)% for large, medium and small sized meals with medium absorption, respectively. The number of hypoglycemic events were 23 and 23, 2 and 13, and 9 and 8 level 1 and 6 and 9, 3 and 12, and 6

Table 5.18: Overall population outcomes of a 15-day simulation with small (15—40 grams) medium absorption meals for three strategies in closed-loop control: missed meal boluses, announced meals, and unannounced meals with a PHRA. There were 450 meals in total.

	Missed Meal Boluses	Announced	PHRA	p*	p†
		Tuning			
Population Median Glucose (mg/dl)	127.1 (125.4, 137.0)	120.7 (119.2, 123.6)	126.3 (125.3, 133.7)	0.006	0.002
Insulin/day	35.4 (28.0, 39.2)	37.8 (30.9, 40.4)	35.5 (28.2, 39.2)	0.002	0.002
Percentage of time spent in... (mg/dl)					
70-180	97.4 (91.4, 99.7)	99.4 (99.0, 99.9)	97.7 (93.8, 99.7)	0.004	0.037
>180	2.6 (0.3, 8.6)	0.1 (0.0, 0.7)	2.3 (0.3, 6.2)	0.004	0.002
>250	0.0 (0.0, 0.0)	0.0 (0.0, 0.0)	0.0 (0.0, 0.0)	1	1
<70	0.0 (0.0, 0.0)	0.1 (0.0, 0.7)	0.0 (0.0, 0.0)	1	0.063
Hypoglycemic Events					
Level 1	0	9	0	1	0.063
Level 2	0	6	0	1	0.25
		Validation			
Population Median Glucose (mg/dl)	126.1 (122.3, 132.1)	119.5 (118.1, 121.8)	125.5 (122.0, 128.0)	0.004	0.002
Insulin/day	35.7 (27.8, 39.2)	37.9 (30.3, 40.4)	35.7 (27.9, 39.2)	0.004	0.002
Percentage of time spent in... (mg/dl)					
70-180	98.3 (94.3, 99.7)	99.8 (99.4, 99.9)	98.4 (94.4, 99.8)	0.008	0.014
>180	1.7 (0.3, 5.7)	0.1 (0.0, 0.3)	1.6 (0.2, 5.6)	0.008	0.002
>250	0.0 (0.0, 0.0)	0.0 (0.0, 0.0)	0.0 (0.0, 0.0)	1	1
<70	0.0 (0.0, 0.0)	0.0 (0.0, 0.3)	0.0 (0.0, 0.0)	1	0.063
Hypoglycemic Events					
Level 1	0	8	0	1	0.125
Level 2	0	7	0	1	0.5

Values reported as median (25th percentile, 75th percentile). *p value between missed meal boluses and PHRA scenarios. †p value between announced and PHRA.

and 7 level 2 events, for the announced meals strategy for large, medium and small sized meals with medium absorption, respectively.

It can be seen in Table 5.13, 5.16, and 5.19 that slow meals are the most challenging to control during the announced meals strategy for both the tuning and validation scenarios leading to 5 (4, 10)% and 4 (4, 12)%, 3 (2, 5)% and 3 (3, 3)%, and 1 (0, 1)% and 1 (0, 2)% of time <70 mgdl for large, medium and small meals with slow absorption, respectively. During these slow absorption meals, the tuning and validation scenarios for the announced meal strategy experienced 52 and

Table 5.19: Overall population outcomes of a 15-day simulation with small (15—40 grams) slow absorption meals for three strategies in closed-loop control: missed meal boluses, announced meals, and unannounced meals with a PHRA. There were 450 meals in total.

	Missed Meal Boluses	Announced	PHRA	p*	p†
		Tuning			
Population Median Glucose (mg/dl)	124.3 (123.0, 131.8)	119.5 (118.5, 123.7)	124.3 (123.0, 130.8)	0.049	0.002
Insulin/day	35.9 (28.0, 39.2)	37.9 (30.6, 40.5)	35.9 (28.0, 39.2)	0.02	0.002
Percentage of time spent in... (mg/dl)					
70-180	99.9 (96.6, 99.9)	99.4 (99.3, 99.7)	99.9 (96.6, 99.9)	0.5	0.625
>180	0.1 (0.1, 3.4)	0.0 (0.0, 0.1)	0.1 (0.1, 3.4)	0.5	0.008
>250	0.0 (0.0, 0.0)	0.0 (0.0, 0.0)	0.0 (0.0, 0.0)	1	1
<70	0.0 (0.0, 0.0)	0.6 (0.2, 0.7)	0.0 (0.0, 0.0)	1	0.004
Hypoglycemic Events					
Level 1	1	18	1	1	0.004
Level 2	0	10	0	1	0.031
		Validation			
Population Median Glucose (mg/dl)	126.7 (124.5, 135.0)	120.7 (118.7, 125.6)	126.5 (124.3, 134.0)	0.004	0.002
Insulin/day	36.0 (28.1, 39.3)	38.2 (30.9, 40.5)	36.0 (28.2, 39.3)	0.002	0.002
Percentage of time spent in... (mg/dl)					
70-180	99.6 (96.6, 99.9)	98.9 (98.0, 99.6)	99.7 (96.7, 99.9)	0.063	0.375
>180	0.4 (0.1, 3.4)	0.2 (0.0, 0.2)	0.3 (0.1, 3.3)	0.063	0.008
>250	0.0 (0.0, 0.0)	0.0 (0.0, 0.0)	0.0 (0.0, 0.0)	1	1
<70	0.0 (0.0, 0.0)	1.0 (0.4, 1.7)	0.0 (0.0, 0.0)	1	0.002
Hypoglycemic Events					
Level 1	0	29	0	1	0.004
Level 2	0	20	0	1	0.031

Values reported as median (25th percentile, 75th percentile). *p value between missed meal boluses and PHRA scenarios. †p value between announced meals and the PHRA.

55, 40 and 42, and 18 and 29 level 1 hypoglycemic events and 125 and 116, 71 and 74, and 10 and 20 level 2 hypoglycemic events for large, medium and small meals, respectively.

For the PHRA, one level 1 and one level 2 hypoglycemic event occurred in the validation for the large fast scenario and one level 1 hypoglycemic event occurred in the tuning for the small slow scenario. All three of these events occurred due to insulin administration in the late postprandial period leading to postprandial hypoglycemia.

A final test to the PHRA was performed using a typical day scenario described in Chapter 5.2.7. Table 5.20 shows the overall outcomes during CLC during missed meal boluses, announced meals, and with the PHRA. For all of the ten subjects, there were 146 fast, 150 medium, and 154 slow absorption meals and 170 small and 280 medium sized meals. The median CHO amount was 46 grams, the 5th percentile was 23 grams, the 95th percentile was 69.5 grams, the minimum was 20 grams, and the maximum was 74 grams.

Table 5.20: Meal related outcomes of a 15-day typical day simulation for three strategies in closed-loop control: missed meal boluses, announced meals, and unannounced meals with a PHRA. There were 450 meals in total.

	Missed Meal Boluses	Announced	PHRA	p^*	$p^\dagger$
Population Median					
Glucose (mg/dl)	140.9 (131.3, 169.4)	121.4 (120.2, 127.5)	135.8 (128.0, 143.5)	0.002	0.002
Insulin/day	36.5 (28.7, 39.5)	41.3 (35.2, 44.6)	36.9 (30.7, 39.8)	0.002	0.002
Percentage of time					
spent in... (mg/dl)					
70-180	81.5 (56.4, 90.9)	96.7 (94.9, 98.4)	86.6 (73.6, 92.4)	0.002	0.002
>180	18.5 (9.1, 43.6)	1.7 (0.2, 4.2)	13.4 (7.6, 26.4)	0.002	0.002
>250	1.3 (0.0, 6.3)	0.0 (0.0, 0.0)	0.5 (0.0, 2.5)	0.031	0.031
<70	0.0 (0.0, 0.0)	1.1 (0.7, 1.6)	0.0 (0.0, 0.0)	1	0.004
Hypoglycemic Events					
Level 1	1	28	1	1	0.004
Level 2	0	22	0	1	0.008

Values reported as median (25th percentile, 75th percentile). *p value between missed meal boluses and PHRA scenarios. †p value between announced and PHRA.

The PHRA in this scenario is able to significantly improve outcomes without increasing the number of hypoglycemic events when compared to missed meal boluses with a percentage of time between 70–180 mg/dl of 87 (74, 92)% (p=0.002) and 13 (8, 26)% of time >180 mg/dl (p=0.002). The percentage of time between 70–180 mg/dl is significantly greater and the percentage of time >180 mg/dl is significantly lower for the announced meals strategy however, the percentage of time <70% mg/dl is increased to 1 (1, 2)% (p=0.004) with 28 level 1 hypoglycemic events (p=0.004) and 22 level 2 hypoglycemic events (p=0.008) over the 15-day period for the ten adult subjects.

Table 5.21: Meal related outcomes of a 15-day typical day simulation for three strategies in closed-loop control: missed meal boluses, announced meals, and unannounced meals with a PHRA. There were 450 meals in total.

	Missed Meal Boluses	Announced	PHRA	p*	p†
		Meal Related Outcomes[a]			
Preprandial Glucose (mg/dl)	124.2 (117.5, 131.8)	118.1 (113.6, 123.3)	121.0 (116.2, 124.5)	0.002	0.0137
Postprandial Peak (mg/dl)	189.0 (172.5, 211.8)	154.9 (148.8, 161.0)	184.5 (172.4, 202.4)	0.049	0.002
Postprandial Nadir (mg/dl)	116.2 (112.7, 124.0)	103.8 (96.9, 109.1)	113.5 (110.9, 120.9)	0.002	0.002
Meal Excursion (mg/dl)	55.1 (47.1, 62.2)	31.0 (26.8, 32.7)	55.6 (49.8, 67.4)	0.02	0.002
		From meal start + 1 hour			
Population Median					
Glucose (mg/dl)	128.6 (123.8, 140.2)	120.3 (115.3, 126.1)	125.6 (122.4, 133.7)	0.002	0.002
Insulin/meal	82.3 (65.0, 94.6)	191.5 (155.9, 227.9)	89.2 (68.2, 98.6)	1	1
Percentage of time					
spent in... (mg/dl)					
70-180	100.0 (100.0, 100.0)	100.0 (100.0, 100.0)	100.0 (100.0, 100.0)	1	1
>180	0.0 (0.0, 0.0)	0.0 (0.0, 0.0)	0.0 (0.0, 0.0)	1	1
>250	0.0 (0.0, 0.0)	0.0 (0.0, 0.0)	0.0 (0.0, 0.0)	1	1
<70	0.0 (0.0, 0.0)	0.0 (0.0, 0.0)	0.0 (0.0, 0.0)	1	1
Hypoglycemic Events					
Level 1	0	10	0	1	0.125
Level 2	0	20	0	1	0.016
		1 hour after meal start + 1 hour			
Population Median					
Glucose (mg/dl)	170.1 (157.5, 179.0)	123.7 (113.8, 127.4)	163.7 (156.2, 176.0)	0.002	0.002
Insulin/meal	74.6 (59.0, 80.4)	18.6 (11.3, 27.0)	79.5 (66.4, 91.3)	1	1
Percentage of time					
spent in... (mg/dl)					
70-180	94.2 (50.0, 100.0)	100.0 (100.0, 100.0)	100.0 (65.4, 100.0)	0.031	0.125
>180	5.8 (0.0, 50.0)	0.0 (0.0, 0.0)	0.0 (0.0, 34.6)	0.031	0.125
>250	0.0 (0.0, 0.0)	0.0 (0.0, 0.0)	0.0 (0.0, 0.0)	1	1
<70	0.0 (0.0, 0.0)	0.0 (0.0, 0.0)	0.0 (0.0, 0.0)	1	1
Hypoglycemic Events					
Level 1	0	0	0	1	1
Level 2	0	0	0	1	1

Values reported as median (25th percentile, 75th percentile). *p value between missed meal boluses and PHRA scenarios. †p value between announced and PHRA. [a] Meal related outcomes are calculated during a postprandial period of 5 hr.

The meal related outcomes of the typical day are shown in Table 5.21. This table shows that the PHRA is able to significantly improve outcomes compared to missed meal boluses with a postprandial peak of 185 (172, 202) mg/dl (p=0.049), a postprandial nadir of 114 (111, 121) mg/dl (p=0.002), and a meal excursion of 56 (50, 67) mg/dl (p=0.002). During the announced strategy 10 level l (p=0.125) and 20 level 2 (p=0.016) hypoglycemic events occurred from the start of the meals to one hour after the commencement of exercise. From one hour after the start of a meal to two hours after the start of the meal the PHRA is able to significantly improve outcomes when compared to missed meal boluses and the outcomes achieved are not statistically different from that of the announced strategy. The PHRA achieved a percentage of time between 70–180 mg/dl of 100 (65, 100)% (p=0.031 (missed meal bolus) vs. p=0.0125 (announced)) and a percentage of time >180 mg/dl of 0 (0, 35)% (p=0.031 (missed meal bolus) vs. p=0.125 (announced)).

5.2.9 Discussion

In this study, a PHRA that detects a meal and triggers postprandial hyperglycemia mitigation actions was implemented into an existing closed-loop controller and tested in silico on ten adult subjects using the T1D Simulator in realistic and challenging scenarios. The PHRA used three refined tunings based on the methodology found in Chapter 5.1. One difficulty that can be expected to be encountered when applying this methodology in real life is finding the minimum and maximum values required for the scaling of data prior to finding the cross-covariance between D_{diff} and $G(t)$. This will require the acquisition of rich data that represents frequent activities that the subject participates in such as eating out, exercising, etc. Additional data are necessary for the tuning of the PHRA for meal detection as data with a variety of meals without meal boluses are required to adequately tune the PHRA following the methodology used. Therefore, further research on the tuning of the PHRA is required.

Using the data available with different meal types, a methodology was devised to identify rapidly appearing meals using two meal detection tunings, one with a high sensitivity and the other with a low amount of FP. The idea behind this technique is that if the meal is rapidly appearing both detections will be triggered at the same time, i.e., there is a large and rapid disturbance in BG. Although this is an imperfect system for identifying the Ra, it gives the controller insight into meal dynamics and allows actions to be modified accordingly.

A methodology to estimate CHO quantity of a detected meal was also developed using the area under the curve of D, a tunable gain, and the Ra. This technique uses these parameters as indicators of the quantity of CHO ingested. However, the spread of the CHO estimation error is quite large. The estimation error for Detection 1 and Detection 2 were -19 ± 63% (-17 ± 48 grams CHO) and -27 ± 59% (-22 ± 49 grams CHO) for the tuning set and -19 ± 63% (-18 ± 48 grams CHO) and -25 ± 62% (-22 ± 50 grams CHO) for the validation set (mean ± standard deviation). These estimations are larger than those found in human estimates of ~21–40% overestimation and ~12–21% underestimation [30, 136, 137].

Samadi et al. [174] developed a CHO estimation algorithm that determines a distributed approximation of CHO content of an unannounced meal when the slope of the measured BG is positive without satisfaction of a safety criteria that causes the estimation of CHO to be paused. The estimation error achieved using this methodology is -1.7 ± 28.1 grams CHO. Lee and Bequette [5] estimated the CHO of a detected meal using continuous observations of the first and second derivative of glucose to produce series of meal impulses when a set of conditions are satisfied. These meal impulses are converted into grams of CHO by a scaling factor that can be different for each individual and obtained an estimated error of -0.75 ± 9.3 grams CHO. Based on the estimated CHO by other studies the results achieved in this study are poorer in comparison and therefore limited in its ability to aid to meal bolusing.

The aim of the PHRA is to improve glycemic outcomes without increasing the number of hypoglycemic events; unlike several clinical trials [14, 15] where rescue CHO were required due to hypoglycemia caused by meal detection algorithms. Also, contrary to the preliminary tuning of the meal detection algorithm in Chapter 5.1, the PHRA was active at all times to account for those who practice non-standard schedules such as night shift workers. The PHRA utilized a mechanism to increase the $\overline{IOB}_{max}$, which was triggered at each meal detection and remained active until the derivative of BG over three time samples was no longer positive. This type of disturbance rejection adds safety to the system during a FP where the amount of insulin delivered will only increase if it is necessary. The estimation of Ra and CHO were not utilized for bolus suggestions as it was found that bolusing after the consumption of meal increased the likelihood of hypoglycemia.

Cameron et al. [7] developed a meal detection and estimation of total glucose appearance using an evolving probabilistic method by first comparing the CGM signal to no-meal predictions made by a simple insulin-glucose model, then it fits residuals to potential, assumed meal shapes, finally, it compared and combines these fits to detect any meals and estimate the meal total glucose appearance, shape, and total glucose appearance uncertainty. This algorithm was tested in silico in a 36-hour simulation with 100 subjects with meals of 40 (breakfast 7:00h), 50 (lunch 12:00h), 20 (snack 16:00h), and 60 (dinner 18:00h) grams of CHO. The results obtained with disturbance rejection and meal detection were a mean BG of 132 mg/dl, 0% of time <50 mg/dl, 11% of time >180 mg/dl, and 89% of time between 70–180 mg/dl. This scenario most resembles the typical day scenario where our algorithm obtained similar results with a population median BG of 136 mg/dl, 0% of time <70 mg/dl, 13% of time >180 mg/dl, and 87% of time between 70–180 mg/dl.

Lee and Bequette [5] used the same simulation to test their unannounced meals algorithm as the one described in Cameron et al. [7], however, the dinner time meal was 80 grams of CHO. The results obtained with disturbance rejection with meal detection in adult subjects were a mean BG of 132 mg/dl, 0.5% of time <70 mg/dl, and 90% of time between 70-180 mg/dl. These results are also similar to our results.

During slow absorption meals the PHRA is safer than the announced meals strategy which results in many hypoglycemic events. Hypoglycemia in the announced meals strategy due to slow absorption meals, occurs because this strategy is not prepared for this type of meal and results in an increased risk of hypoglycemia. Therefore, other techniques of bolusing for announced meals are required for slow absorption meals as noted by Slattery et al. [132]. The PHRA is able to significantly reduce the number of level 1 and level 2 hypoglycemia events, increasing patient safety during meals of slower absorption rates.

Fast absorption meals are difficult for the PHRA to control and the time between 70–180 mg/dl for the announced meals strategy is higher for all meal sizes. However, meals consumed are generally mixed and contain both fat and protein, which slow down absorption [35]. Meals with a CHO content >80 grams also prove to be challenging in all three cases of missed meal boluses, announced meals, and unannounced meals with the PHRA. The announced meals strategy obtained the highest amount of time between 70–180 mg/dl, however, resulted in many hypoglycemic events. The PHRA obtained significantly better results than the missed meal boluses case; however, this type of meal poses a challenge to the system and is a limitation of the PHRA. This is in part due to the delay in meal detection and also in part due to the delay of subcutaneously delivered insulin.

Due to the delay of insulin action, the development of a PHRA is necessary to handle meals that have not been announced to the controller and that no premeal bolus has been given. If there were no delay in insulin action, this would not be necessary as the majority of meals could be handled by the feedback response of the controller to rising BG levels. Additionally, the delay in the insulin action means that the PHRA is unable to prevent early postprandial hyperglycemia, which will continue to be a persistent problem with unannounced meals until improved fast-acting insulin formulations are available.

5.3 Summary

In this study, a PHRA that detects meals, determines its Ra, estimates CHO quantity, and triggers postprandial hyperglycemia mitigation actions was implemented into an existing closed-loop controller and tested in silico using the T1D Simulator in several scenarios. The meal detection algorithm was tuned empirically according to patient population outcomes and is more sensitive to large and fast absorption meals, which it can detect in a relatively short period of time with little change to BG. After meal detection, the PHRA allows the $\overline{IOB}_{max}$ to increase to allow additional insulin administration. The PHRA outperforms a CLC controller with missed meal boluses in all scenarios tested and is typically able to reduce severe hyperglycemia (>250mg/dl) without increasing the likelihood of a hypoglycemic event. The PHRA is still unable to prevent hyperglycemia during fast absorption and large meals due to the delays in meal detection and insulin action.

CHAPTER 6

Unannounced Aerobic Exercise Detection and Postexercise Glycemic Control

Closed-loop control systems intended for BG control in people with T1D, i.e. AP systems, lack exercise-induced hypoglycemia prevention strategies. Current hybrid CLC systems suggest that patients temporarily raise their target glucose to 150 mg/dl from 120 mg/dl before aerobic exercise. However, this recommendation has been found insufficient in preventing hypoglycemia due to aerobic exercise [175]. Additional recommendations include ingesting CHO before and during prolonged exercise and lowering basal insulin levels before the commencement of exercise [34]. However, these recommendations are not realistic as they require the patient to concurrently calculate CHO and control basal insulin levels prior to exercise. Additionally, anaerobic exercise, which produces a paradoxical increase in BG, is not considered in this scheme.

The objective of this work was to build an exercise-induced hypoglycemia reduction algorithm (EHRA) that detects exercise without the use of additional physiological signals and triggers automatic disturbance rejection actions that safely and effectively reduce hypoglycemia induced by aerobic exercise. Therefore, we hypothesize that the proposed EHRA provides sufficient sensitivity and reliability to be used safely and effectively within an AP system.

6.1 Diabetes Simulation Scenario

The T1D Simulator (see Chapter 3.2) coupled with an exercise model described in Bertachi et al. [160] was used to build a 15-day scenario with ten adult subjects. Additionally, the effect of fast absorption rescue CHO on glucose was added to the simulator using a two-compartment model [166]:

$$\dot{G_p}(t) = \frac{-G_p(t)}{\tau_{max}} + u_{CHO}(t) \cdot A_g \tag{6.1}$$

$$\dot{G_t}(t) = \frac{G_p(t) - G_t(t)}{\tau_{max}} \tag{6.2}$$

$$u_G = \frac{G_t(t)}{\tau_{max}} \tag{6.3}$$

where u_G is the glucose absorption rate into the plasma, A_g is the CHO bioavailability, τ_{max} is the time-to-maximum glucose absorption set to 20 minutes for fast absorption CHO.

The scenario included eight exercise sessions with a duration of 50 minutes at 60% VO_{2max} distributed on days 1, 3, 5, 7, 9, 11, 13, and 15 at 7:00h, 14:00h, 20:00h, 10:00h, 7:00h, 18:00h, 23:00h, and 12:00h, respectively. There were three meals per day with varying CHO content following a normal distribution with mean 30 grams at 8:30h (breakfast), 60 grams at 13:00h (lunch), and 50 grams at 19:00h (dinner). The coefficient of variation for the meal size was ±20%. For each meal, a meal absorption profile was randomly selected from a meal library of eleven meals. Meal absorption rate and subcutaneous insulin absorption rate were varied at each meal according to a uniform distribution of ±10% and ±30%, respectively. Circadian insulin sensitivity variation (sinusoidal type with 24-hour period [162]) was implemented with random amplitude according to a uniform distribution of ±30% and random phase. Finally, CGM error was according to the default model in the T1D simulator.

6.2 Exercise Detection Algorithm

The EHRA presented in this thesis was tested in silico on a 15-day scenario with eight exercise sessions on alternating days. The algorithm collects glucose and insulin infusion rate values and computes a disturbance parameter, $D(t)$, from an augmented minimal model using an UKF (see Chapter 4). A patient-specific threshold, k_{TH} was determined using the minimum $D(t)$ value found in an in silico 15-day, well-controlled, closed-loop scenario without exercise. This threshold was used to detect aerobic exercise and in turn trigger disturbance rejection actions that aim to reduce the risk of exercise-induced hypoglycemia. Exercise is detected if the threshold is crossed and more than 60 minutes have elapsed since the last detection (Figure 6.1).

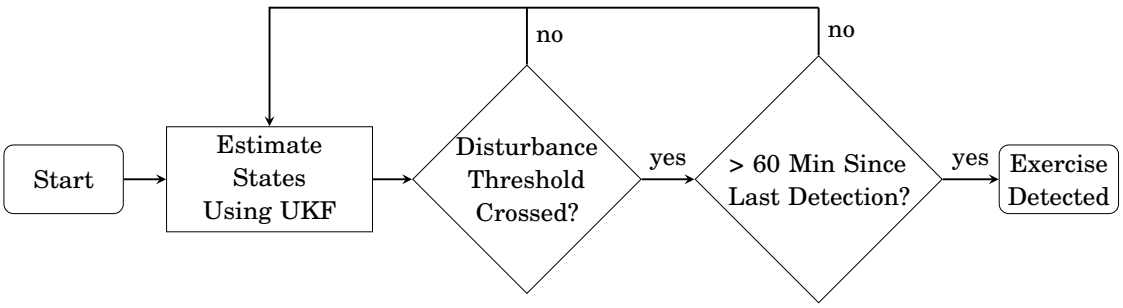

Figure 6.1: Flow Chart of Exercise Detection Algorithm. First the states of a minimal model are estimated using an UKF. A threshold is applied to the UKF estimated disturbance parameter, once crossed and there has not been a detection for at least 60 min, exercise is detected.

6.2.1 Performance Metrics

Seven performance metrics were used. Sensitivity, TP, FP, FN, FP/day, detection time, and Δ glucose. TN and specificity cannot be determined in this framework due to the fact that one TP can span multiple time points depending on exercise duration; however, a TN can be counted at each time sample when a negative occurrence is correctly identified. This skews the specificity to the higher end of the spectrum. Therefore, sensitivity and FP were used as measures of performance. Sensitivity measures the percentage of positive results that are correctly identified. Correct detection (a TP) is when the algorithm has detected an exercise session from the beginning of exercise to 480 minutes after the time of the commencement of exercise. A FP is when detection is positive without the occurrence of exercise. Negative detection or a FN is when an exercise session has not been detected up to 480 minutes after commencement. FP/day values are included for easy comparison between studies. Detection time reflects the time at which a TP is detected with respect to exercise time and Δ glucose reflects the change in glucose from the start of exercise to the time when exercise was detected. All values are reported as mean $\pm$ standard deviation and median (5th percentile, 95th percentile).

6.2.2 Results

The exercise detection algorithm threshold, k_{TH} was obtained using the lowest estimated $D(t)$ value for each patient in a 15-day in silico simulation with no exercise. The scenario is the same as the scenario described in Section 6.1 with the exclusion of exercise. The overall, daytime, and nighttime outcomes were reported as median glucose, percentage of time spent between 70–180 mg/dl, >180 mg/dl, <70 mg/dl, <54 mg/dl, and hypoglycemic events separated between level 1 and level 2 are shown in Table 6.1. This is a well-controlled simulation with no time below 70 or 54 mg/dl and with 1 level 1 hypoglycemic event. No nocturnal hypoglycemia was experienced. Daytime outcomes reveal 8 (5, 9)% of time above 180 mg/dl due to meals.

The exercise detection algorithm was tested in a 15-day in silico scenario with eight exercise

Table 6.1: Outcomes of a 15-day in silico simulation with no exercise.

Median Glucose (mg/dl)	Percentage of time spent in (mg/dl)				Hypoglycemic Events	
	<54	<70	70-180	>180	Level 1	Level 2
Overall Outcomes						
131.4 (128.2, 136.4)	0 (0, 0)	0 (0, 0)	94.5 (93.4, 96.5)	5.5 (3.5, 6.6)	1	0
Daytime Outcomes						
138.9 (136.4, 145.6)	0 (0, 0)	0 (0, 0)	92.5 (90.6, 95)	7.5 (5, 9.4)	1	0
Nighttime Outcomes						
100 (99.1, 100)	0 (0, 0)	0 (0, 0)	100 (99.1, 100)	0 (0, 0.9)	0	0

Values reported as median (25th percentile, 75th percentile).

sessions at 60% VO_{2max} on alternating days. The intensity of exercise in the scenario described in Section 6.1 was then decreased and increased by 25% to test the exercise detection algorithm and exercise-induced hypoglycemia mitigation strategies for robustness. The population performance metrics can be found in Table 6.2. The exercise detection algorithm for the nominal intensity (60% VO_{2max}) was able to detect all 80 sessions. The Δ glucose had a mean drop of 54 $\pm$ 22 mg/dl and median drop of 52 (24, 89) mg/dl. The time to detection was mean 41 $\pm$ 10 minutes and median 40 (30, 63) minutes. The number of FP were mean 2 $\pm$ 2 and median 2 (0, 6) with a FP/day of mean of 0.2 $\pm$ 0.4 and median 0 (0, 1). There were no FN occurrences. Compared to the nominal intensity (60% VO_{2max}) the exercise detection metrics with the intensity decreased by 25% had a lower sensitivity, FP, FP/day and a higher detection time and FN. The Δ glucose had a negligible change. Compared to the nominal intensity (60% VO_{2max}) the exercise detection metrics with the intensity increased by 25% had the same sensitivity and FN, a lower detection time, FP, and FP/day, and a higher Δ glucose.

Table 6.2: Population performance metrics of exercise detection algorithm in 15-day scenario with a total of eight exercise sessions per patient with a nominal (60% VO_{2max}), decreased by 25% and increased by 25% intensity.

	Sensitivity (%)	Δ Glucose (mg/dl)	Detection Time (min)	TP	FP	FN	FP/day
Nominal Exercise Intensity (60% VO_{2max})							
Mean	100 $\pm$ 0	53.7 $\pm$ 21.8	41.1 $\pm$ 9.7	8 $\pm$ 0	0.7 $\pm$ 0.7	0 $\pm$ 0	0.0 $\pm$ 0.0
Median	100 (100, 100)	52 (23.7, 89.4)	40 (30, 62.5)	8 (8, 8)	1 (0, 2)	0 (0, 0)	0 (0, 0.1)
Exercise Intensity Decreased by 25%							
Mean	96.3 $\pm$ 6.0	53.6 $\pm$ 22.3	50.5 $\pm$ 20	7.7 $\pm$ 0.5	0.6 $\pm$ 0.7	0.3 $\pm$ 0.5	0.0 $\pm$ 0.0
Median	100 (87.5, 100)	51.6 (24.0, 90.4)	45 (31.8, 73.3)	8 (7, 8)	0.5 (0, 2)	0 (0, 1)	0 (0, 0.1)
Exercise Intensity Increased by 25%							
Mean	100 $\pm$ 0	55.0 $\pm$ 21.0	37.3 $\pm$ 7.7	8 $\pm$ 0	0.6 $\pm$ 0.7	0 $\pm$ 0	0.0 $\pm$ 0.0
Median	100 (100, 100)	55.6 (27.1, 94.3)	35 (25, 52.5)	8 (8, 8)	0.5 (0, 2)	0 (0, 0)	0 (0, 0.1)

Values reported as mean $\pm$ standard deviation and median (5th percentile, 95th percentile).

Figure 6.2 illustrates the cumulative detection rates over change in Δ glucose drop and time from the onset of exercise for the three intensities of exercise and demonstrates that the detection algorithm is increases in the detection rate as the drop in BG increases across all three intensities of exercise.

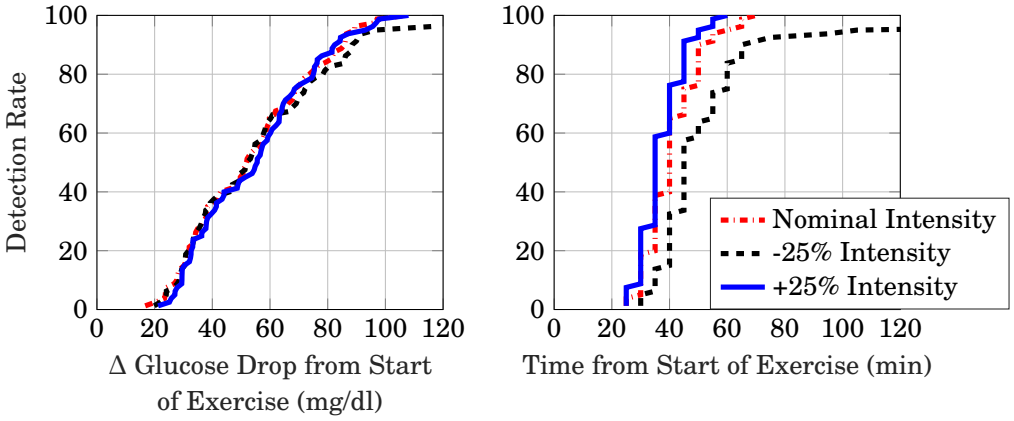

Figure 6.2: Cumulative detection rates over change in Δ glucose and time from the start of exercise for the EHRA for nominal (60% VO_{2max}), -25%, and +25% intensities of exercise.

6.3 Postexercise Glucose Control

6.3.1 The Exercise-Induced Hypoglycemia Reduction Algorithm

The closed-loop controller previously described in Chapter 3 has been modified to include an exercise rejection loop as seen in Figure 6.3. The middle loop is the exercise rejection loop that comprises of the EHRA that uses an UKF to estimate the disturbance parameter, D, which is used to detect exercise and apply exercise-induced hypoglycemia mitigation actions.

The exercise rejection loop applies heuristic actions to the closed-loop controller only when exercise is detected and escape conditions are not met. If at any point the escape conditions are met, all three disturbance rejection actions (described below) are removed. The escape conditions, which are checked once exercise has been detected, are defined as:

$$escape = \begin{cases} true & \text{if } G(k) > 120 \wedge \dot{G}(k) > 0, \quad \forall k \in (t-2,...,t) \\ & \vee\ (G(k) > 90 \wedge \dot{G}(k) > 1), \quad \forall k \in (t-2,...,t) \\ & \vee\ (\dot{G}(k) > 0 \wedge u_{IFB}(k) > 0), \quad \forall k \in (t-2,...,t) \\ & \vee\ (\dot{G}(j) > 1.5 \wedge u_{IFB}(j) > 0), \quad \forall j \in (t-1,t) \\ false & \text{otherwise.} \end{cases} \tag{6.4}$$

where k and j represent multiple time points for a given sampling time, t, $G(t)$ is represented in mg/dl, $\dot{G}(t)$ is the derivative of glucose in mg/dl/min and u_{IFB} is the delivered insulin.

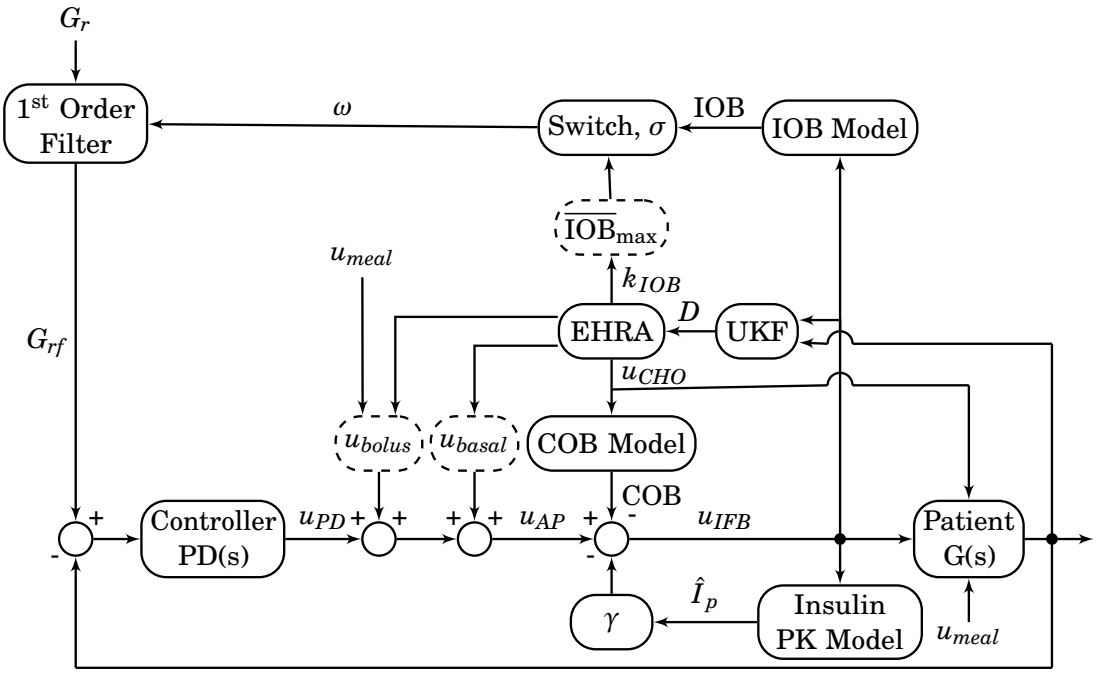

Figure 6.3: Closed-loop controller composed of an inner control loop that contains a PD controller with IFB designed to drive the measured glucose value (G) to a target value (G_r), a top outer loop that acts as a safety supervisory loop and uses SMRC to modulate G_r to G_{rf} based on the estimated IOB, and a top inner loop that uses an UKF to estimate the disturbance parameter, D that is then introduced into an EHRA, which when activated applies disturbance rejection actions to reduce exercise-induced hypoglycemia by modifying $\overline{\text{IOB}}_{\text{max}}$, u_{basal}, u_{bolus}, and suggesting carbohydrates, u_{CHO}.

Three disturbance rejection actions adapted from Bertachi et al. [160] are applied when exercise is detected:

1. Basal insulin (u_{basal}) is reduced to zero and k_{IOB} is reduced to 0.85
2. The following meal insulin bolus (u_{bolus}) is reduced by 30%
3. A specified amount of CHO is suggested to the patient

where k_{IOB} is defined as a gain that regulates the amplitude of the upper limit of the IOB ($\overline{IOB}_{max}(t)$). The time-variant $\overline{IOB}_{max}(t)$ is computed as follows:

$$\overline{IOB}_{max}(t) = k_{IOB}\frac{2u_{basal}(t)}{60k_{DIA}} \tag{6.5}$$

where k_{DIA} is a tuned gain for the duration of insulin action (DIA) [162]. At exercise detection, the first action is applied for 60 minutes and then these values are linearly returned to their nominal values over a period of 120 min. The CHO suggestion is calculated at the moment of

detection as follows:

$$u_{CHO}(t) = \frac{G_{ex} - G(t)}{k_{CHO}} \cdot \frac{D(t)}{k_{TH}} k_{FF} \tag{6.6}$$

where G_{ex} is the maximum desired BG level during exercise (mg/dl), k_{CHO} is a insulin-to-carbohydrate correction factor, k_{TH} is the threshold of the EHRA, and $k_{FF}(t)$ is a tunable gain that decreases by 50% if there is a second exercise detection within eight hours of the previous one and $D(t)$ is less than $D(t^*)$ (D at the previous detection). This second detection is considered to be of the same exercise session and accounts for late-onset postexercise hypoglycemia [176]. u_{CHO} is rounded to the nearest 5.

The carbohydrates-on-board (COB) or $COB(t)$ is then estimated using a two-compartment chain [166]:

$$\widehat{COB}(t) = 1 - \int_{t^*+1}^{t} \frac{u_{CHO}(t^*+1) A_g \tau e^{-\frac{\tau}{\tau_{max}}}}{{\tau_{max}}^2} d\tau \Big/ A_g u_{CHO}(t^*+1) \tag{6.7}$$

where $t^* + 1$ is the time instant of CHO consumption (assumed to be one time sample after detection). The COB estimation can be approximated using a discrete FIR filter as follows:

$$\widehat{COB}(k) = \sum_{i=1}^{N} \delta_i u_{CHO}(k - i + 1) \tag{6.8}$$

where $\widehat{COB}(k)$ is the percentage of active CHO at time instant, k. δ_i are the FIR parameters that model the absorption of the consumed CHO that have yet to appear in the plasma and can be identified for individual patients using the BG response in basal conditions of the desired fasting-acting CHO, i.e. glucose gels or tablets. The calculated $\widehat{COB}(t)$ is used to prevent controller overcorrection by inhibiting the insulin action:

$$u_{IFB}(t) = u_{AP} - \gamma(\hat{I}_p(t) - \hat{I}_p^*(t)) - \beta \widehat{COB}(t) \tag{6.9}$$

where $\hat{I}_p(t)$ (estimated plasma insulin concentration), $\hat{I}_p^*(t)$ (estimated basal plasma insulin concentration at steady-state), and γ (IFB gain [177]) are parameters belonging to the IFB component. β is an adjustable carbohydrate-to-insulin inhibition gain. The controller parameters for the EHRA can be found in Table 6.3.

Table 6.3: EHRA Controller parameter values.

Symbol	Quantity	Value	Units
G_{ex}	Maximum desired glucose level during exercise	250	mg/dl
k_{CHO}	Carbohydrates correction factor	2.7	unitless
k_{TH}	Threshold of the exercise detection algorithm	patient specific	unitless
k_{FF}	Gain on carbohydrate estimation	0.6	unitless
A_g	Carbohydrate bioavailability	0.9	unitless
τ_{max}	Time-to-maximum glucose absorption	20	min
β	Carbohydrate-to-insulin gain	0.5	g/U

6.3.2 Performance Metrics

Glucose values are measured as median glucose (median of the median value for each subject), percentage of time between 70-180 mg/dl, >180 mg/dl, <70 mg/dl and <54 mg/dl. The number of hypoglycemic events are categorized as either a level 1 or level 2 event defined as BG <70 mg/dl and ≥54 mg/dl and BG <54 mg/dl, respectively [65]. A hypoglycemic event requires a minimum duration of 15 minutes below/within threshold, with a separation of at least 30 minutes [173]. All values are reported as median (25th percentile, 75th percentile). The Wilcoxon signed-rank test was used to obtain p values where a p value of <0.05 is considered significant. The percentage of time between 70-180 mg/dl, <70 mg/dl and <54 mg/dl are used as measures of performance, where higher values are desirable for the percentage of time between 70-180 mg/dl and lower values are desirable for the percentage of time <70 mg/dl and <54 mg/dl.

6.3.3 Insulin-Only Closed-Loop Strategy with Unannounced Exercise

The unannounced exercise strategy is tested in the same scenario described in Chapter 6.1, however, exercise is not unannounced and no strategy is used to avoid exercise-induced hypoglycemia. This strategy includes rescue CHO when the patient's BG drops below 70 mg/dl. The patient ingests 15 grams of fast absorption CHO if their BG level is <70 mg/dl, waits 20 minutes and if BG is still <70 mg/dl, they consume another 15 grams of CHO. This process repeats until BG is >70 mg/dl. Rescue CHO are consumed exercise is ongoing.

6.3.4 Insulin-Only Closed-Loop Strategy with Announced Exercise

The announced exercise strategy is tested in the same scenario described in Chapter 6.1, however, exercise is announced. This strategy has been previously published [160] and follows the consensus recommendations for conventional insulin therapy [34]. The strategy involves the patient ingesting a controller-calculated amount of CHO 20 minutes before the commencement of exercise. The absorption profile for these CHO is randomly selected from a meal library of 31 fast absorption meals. This type of CHO is tailored to resemble a snack such as a sandwich or fruit. The controller also makes adjustments to the k_{IOB}, u_{basal}, τ_d (PD gain tuned based on individual insulin requirements), and ω^+ (amplitude of discontinuous change in glucose set-point by SMRC loop [178]), as well as reducing the insulin bolus by 50% and omiting any correction bolus for the next meal.

6.3.5 Results

Three insulin-only closed-loop control strategies of unannounced exercise, announced exercise, and unannounced exercise with the EHRA were tested using the scenario described in Chapter 6.1. Tables 6.4 and 6.5 show the overall outcomes and exercise related outcomes during CLC for the three control strategies. The data show that the EHRA is able to outperform the unannounced strategies, this is primarily shown in the number of level 1 and level 2 hypoglycemic events and the percentage of time <70 mg/dl and <54 mg/dl. The EHRA is able to prevent severe hypoglycemia and therefore there are no level 2 hypoglycemic events. Between the announced strategy and the EHRA, there was only a significant difference in the percentage of time <70 mg/dl (p=0.006). The difference between the strategies is even more stark when compared for the two hours after the start of exercise. Here we can see that the drop in glucose is decreased by ~21 mg/dl (p=0.002) and the percentage of time <70 mg/dl is reduced from 28% to 1% (p=0.002) when comparing the unannounced exercise strategy with the EHRA. Additionally, the percentage of time >180 mg/dl is reduced from 3% to 0% when comparing the announced exercise strategy with the EHRA (p=0.063). The results from two hours after the start of exercise to six hours after the start of exercise show how the lasting effects of aerobic exercise affect BG control. Here we can see similar performance for both the announced strategy and the EHRA, with both strategies able to prevent all level 2 hypoglycemic events with 0% of time <54 mg/dl (p=1).

Table 6.4: Overall population outcomes of a 15-day simulation for three strategies in closed-loop control: unannounced exercise, announced exercise, and unannounced exercise with an EHRA. There were 80 exercise sessions in total.

	Unannounced	Announced	EHRA	p*	p†
Overall Outcomes					
Population Median Glucose (mg/dl)	119.6 (118.7, 124.5)	126.4 (122.4, 129.0)	125.1 (120.7, 130.4)	0.002	0.375
CHO/day (g/day)	27.9 (22.5, 39.6)	31.1 (28.6, 32.9)	33.4 (28.9, 37.1)	0.109	0.232
Percentage of time spent in... (mg/dl)					
70–180	93.8 (93.2, 95.9)	93.8 (91.7, 95.0)	93.6 (90.8, 93.9)	0.084	0.492
>180	4.2 (2.0, 4.6)	5.9 (4.5, 7.8)	6.4 (6.0, 8.7)	0.002	0.432
<70	1.9 (1.5, 2.8)	0.4 (0.2, 0.6)	0.1 (0.0, 0.1)	0.002	0.006
<54	0.2 (0.1, 0.5)	0.0 (0.0, 0.0)	0.0 (0.0, 0.0)	0.004	0.25
Hypoglycemic Events					
Level 1	118	15	6	0.002	0.117
Level 2	24	2	0	0.008	0.5

Values reported as mean ± standard deviation and median (25th percentile, 75th percentile). * p value between unannounced and EHRA scenarios. † p value between announced and EHRA.

Table 6.5: Exercise related outcomes of a 15-day simulation for three strategies in closed-loop control: unannounced exercise, announced exercise, and unannounced exercise with an EHRA. There were 80 exercise sessions in total.

	Unannounced	Announced	EHRA	p*	p†
BG at exercise start (mg/dl)	136.9 (132.6, 148.0)	151.2 (145.0, 158.8)	137.2 (132.8, 148.0)	1	0.002
Pre-exercise CHO/session (g/session)	0.0 (0.0, 0.0)	45.0 (37.5, 47.5)	0.0 (0.0, 0.0)	1	0.002
From exercise start + 2 hours					
Population Median Glucose (mg/dl)	91.6 (84.8, 94.7)	125.1 (122.1, 132.3)	113.5 (111.6, 119.6)	0.002	0.004
BG drop (mg/dl)	82.7 (77.5, 93.6)	62.9 (57.2, 73.0)	62.0 (58.4, 63.9)	0.002	0.92
CHO/session (g/session)	30.0 (30.0, 30.0)	0.0 (0.0, 0.0)	45.0 (42.5, 45.0)	0.004	0.002
Percentage of time spent in... (mg/dl)					
70–180	71.0 (66.0, 78.0)	93.0 (90.0, 100.0)	100.0 (98.0, 100.0)	0.002	0.102
>180	0.0 (0.0, 0.0)	3.0 (0.0, 10.0)	0.0 (0.0, 0.0)	1	0.063
<70	28.0 (22.0, 32.0)	0.0 (0.0, 0.0)	0.0 (0.0, 0.0)	0.002	1
<54	0.0 (0.0, 12.0)	0.0 (0.0, 0.0)	0.0 (0.0, 0.0)	0.25	1
Hypoglycemic Events					
Level 1	52	6	5	0.004	0.594
Level 2	23	1	0	0.008	1
2 hours after exercise start + 4 hours					
Population Median Glucose (mg/dl)	92.8 (87.7, 97.5)	126.7 (119.4, 135.1)	114.7 (112.0, 120.1)	0.002	0.002
CHO/session (g/session)	15.0 (0.0, 22.5)	0.0 (0.0, 0.0)	0.0 (0.0, 0.0)	0.125	0.5
Percentage of time spent in... (mg/dl)					
70–180	92.9 (88.8, 100.0)	100.0 (100.0, 100.0)	100.0 (100.0, 100.0)	0.016	0.5
>180	0.0 (0.0, 0.0)	0.0 (0.0, 0.0)	0.0 (0.0, 0.0)	1	1
<70	7.1 (0.0, 11.2)	0.0 (0.0, 0.0)	0.0 (0.0, 0.0)	0.016	1
<54	0.0 (0.0, 0.0)	0.0 (0.0, 0.0)	0.0 (0.0, 0.0)	1	1
Hypoglycemic Events					
Level 1	58	7	1	0.002	0.063
Level 2	1	0	0	1	1

Values reported as mean ± standard deviation and median (25th percentile, 75th percentile). * p value between unannounced and EHRA scenarios. † p value between announced and EHRA.

Figure 6.4 shows an aggregated plot of the CGM readings, insulin delivery, and delivered CHO for all 80 exercise sessions (eight sessions per patient). Exercise commenced at hour zero for a duration of 50 minutes. The improvement in BG control one hour before exercise and six hours after exercise for the EHRA can be visualized in this plot, which shows a lower prevalence in median (25th percentile, 75th percentile) glucose values above 180 mg/dl and below 70 mg/dl

when compared to the unannounced and announced exercise strategies. Additionally, it can be seen that during the unannounced exercise strategy the controller overcorrects for consumed rescue CHO resulting in unnecessary insulin delivery.

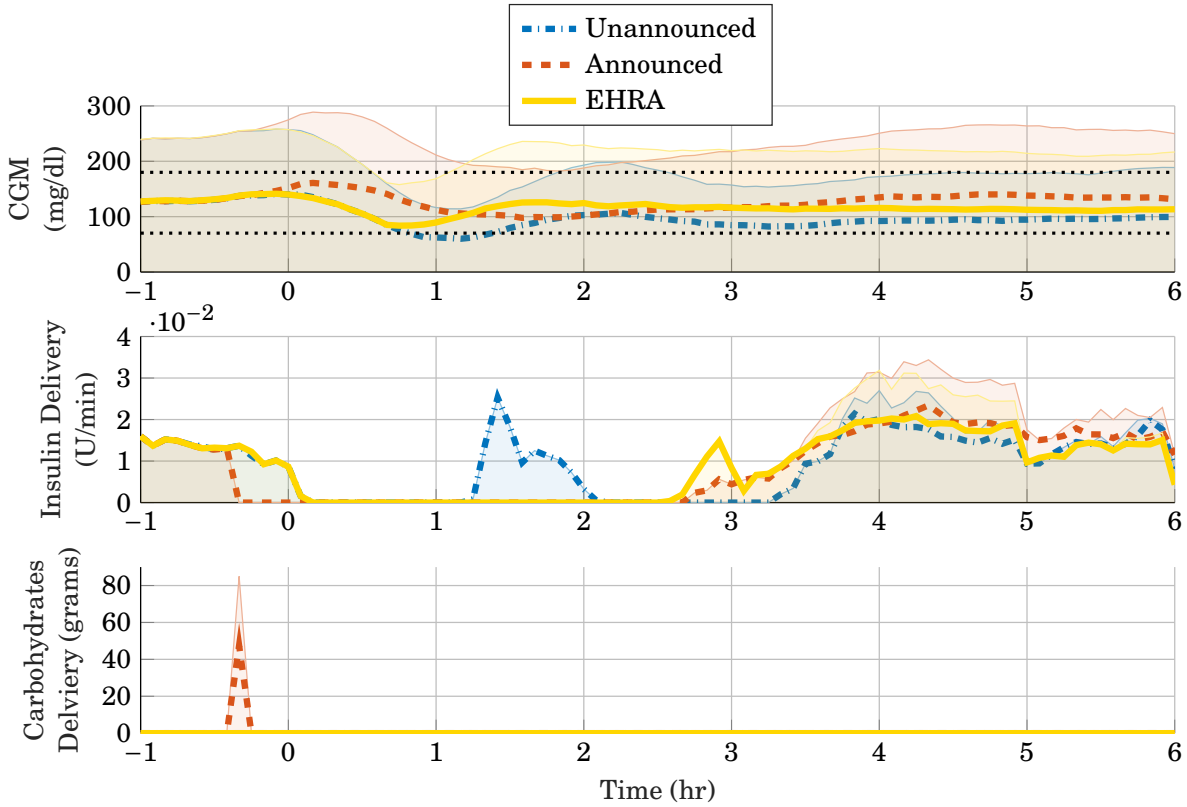

Figure 6.4: Aggregated population CGM readings (mg/dl), insulin delivery (U/min), and carbohydrates delivery (grams) for 80 exercise sessions for the unannounced, announced and EHRA control strategies. Exercise commenced at hour 0 for a duration of 50 min. Graph reported as median (bold lines), 25th percentile and 75th percentile (lightly shaded area), hypoglycemia threshold of 70 mg/dl (dotted lower line), and hyperglycemia threshold of 180 mg/dl (dotted upper line).

The intensity of exercise in the scenario previously described was decreased and increased by 25% from the nominal value of 60% VO_{2max} to test the EHRA for robustness. Table 6.6 shows the overall outcomes for the three control with the exercise intensity decreased and increased by 25%. Here we can see the ability of the EHRA to respond to different exercise intensities as the amount of CHO/day is increased from 29 to 41 g/day from -25% intensity to +25% intensity. While the announced exercise strategy performs well with -25% intensity with no significant difference in the number of hypoglycemic events when compared to the EHRA (p=1), it performs poorly with +25% intensity. The announced exercise strategy produces seven level 2 hypoglycemic events compared to the EHRA, which is able to avoid all level 2 hypoglycemic events (p=0.031).

The overall outcomes for the EHRA for all three intensities of aerobic exercise (see Tables

Table 6.6: Overall population outcomes of a 15-day simulation with exercise intensity decreased and increased by 25% for three strategies in closed-loop control: unannounced exercise, announced exercise, and unannounced exercise with an EHRA. There were 80 sessions of exercise in total.

	Unannounced	Announced	EHRA	p*	p†
Exercise Intensity Decreased by 25%					
Population Median Glucose (mg/dl)	120.6 (119.3, 124.9)	129.2 (124.1, 132.6)	126.0 (123.0, 132.8)	0.002	0.16
CHO/day (g/day)	21.4 (13.9, 27.9)	31.1 (28.6, 32.9)	28.8 (26.4, 34.6)	0.004	0.951
Percentage of time spent in... (mg/dl)					
70–180	94.5 (93.8, 96.5)	92.7 (89.2, 93.9)	93.4 (91.0, 94.3)	0.014	0.412
>180	4.3 (2.0, 4.6)	7.3 (5.9, 10.8)	6.6 (5.7, 9.0)	0.002	0.557
<70	1.4 (0.9, 1.9)	0.0 (0.0, 0.1)	0.0 (0.0, 0.0)	0.002	0.25
<54	0.0 (0.0, 0.1)	0.0 (0.0, 0.0)	0.0 (0.0, 0.0)	0.063	1
Hypoglycemic Events					
Level 1	97	3	2	0.002	1
Level 2	7	1	0	0.125	1
Exercise Intensity Increased by 25%					
Population Median Glucose (mg/dl)	119.1 (118.5, 124.7)	124.1 (121.5, 128.0)	124.8 (121.5, 130.4)	0.002	0.131
CHO/day (g/day)	34.8 (27.9, 46.1)	31.1 (28.6, 32.9)	41.3 (40.4, 48.9)	0.008	0.002
Percentage of time spent in... (mg/dl)					
70–180	93.6 (92.6, 95.4)	93.6 (91.0, 95.3)	92.0 (90.9, 92.7)	0.01	0.02
>180	4.2 (2.0, 4.6)	5.6 (3.9, 7.6)	7.6 (7.1, 9.1)	0.002	0.004
<70	2.4 (1.9, 3.4)	0.7 (0.2, 1.4)	0.1 (0.0, 0.2)	0.002	0.006
<54	0.3 (0.2, 0.8)	0.1 (0.0, 0.2)	0.0 (0.0, 0.0)	0.002	0.031
Hypoglycemic Events					
Level 1	133	25	13	0.002	0.094
Level 2	36	7	0	0.002	0.031

Values reported as mean ± standard deviation and median (25th percentile, 75th percentile).* p value between unannounced and EHRA scenarios. † p value between announced and EHRA.

6.4 and 6.6) show no significant difference in the percentage of time between 70–180 mg/dl with p=0.625 (nominal vs. -25%), p=0.064 (nominal vs. +25%), and p=0.416 (-25% vs. +25%). There was also no significant difference in the percentage of time <54 mg/dl with p=1 for nominal vs. -25%, nominal vs. +25%, and -25% vs. +25%. However, there was a significant difference in the percentage of time <70 mg/dl with p=0.031 (nominal vs. -25%), p=0.016 (nominal vs. +25%), and p=0.008 (-25% vs. +25%). Although with greater intensities of exercise there is an increase in the amount of hypoglycemia experienced as seen in the percentage of time <70 mg/dl, the EHRA is able to prevent severe hypoglycemia (BG <54 mg/dl) for all intensities of exercise tested, thereby

increasing the level of safety to the patient.

The EHRA was then tested when the patient decides not to comply with the suggested CHO consumption and instead consume rescue CHO only when BG is <70 mg/dl similar to the unannounced case (Chapter 6.3.3). Table 6.7 are the results during the three intensities with the intensity decreased by 25%, the nominal intensity of 60% VO_{2max}, and the intensity increased by 25%. Here we can see that when compared to unannounced exercise, although the amount of level 1 hypoglycemic events are reduced from 97 to 67, 118 to 59, and 133 to 52 for the three different intensities, the amount of the level 2 hypoglycemic events have not been markedly reduced from 7 to 6, 24 to 22, and 36 to 34.

Table 6.7: Overall population outcomes of a 15-day simulation with exercise intensity decreased by 25% (-25%), for the nominal intensity of 60% VO_{2max} (nominal), and with the intensity increased by 25% (+25%) during unannounced exercise with an exercise-induced hypoglycemia reduction algorithm (EHRA) without suggested carbohydrate consumption. There were 80 sessions of exercise in total.

	-25%	Nominal	+25%
		Overall Outcomes	
Population Median Glucose (mg/dl)	123.7 (121.5, 130.7)	123.1 (120.5, 129.0)	122.5 (120.2, 128.0)
CHO/day (g/day)	16.1 (10.7, 18.2)	18.2 (13.9, 22.5)	19.8 (16.1, 24.6)
Percentage of time spent in (mg/dl)			
70–180	93.6 (92.3, 95.1)	93.2 (91.7, 95.5)	92.8 (91.6, 94.7)
>180	5.5 (3.7, 6.5)	5.5 (3.1, 7.0)	5.6 (3.8, 7.2)
<70	1.1 (0.6, 1.2)	1.3 (0.9, 1.6)	1.4 (1.1, 1.9)
<54	0.0 (0.0, 0.1)	0.1 (0.1, 0.5)	0.2 (0.1, 0.8)
Hypoglycemic Events			
Level 1	67	59	52
Level 2	6	22	34

Values reported as mean ± standard deviation and median (25th percentile, 75th percentile).

6.4 Discussion

In this study, an EHRA that detects aerobic exercise and triggers exercise-induced hypoglycemia mitigation actions was implemented into an existing closed-loop controller and tested in silico using the T1D Simulator extended with the exercise model [160] in a realistic and challenging scenario. The EHRA was tuned using the lowest D value in a well-controlled in silico simulation without exercise that represented normal patient dynamics and variation. The principal idea behind the tuning of the EHRA was that glucose uptake during aerobic exercise produces a more profound effect on D than the effect of insulin-promoted glycogenesis; therefore, D values during exercise should be lower than those experienced in the absence of exercise. To effectively use the

methodology outlined in this study, the threshold must be optimally adjusted for each patient as it plays a central role in both the detection of exercise and in CHO dosing. Primarily, the EHRA responds to glycemic impact of exercise and detects a prominent and inexplicable decrease in glucose that is assumed to be aerobic exercise as seen in the Δ glucose in Figure 6.2.

In a real-life setting, the threshold tuning can be performed with retrospective data from patients or using an adaptive threshold. Ideally, three sets of clincal data are required to tune and validate the EHRA: 1) a well-controlled scenario for tuning, 2) a scenario without announced exercise for testing the threshold, and 3) a scenario without announced exercise for validation of the threshold. However as seen in Table 6.1, this well-controlled scenario may be overly optimistic as to gain these results requires a very well-tuned controller, a period of fasting, or a period of consuming small meals. Furthermore, more research is required on the state estimations performed and on the methodologies required to identify different tuning methodologies.

Dasanayake et al. [19] reported detection times of both the start and end of 60 and 90 minutes exercise sessions of 30% and 50% predicted heart rate reserve (HRR). An accelerometer and HRM were used to detect exercise using principal component analysis. Onset was identified within 6 $\pm$ 3 minutes and 5 $\pm$ 2 minutes (mean $\pm$ standard deviation), while completion was detected within 3 $\pm$ 8 minutes and 6 $\pm$ 5 minutes, respectively. Δ glucose from start of exercise to detection time was 1 $\pm$ 6 mg/dl and –1 $\pm$ 3 mg/dl, and, from the end of exercise to detection time was 6 $\pm$ 4 mg/dl and –17 $\pm$ 13 mg/dl, respectively, for the two exercise sessions. FP and FN ratios were 4 $\pm$ 2% and 21 $\pm$ 22%. Here we can see that the use of external physiological signals allow exercise to be detected at an earlier time with little change in glucose when compared to the EHRA. However, there is a high FP and FN ratio compared to the EHRA having a FP/day of mean 0 $\pm$ 0 (median: 0 [0, 0.1]) with no FN occurrences. There is also an added burden with the use of these devices as they must be maintained and worn by the user. It should be noted that these values cannot be directly compared because HRR is not equivalent to VO_{2max}, but is instead equivalent to a percentage of the difference between resting and maximal VO_2 or the $VO_{2reserve}$ [179].

Jacobs et al. [20] performed a study that included 13 subjects with T1D using an accelerometer and HRM. Each subject underwent 45 minutes of mild aerobic exercise (30-50% VO_{2max}). Exercise was detected using an accelerometer and a HRM as inputs into a validated regression model. Their detection algorithm was reported to have a sensitivity of 97.2% and a specificity of 99.5%. This intensity of exercise can be likened to the scenario with exercise decreased by 25% where the sensitivity obtained was marginally lower at 96 $\pm$ 6% (median: 100 [88, 100]%). Although, the specificity was not calculated it is suggested that the high specificity obtained in Jacobs et al. [20] means there were very few FP occurrences, which is similar to our FP/day results of 0 $\pm$ 0 (median: 0 [0, 0.1]).

The outcomes reported in this study are unable to be compared to other exercise detection studies with exercise-induced hypoglycemia mitigation strategies [16, 17, 21] because results for

these studies were compared among different arms in their respective study but they failed to provide general comparable metrics such as time between 70–180 mg/dl or number of hypoglycemic events.

Although the lasting effects of aerobic exercise are not fully understood, and it is unknown if they are well represented in the exercise model implemented, results obtained in this study are in keeping with the literature [26, 176] where the exercise detections up to eight hours after the initial detection of exercise can be attributed to the persistent effect of aerobic exercise. This also explains the need for two values of k_{FF}, where if there is a second detection within eight hours of the previous one and $D(t)$ is less than $D(t^*)$ it is assumed that it is a second detection of the same exercise session due to late-onset postexercise hypoglycemia. This allows the controller to perform disturbance rejection actions with a reduced CHO suggestion to account for the delayed effect of aerobic exercise on BG. This persistent effect of aerobic exercise on BG control further reinforces the need for exercise detection as it is particularly challenging for patients to control on their own.

As stated before, the EHRA exploited in this study detects a profound and pervasive drop in BG that is assumed to be provoked by a physiological process other than insulin-promoted glycogenesis, i.e. drops in glucose that are not a result of insulin delivery. If a FP occurs, the patient is likely in a state where action is required to prevent a hypoglycemic event. Therefore, the outcomes of the actions implemented by the EHRA are unlikely to produce a negative effect. Additionally, the controller returns to its nominal state when certain escape conditions are met and ensures that the patient will not enter into extreme hyperglycemia due to these actions.

An increase of 25% in the intensity was chosen as any greater increase may result in the activation of the anaerobic system, where glucose dynamics and patient requirements are different and not represented in the implemented exercise model. The nominal intensity of exercise (60% VO_{2max}) was increased and decreased by manipulating the fitted heart rate value [160] in the Model C exercise model found in Dalla Man et al. [159], which increased or decreased the impact of exercise on BG. The different intensities tested can also account for the wide variability in glucose profiles present before, during and after exercise [180] attributed to a multitude of factors such as the amount of IOB, starting glucose, total muscle mass, BMI, age, duration of T1D, progression of T1D, stress level, insulin sensitivity, rate of glucose uptake, etc.

In the previous simulations described it is assumed that the user will consume CHO in the time sample following exercise detection. However, it is known that one major challenge of systems such as these is user adherence and despite CHO suggestions, users will opt out of CHO consumption. Therefore, a simulation was included that assumed that the user ignored or did not hear the alarm to consume CHO. Table 6.7 shows that there is a degradation in system performance and user glycemic outcomes especially in the amount of level 2 hypoglycemic events experienced. This suggests that without preemptive CHO consumption, these severe hypoglycemic events cannot be prevented during unannounced aerobic exercise with the current

EHRA implementation. Despite the challenges associated with user adherence, it is also possible for the user to improve the system by confirming or denying exercise, improving system outcomes and avoiding severe hyperglycemia caused by unnecessary rescue CHO consumption.

It can be seen that a downfall of the announced exercise strategy is that the alternations to the controller and number of CHO given to the patient remain the same regardless of exercise intensity. Here we can see that the EHRA is adaptive based on the glycemic impact of the exercise session, as less CHO are suggested during lower intensity exercise and more are suggested during higher intensity exercise. The IOB is also lower when the EHRA detects exercise and therefore, the rescue CHO have a greater effect on glycemia when compared to the announced strategy where CHO are given before exercise. The EHRA also includes a COB calculation, which prevents a calculated amount of insulin relative to the amount of CHO consumed from being delivered that in turn prevents an overcorrection by the controller due to rescue CHO. However, a similar COB strategy could also be implemented into an exercise announcement strategy. Furthermore, the EHRA has the added benefit of calculating the amount of CHO required to prevent hypoglycemia, further removing the burden from the patient. This COB calculation can be tailored to any type of fast-acting CHO, according to user preference (e.g. glucose gels or sports drinks). In this application, fast-acting CHO where the carbohydrate quantities are easily found on the packaging are desirable. However, this would require tuning for each subject and each type of CHO, which must be further explored. For simplicity, the carbohydrate-to-insulin gain, β, was given a populational value, however in a real-life setting this value should be patient specific and must also be further explored.

The EHRA relies on the accuracy of CGM readings as they are a direct input to the UKF. However, it has been shown that there is a tendency for the MARD to increase during periods of aerobic exercise [50–53]. Several factors have been attributed to this degradation in CGM accuracy including microcirculation perturbation, variations of the oxygen concentration in the blood, increase in body temperature, rapid BG changes in the plasma caused by exercise, and mechanical forces where the sensor is placed or movement around or within the insertion area and sensor during aerobic exercise. After the cessation of exercise, it has been found that CGM accuracy returns to baseline values. Therefore, one major possible downfall of this strategy lies in inaccurate CGM readings, however, with new CGM generations these short comings might be addressed. Another possible downfall lies in current insulin formulations that experience a delay between its administration and insulin action. The delays associated with subcutaneous insulin administration contribute to increased amounts of IOB, which increase the risk of hypoglycemic events during aerobic exercise.

An advantage of the EHRA is that it is linked to a profound drop in BG as seen in Figure 6.2 and is therefore unlikely to be triggered in the presence of anaerobic exercise due to the increase in BG experienced during this type of exercise.

6.5 Summary

In this study, an EHRA that detects aerobic exercise and triggers exercise-induced hypoglycemia mitigation actions was implemented into an existing closed-loop controller and tested in silico using the T1D Simulator extended with an exercise model in a 15-day scenario with eight exercise sessions on alternating days. The EHRA was tuned using the lowest D value in a well-controlled in silico simulation without exercise that represented normal patient dynamics and variation. The exercise detection algorithm is able to detect all exercise events with a detection time of 41.1 ± 9.7 minutes (median: 40 (30, 62.5) minutes) and a drop in glucose of 53.7 ± 21.8 mg/dl (median: 52 (23.7, 89.4) mg/dl) during exercise at 60% VO_{2max}. After exercise detection, the EHRA triggers a CHO suggestion, a decrease in basal insulin, and a reduction of the next meal bolus. The EHRA outperforms both unannounced and announced aerobic exercise strategies in terms of BG control and is able prevent all severe hypoglycemic events (<54 mg/dl) without causing excess hyperglycemia due to CHO suggestions and has been proven robust during an intensity of 60% VO_{2max} and when this intensity is decreased and increased by 25%. However, if the suggested CHO are not consumed, BG control deteriorates and level 2 hypoglycemic events cannot be prevented.

CHAPTER 7

CONCLUSION

Hybrid closed-loop AP systems are gradually moving towards a fully closed-loop design. Therefore, the user of the system will be required to perform less actions and have less responsibility for their overall T1D management. The first step to closing the loop is removing meal and aerobic exercise announcement; however, many challenges still remain due to the delay in meal detection, insulin action lag time, and the discrepancy in postprandial hyperglycemia, which is dependent on meal composition and intra-patient variability.

A PHRA and EHRA that use CGM values and a disturbance parameter, D, estimated from an adapted minimal model using an UKF have been presented. Tuning of the PHRA is complicated by the need to administer insulin as soon as possible due to the lag in insulin action. Therefore, three tunings that are useful for the mitigation of postprandial hyperglycemia, Ra discrimination, and CHO estimation methodologies and postprandial mitigation actions have been explored. Furthermore, an EHRA tuned using the lowest value of D in a well-controlled in silico simulation without exercise along with disturbance rejection actions to prevent exercise-induced hypoglycemia have been tested. Both the PHRA and EHRA were implemented using the T1D Simulator, a modified version of the UVA/Padova T1D Simulator well-known as a tool for the testing of novel technologies in diabetes care and a well-established starting point for evaluating the presented PHRA and EHRA.

Limitations to the proposed strategies include the lag in insulin action, which complicates control during the postprandial period and aerobic exercise. The CHO estimation methodology presented has a large estimation error that limits is usefulness. The methodology to identify fast absorption meals, although effective, has not been utilized for postprandial hyperglycemic mitigation and further research is required here. Lastly, the degradation in performance of the EHRA due to the user not consuming the suggested CHO is a limitation to this strategy, as severe

hypoglycemia cannot be prevented without the consumption of the these sugeested CHO.

This thesis concludes by providing a summary of the contributions of this thesis and a discussion of potential future research on the subject of this thesis.

7.1 Contributions

The main contribution of this thesis is the development of effective and safe CLC strategies for postprandial and postexercise glucose control in patients with T1D, which is the beginning steps of the realization of the AP as a fully CLC system. A postprandial hyperglycemia reduction algorithm (PHRA) and a exercise-induced hypoglycemia reduction algorithm (EHRA), which were designed and developed in this thesis, will be extensively evaluated in silico and then are expected to be validated clinically. As a result of this thesis the following contributions have been made:

- The development of a detection system able to detect perturbations using a state estimator, which consists of an augmented minimal model and an UKF. This system has the ability to be used and tested with other disturbances present in T1D patients such as during stress or illness.
- The development of a novel meal detection algorithm that uses the state estimator to estimate a disturbance parameter. The cross-covariance between the glucose data and the forward difference of computed disturbance parameter is then calculated over different sliding windows. A threshold is then applied, different for each sliding window. This algorithm able to detect large and rapidly appearing meals quickly with very little change in glucose at detection.
- The implementation of a PHRA, which includes three tunings able to detect meals with varying detection times and sensitivities. Using the three tunings, disturbance rejection actions are applied and are able to reduce postprandial hyperglycemia.
- The implementation of a EHRA, that offers a reliable and easy tuning methodology. Disturbance rejection actions are applied after detection that include a CHO estimation and changes in controller dependent and independent variables. This EHRA has been proven to be robust during exercise of varying intensities.

7.2 Future Work

To continue the research initiated by this thesis, several improvements should be made to the developed systems to be employed in a real life situation:

- To obtain rich clinical data that represents frequent activities that the subject participates in such as eating out, exercising, etc., in order to develop a methodology for determining the minimum and maximum values required for the scaling of data prior to finding the cross-covariance between D_{diff} and $G(t)$ in the PHRA.
- To obtain the clinical data necessary for the tuning of the PHRA for meal detection. This requires data with a variety of meals without meal boluses, in which a detection bank of multiple thresholds and windows can be developed and the most favorable tunings selected.
- To obtain three sets of clinical data to tune and validate the EHRA: 1) a well-controlled scenario for tuning, 2) a scenario with unannounced exercise for testing the threshold, and 3) a scenario with unannounced exercise for validation of the threshold.
- The integration of the two strategies into current hybrid systems to increase their efficacy and safety during meals and exercise. This includes combining the meal type discrimination to lower hypoglycemic events during slow absorption meals, including CHO suggestions before and during aerobic exercise to to lower the burden to the patient, and including COB to prevent controller overcorrection allowing the patient to enter CHO amounts anytime rescue CHO are consumed.
- The exploration of the $\overline{IOB}_m in$, which may be necessary during aerobic exercise where the omission of insulin administration over an extended period of time can lead to life threatening DKA.
- To join the two algorithms developed in this thesis into a unified system. This will include significant alterations to the two algorithms to prevent systems clashes.
- To explore other ways in which improvement to BG control during the postprandial periods can be improved, such as the infusion of other hormone replacements e.g. pramlintide and GLP-1 receptor agonists.

APPENDIX A

THE UNIVERSITY OF VIRGINIA/PADOVA MIXED MEAL SIMULATION MODEL

The mixed meal simulation model found in the UVA/Padova T1D Simulator is shown in Figure A.1 is outlined below.

Glucose Subsystem

A two compartment model was used to describe glucose kinetics:

$$\begin{aligned} \dot{G}_p(t) &= EGP(t) + Ra(t) - U_{ii} - E(t) - k_1 \cdot G_p(t) + k_2 \cdot G_t(t) \quad G_p(0) = G_{pb} \\ \dot{G}_t(t) &= -U_{id}(t) + k_1 \cdot G_p(t) - k_2 \cdot G_t(t) \quad G_t(t) = 0 \\ G(t) &= \frac{G_p(t)}{V_G} \quad G(0) = G_b \end{aligned} \tag{A.1}$$

where G_p and G_t (mg/kg) are glucose masses in plasma and rapidly-equilibrating tissues, and in slowly-equilibrating tissues, respectively, G (mg/dl) is the plasma glucose concentration where suffix b denotes basal state, EGP is the endogenous glucose production (mg/kg/min), Ra is the glucose rate of appearance in plasma (mg/kg/min), E is the renal excretion (mg/kg/min), U_{ii} and U_{id} are the insulin-independent and –dependent glucose utilizations (mg/kg/min), V_G is the glucose distribution volume (dl/kg), and k_1 and k_2 (min^{-1}) are rate parameters.

Insulin Subsystem

A two-compartment model was used to describe insulin kinetics:

$$\begin{aligned} \dot{I}_p(t) &= -(m_2 + m_4) \cdot I_p(t) + m_1 \cdot I_l(t) + R_{ai}(t) \quad I_p(0) = I_{pb} \\ \dot{I}_l(t) &= -(m_1 + m_3) \cdot I_l(t) + m_2 \cdot I_p(t) \quad I_l(0) = I_{lb} \\ I(t) &= \frac{I_p(t)}{V_I} \quad I(0) = I_b \end{aligned} \tag{A.2}$$

where I_p and I_l (pmol/kg) are insulin masses in plasma and in liver, respectively, I (pmol/l) is the plasma insulin concentration, R_{ai} is insulin secretion (pmol/kg/min), V_I is the insulin distribution volume (l/kg), and m_1, m_2, m_4 (min^{-1}) are rate parameters. Here a linear peripheral degradation (m_3) is assumed, while hepatic extraction (HE) is:

$$\begin{aligned} HE(t) &= -m_5 \cdot R_{ai}(t) + m_6 \quad HE(0) = HE_b \\ m_3(t) &= \frac{HE(t) \cdot m_1}{1 - HE(t)} \end{aligned} \tag{A.3}$$

where m_5 and m_6 (min^{-1}) are rate parameters.

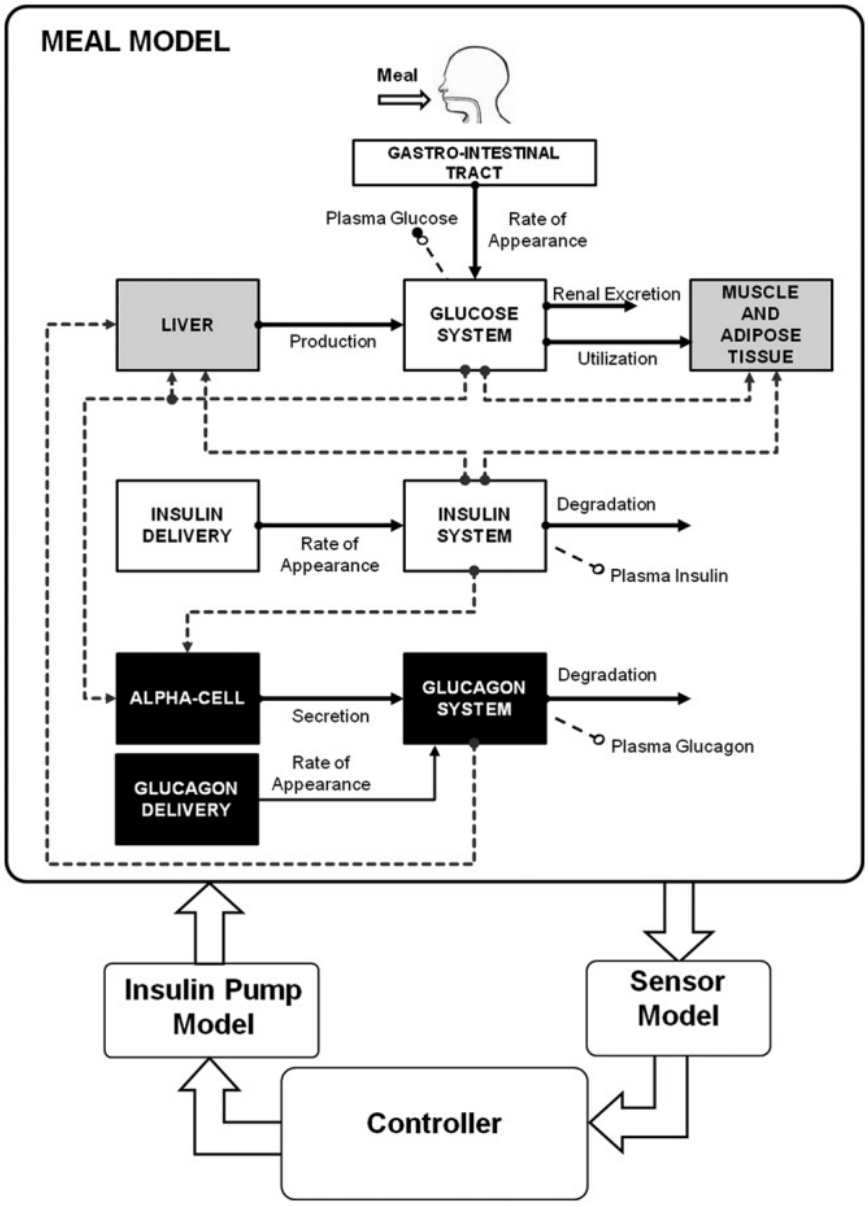

Figure A.1: Model scheme of the the UVA/Padova T1D Simulator [155].

Endogenous Glucose Production

The functional description of endogenous glucose production (EGP) comprises of a direct glucose signal of both delayed and anticipated insulin signals. The model has been updated to assume that EGP is stimulated by the basal glucagon concentration with a delay:

$$\begin{aligned} EGP(t) &= k_{p1} - k_{p2} \cdot G_p(t) - k_{p3} \cdot X^L(t) + \xi \cdot X^H(t) & EGP(0) &= EGP_b \\ \dot{X}^L(t) &= -k_i \cdot (X^L(t) - I'(t)) & X^L(0) &= I_b \\ \dot{I}'(t) &= -k_i \cdot (I'(t) - I(t)) & I'(0) &= I_b \\ \dot{X}^H(t) &= -k_H \cdot X^H(t) + k_H \cdot max((H(t) - H_b), 0) & X^H(0) &= 0 \end{aligned} \tag{A.4}$$

where $X^L(t)$ is the delayed insulin action in the liver, k_i, k_{p1}, k_{p2}, and k_{p3} are rate parameters, $H(t)$ is the plasma glucagon concentration, $X^H(t)$ is the delayed glucagon action on EGP, ξ is the liver responsivity to glucagon, and $1/k_H$ is the delay between the glucagon concentration and action.

Glucose Rate of Appearance

Glucose intestinal absorption is modeled as:

$$\begin{aligned} Q_{sto}(t) &= Q_{sto1}(t) + Q_{sto2}(t) & Q_{sto}(0) &= 0 \\ \dot{Q}_{sto1}(t) &= -k_{gri} \cdot Q_{sto1}(t) + D \cdot \delta(t) & Q_{sto1}(0) &= 0 \\ \dot{Q}_{sto2}(t) &= -k_{empt}(Q_{sto}) \cdot Q_{sto2}(t) + k_{gri} \cdot Q_{sto1}(t) & Q_{sto2}(0) &= 0 \\ \dot{Q}_{gut}(t) &= -k_{abs} \cdot Q_{gut}(t) + k_{empt}(Q_{sto}) \cdot Q_{sto2}(t) & Q_{gut}(0) &= 0 \\ Ra(t) &= \frac{f \cdot k_{abs} \cdot Q_{gut}(t)}{BW} & Ra(0) &= 0 \end{aligned} \tag{A.5}$$

where Q_{sto} (mg) is amount of glucose in the stomach (solid, Q_{sto1}, and liquid phase, Q_{sto2}), Q_{gut} (mg) is the glucose in the intestine, k_{gri} (min^{-1}) is the rate of grinding, k_{abs} (min^{-1}) is a rate constant of intestinal absorption, f is the fraction of intestinal absorption which appears in plasma, D (mg) is the amount of ingested glucose, and BW (kg) is body weight. $k_{empt}(Q_{sto})$ (min^{-1}) is a rate constant of gastric emptying which is a nonlinear function of Q_{sto} calculated as:

$$k_{empt}(Q_{sto}) = k_{min} + \frac{k_{max} - k_{min}}{2} \cdot \Big(tanh\big(\alpha(Q_{sto} - b \cdot D)\big) - tanh\big(\beta(Q_{sto} - c \cdot D)\big) + 2 \Big) \tag{A.6}$$

where k_{max} is when the stomach contains the amount of ingested glucose D, α is the rate at which k_{max} decreases to a minimum (k_{min}), and β is the rate at which k_{min} increases back to its maximum (k_{max}) [172].

Glucose Utilization

Glucose utilizations by body tissues is made up of two components U_{ii} and U_{id}. Insulin-independent utilization takes place in the first compartment, is constant, and represents glucose uptake by the brain and erythrocytes (Fcns):

$$U_{ii}(t) = F_{cns} \tag{A.7}$$

Insulin-dependent utilization occurs in the remote compartment, which represents peripheral tissues and depends nonlinearly, i.e., via Michaelis–Menten kinetics, on glucose in tissues:

$$U_{id}(t) = \frac{\left(V_{m0} + V_{mx} \cdot X(t) \cdot (1 + r_1 \cdot risk)\right) \cdot G_t(t)}{K_{m0} + G_t(t)} \tag{A.8}$$

where G_t (mg/kg) is glucose mass in the remote compartment and V_{m0} is assumed to be linearly dependent on X (pmol/l), which represents remote insulin described by:

$$\dot{X}(t) = -p_{2U} \cdot X(t) + p_{2U}(I(t) + I_b) \qquad X_i(0) = 0, \tag{A.9}$$

where I_b plasma insulin in the basal states, and p_{2U} (min^{-1}) is the rate constant of insulin action on peripheral glucose utilization. The model assumes that $U_{id}(t)$ increases when glucose decreases below a certain threshold, following the BG risk function:

$$\begin{aligned} risk &= \begin{cases} 0 & if G \geq G_b \\ 10 \cdot (f(G))^2 & if G_{th} \leq G < G_b \\ 10 \cdot (f(G_{th}))^2 & if G < G_{th} \end{cases} \\ f(G) &= \left(log(G)\right)^{r_2} - \left(log(G_b)\right)^{r_2} \end{aligned} \tag{A.10}$$

where G_{th} is the hypoglycemic threshold set at 60 mg/dl and r_1 and r_2 are model parameters.

Renal Excretion

Glucose excretion by the kidney occurs if G_p exceeds a certain threshold and can be modeled by a linear relationship with G_p:

$$E(t) = \begin{cases} k_{e1} \cdot (G_p(t) - k_{e2}) & if G_p(t) > k_{e2} \\ 0 & if G_p(t) \leq k_{e2} \end{cases} \tag{A.11}$$

where k_{e1} (min^{-1}) is the glomerular filtration rate and k_{e2} (mg/kg) is the renal threshold of glucose.

Subcutaneous Insulin Kinetics

Insulin secretion is represented by a two compartment model:

$$\begin{aligned} R_{ai}(t) &= k_{a1} \cdot I_{sc1}(t) + k_{a2} \cdot I_{sc2}(t) \\ \dot{I}_{sc1}(t) &= -(k_d + k_{a1}) \cdot I_{sc1}(t) + IIR(t) \quad I_{sc1}(0) = I_{sc1ss} \\ \dot{I}_{sc2}(t) &= k_d \cdot I_{sc1}(t) - k_{a2} \cdot I_{sc2}(t) \quad I_{sc2}(0) = I_{sc2ss} \end{aligned} \tag{A.12}$$

where I_{sc1} and I_{sc2} are insulin in the first and second subcutaneous compartments, respectively, k_d (min^{-1}) is the rate constant of insulin dissociation, and k_{a1} and k_{a2} are rate constants of nonmonomeric and monomeric insulin absorption, respectively.

Subcutaneous Glucose Kinetics

The blood to interstitial glucose dynamics are described as a first-order linear system:

$$\dot{G}_s(t) = -\frac{1}{T_s}G_s(t) + \frac{1}{T_s}G(t) \qquad G_s(0) = G_b \tag{A.13}$$

where G_s represents subcutaneous glucose and T_s represents the time constant of the system.

Glucagon Kinetics and Secretion

Glucagon kinetics are described by a one compartment linear model:

$$\dot{H}(t) = -n \cdot H(t) + SR_H(t) + Ra_H(t) \quad H(0) = H_b \tag{A.14}$$

where $H(t)$ is the plasma glucagon concentration, $SR_H(t)$ is the glucagon secretion ($SR^b_H(t)$ is the basal value), and n is the clearance rate. Glucagon secretion is described as a sum of two compartments:

$$\begin{aligned} SR_H(t) &= SR^s_H(t) + SR^d_H(t) \\ \dot{SR}^s_H(t) &= \begin{cases} -\rho \cdot \left(SR^s_H(t) - max\left(\sigma_2 \cdot (Gth - G(t)) + SR^b_H, 0\right)\right) & \text{if } G(t) \geq G_b \\ -\rho \cdot \left(SR^s_H(t) - max\left(\frac{\sigma \cdot (Gth - G(t))}{I(t)+1} + SR^b_H, 0\right)\right) & \text{if } G(t) < G_b \end{cases} \end{aligned} \tag{A.15}$$

where σ and σ_2 are alpha-cell responsivity to glucose level, $1/\rho$ is the delay between static glucagon secretion and plasma glucose. In this way, static secretion is stimulated when $G_p < G_b$ (but modulated by insulin) and inhibited when $G_p \geq G_b$. The second component is proportional to glucose rate of change:

$$SR^d_H(t) = \delta \cdot max\left(-\frac{dG(t)}{dt}, 0\right) \tag{A.16}$$

where $dG(t)/dt$ is the glucose rate of change and δ is the alpha-cell responsivity to glucose rate of change.

Subcutaneous Glucagon Kinetics

The interstitial to blood glucagon dynamics are described as a two compartment model:

$$\begin{aligned} R_{aH}(t) &= k_{h3} \cdot H_{sc2}(t) \\ \dot{H}_{sc1}(t) &= -(k_{h1} + k_{h2}) \cdot H_{sc1}(t) + H_{inf}(t) \quad H_{sc1}(0) = H_{sc1b} \\ \dot{H}_{sc2}(t) &= k_{h1} \cdot H_{sc1}(t) - k_{h3} \cdot H_{sc2}(t) \quad H_{sc2}(0) = H_{sc2b} \end{aligned} \tag{A.17}$$

where H_{sc1} and H_{sc2} are glucagon in the first and second subcutaneous compartments, respectively, H_{inf} is the glucagon infusion rate, and k_{h1}, k_{h2} and k_{h3} are rate constants.

APPENDIX B

CLOSED-LOOP CONTROLLER

The closed-loop controller is composed of two loops: the inner control loop, which is a PD controller with IFB designed to drive the measured glucose to a target value and the outer loop, which is a safety supervisory loop that uses SMRC to modulate the glucose target value based on the estimated IOB, which reduces the risk of hypoglycemia due to controller overcorrection [161–163].

B.1 The Proportional-Derivative Controller Loop

The total insulin control action of the inner loop is described as:

$$u_{AP}(t) = u_{basal}(t) + u_{bolus}(t) + u_{PD}(t) \tag{B.1}$$

where $u_{basal}(t)$ is the basal insulin needed by the patient to keep a normal plasma glucose concentration between meals and at night (usually around 100 mg/dl), $u_{bolus}(t)$ is the feed-forward meal bolus derived as:

$$u_{bolus}(t^*) = \frac{u_{meal}}{K_{i2c}} + \frac{\int_{t^*}^{t^*+60} u_{basal}(\tau)d\tau}{60} + \frac{G(t^*) - G_r(t^*)}{K_{cf}}, \tag{B.2}$$

where t^* is the meal time. $u_{PD}(t)$ is the PD control algorithm:

$$u_{PD}(t) = k_p(G(t) - G_{rf}(t)) + k_p\tau_d\dot{G}(t), \tag{B.3}$$

k_p is the proportional gain tuned according to [177]:

$$k_p = \frac{60}{\tau_d}\frac{I_{TDD}}{1500}$$

where u_{meal} is the meal carbohydrate content in grams, K_{i2c} (U/g) is the insulin-to-carbohydrate ratio, $G(t)$ is the measured glucose value, $G_r(t)$ is the predefined glucose target (usually constant),

K_{cf} (mg/dl/U) is the correction factor, $G_{rf}(t)$ is the modulated glucose target described in Section B.2, τ_d (min)is the derivative time, and I_{TDD} (U/day) is the patient's total daily insulin.

The use of an IFB component is widely used in AP applications [116] and is based on the assumption that plasma-insulin concentration inhibits insulin secretion directly at the β-cell level [177]. To replicate this effect in the control algorithm, the plasma insulin concentration (I_p) is estimated as follows [181]:

$$\dot{I}_p(t) = \frac{k_{DIA} \cdot C_2(t)}{BW \cdot V_I} - k_e \cdot I_p(t) \tag{B.4}$$

where t_s (min) is the sampling time, k_{DIA} (min^{-1}) is the subject-specific time constant for the duration of insulin action [162], BW (kg) is the body weight of the patient, V_I (l/kg) is the volume of the plasma insulin compartment, and k_e (min^{-1}) is the fractional elimination rate of insulin from plasma. $C_2(t)$ is an insulin mass compartment described in Section B.2, Equation B.13. Then, using the estimated $I_p(t)$, the insulin control action is proportionally inhibited as follows:

$$u_{IFB}(t) = u_{AP}(t) - \gamma(I_p(t) - I_p^*) \tag{B.5}$$

where γ (l/h) is a IFB term tuned according to [177] and I_p^* is the estimated basal plasma insulin, so that under basal conditions this additional term is nullified.

B.2 Safety Supervisory Loop

The safety supervisory outer control loop is a SMRC [178] module, which modulates G_r in order to avoid violating the IOB constraints. SMRC originates from concepts of invariance control and acts as a transitional mode of operation. For simplicity, $\overline{IOB}_{min}(t)$ is set to zero and the time-variant $\overline{IOB}_{max}(t)$ is computed as follows:

$$\overline{IOB}_{max}(t) = k_{IOB} \cdot \frac{2 \cdot u_{basal}(t)}{60 \cdot k_{DIA}} \tag{B.6}$$

where k_{IOB} is a gain on $\overline{IOB}_{max}$. Given the upper and lower IOB limits (possibly time-variant) and denoting $x(t)$ system's state, the sets:

$$\Sigma^- := \left\{ x(t) | IOB(t) \leq \overline{IOB}_{max}(t) \right\} \tag{B.7}$$

$$\Sigma^+ := \left\{ x(t) | IOB(t) \geq \overline{IOB}_{min}(t) \right\} \tag{B.8}$$

are invariant for a discontinuous signal $\omega(t)$ of the form:

$$\omega(t) = \begin{cases} \omega^+ & \text{if } \sigma^-(t) > 0, \\ \omega^- & \text{if } \sigma^+(t) < 0, \\ 0 & \text{otherwise.} \end{cases} \tag{B.9}$$

where ω^+ and ω^- are set according to [178] and the switching function, σ is defined as:

$$\sigma^-(t) = \begin{cases} 1 & \text{if } IOB(t) - \overline{IOB}_{max}(t) + \sum_{i=1}^{l-1} \tau_i \left(IOB(t)^{(i)} - \overline{IOB}_{max}(t)^{(i)} \right) < 0, \\ 0 & \text{otherwise.} \end{cases} \tag{B.10}$$

$$\sigma^+(t) = \begin{cases} 1 & \text{if } IOB(t) - \overline{IOB}_{min}(t) + \sum_{i=1}^{l-1} \tau_i \left(IOB(t)^{(i)} - \overline{IOB}_{min}(t)^{(i)} \right) > 0, \\ 0 & \text{otherwise.} \end{cases} \tag{B.11}$$

where $d_{IOB}(t)$ is calculated as:

$$d_{IOB}(t) = \frac{IOB(t) - IOB(t-1)}{t_s} \tag{B.12}$$

where τ_i is a constant gain and $\overline{IOB}_{max}(t)$ and $\overline{IOB}_{min}(t)$ are the maximum and mimimum IOB limits, respectively. $IOB(t)$ is estimated using a two-compartment model [182] expanded to account for basal and deviation IOB:

$$\begin{aligned} \dot{C}_1(t) &= u_{IFP}(t) - k_{DIA} C_1(t) \\ \dot{C}_2(t) &= k_{DIA} \left(C_1(t) - C_2(t) \right) \\ IOB(t) &= C_1(t) + C_2(t) \end{aligned} \tag{B.13}$$

where $C_1(t)$ and $C_2(t)$ are the insulin mass in the two subcutaneous compartments that account for basal conditions. G_r is filtered using a low-pass first-order filter that induces smooth changes in the target value:

$$\dot{G}_{rf}(t) = \lambda G_{rf}(t) + \lambda \left(G_r(t) + \omega(t) \right) \tag{B.14}$$

where λ is the filter cut-off frequency [162]. The parameter values used in this controller can be found in Table B.1.

B.3 Clinical Trials

The controller previously described has been tested thus far in two clinical settings [161]. The first was a crossover randomized study performed in two clinical centers with 20 T1D subjects used to compare the CLC system to open loop (OL) therapy during announced meals. For the CLC versus OL, the percent of time-in-range was higher (80% vs. 64%; p<0.001). There was no significant difference in the percent of time below 70 mg/dl (6.1% vs. 3.2%; p>0.05; CLC vs. OL) or the number of rescue CHO (40% vs. 22.5%; p>0.05; CLC vs. OL).

The second study was crossover randomized study with five T1D subjects used to test the CLC system compared to the OL therapy during aerobic and anaerobic exercise. Each subject performed six exercise sessions, which at least one week between each session. Three of the sessions included aerobic exercise and three of the session included anaerobic exercise. after each exercise sessions the patient evaluated the intensity of exercise using the Borg Scale of Perceived

Table B.1: Controller parameter values

Symbol	Quantity	Value	Units
K_{i2c}	Insulin-to-carbohydrate ratio	patient specific	U/g
k_{cf}	Insulin correction factor	patient specific	mg/dl/U
τ_d	Derivative of time	90	min
I_{TDD}	Total daily insulin	patient specific	U/day
G_r	Predefined glucose target	100	mg/dl
k_{DIA}	Gain of the duration of insulin action	0.013	min^{-1}
ω^+	Lower switching signal	0	mg/dl
ω^-	Upper switching signal	350	mg/dl
τ_i	Sensitivity of SMRC for IOB changes	10	min
λ	Filter cut-off frequency	0.1	unitless
γ	Insulin-feedback term	25.2	l/h
k_e	Insulin elimination from plasma	0.138	min^{-1}
V_I	Insulin distribution volume	0.12	l/kg
BW	Body weight of the patient	patient specific	kg
t_s	Sample time of the SMRC algorithm	0.5	min

Exertion. For aerobic exercise, the subjects performed three sets of 15 min in a cycloergometer at 60% VO_{2max} with five min of rest between sets. For anaerobic exercise, subjects performed five series of eight repetitions of four weighted exercises with 90 s of rest between sessions. Each of the four exercises implicated different muscular groups with a weight corresponding to 70% of the patient's maximum exercise capacity. Rescue CHO of 15 grams in the form of glucose gels were given by the clinician if the patient was below 60 mg/dl for ten min or more; following this, CHO were given every 15 min until BG was above 70 mg/dl.

The mean glucose level was 124.0 ± 25.1 mg/dl in the aerobic studies and 152.1 ± 34.1 mg/dl in the anaerobic studies. Percentage of time in the different glucose ranges of 70-180, >180 and <70 mg/dl for aerobic vs. anaerobic sessions were 89.8 ± 18.6%, 7.7 ± 18.4%, and 2.5 ± 6.3% vs. 75.9 ± 27.6%, 23.2 ± 28.0%, and 1.0 ± 3.6%. Six rescues with CHO were required during the studies (4 in aerobic and 2 in anaerobic) [183].

Currently, a third clinical trial is ongoing that includes ten T1D subjects to test a new PD CHO controller added to the controller previously described. Each subject will undergo three aerobic exercise tests, each one at 1-3 week intervals in a random order. The CLC algorithm will be used in two of the exercise tests (one with announced exercise and the other without). For the third exercise test, the control study, the patient will wear a CSII system with a Dexcom G5 Mobile CGM in blinded mode. The trial is expected to be completed in April 2019.

BIBLIOGRAPHY

[1] International Diabetes Federation., *IDF Diabetes Atlas*, 8 ed.; International Diabetes Federation: Brussels, Belgium, 2017.

[2] Russell, S.J.; El-Khatib, F.H.; Sinha, M. et al., Outpatient Glycemic Control with a Bionic Pancreas in Type 1 Diabetes., *The New England Journal of Medicine* **2014**, *371*, 313–25.

[3] Thabit, H.; Tauschmann, M.; Allen, J.M. et al., Home Use of an Artificial Beta Cell in Type 1 Diabetes, *New England Journal of Medicine* **2015**, *373*, 2129–40.

[4] Dassau, E.; Bequette, B.W.; Buckingham, B.A.; Doyle III, F.J., Detection of a Meal Using Continuous Glucose Monitoring, *Diabetes Care* **2008**, *31*, 295–300.

[5] Lee, H.; Bequette, B.W., A closed-loop artificial pancreas based on model predictive control: Human-friendly identification and automatic meal disturbance rejection, *Biomed Signal Process Control* **2009**, *4*, 347–54.

[6] Lee, H.; Buckingham, B.a.; Wilson, D.M.; Bequette, B.W., A closed-loop artificial pancreas using model predictive control and a sliding meal size estimator., *J Diabetes Sci Technol* **2009**, *3*, 1082–90.

[7] Cameron, F.; Niemeyer, G.; Buckingham, B.A., Probabilistic evolving meal detection and estimation of meal total glucose appearance., *J Diabetes Sci Technol* **2009**, *3*, 1022–30.

[8] Cameron, F.; Niemeyer, G., Predicting Blood Glucose Levels Around Meals for Patients With Type I Diabetes, ASME 2010 Dynamic Systems and Control Conference, Volume 1. ASME, 2010, pp. 289–96.

[9] Chen, S.; Weimer, J.; Rickels, M.; Peleckis, A.; Lee, I., Towards a Model-based Meal Detector for Type I Diabetics, 6th Medical Cyber-Physical Systems Workshop, 2015, Vol. April.

[10] Weimer, J.; Chen, S.; Peleckis, A.; Rickels, M.R.; Lee, I., Physiology-Invariant Meal Detection for Type 1 Diabetes, *Diabetes Technol Ther* **2016**, *18*, 616–24.

[11] Xie, J.; Wang, Q., Meal Detection and Meal Size Estimation for Type 1 Diabetes Treatment: A Variable State Dimension Approach, ASME 2015 Dynamic Systems and Control Conference, Volume 1. ASME, 2015, p. V001T15A003.

[12] Turksoy, K.; Samadi, S.; Feng, J. et al., Meal detection in patients with type 1 diabetes: A new module for the multivariable adaptive artificial pancreas control system, *IEEE J Biomed Health Inform* **2016**, *20*, 47–54.

[13] Mahmoudi, Z.; Nørgaard, K.; Poulsen, N.K.; Madsen, H.; Jørgensen, J.B., Fault and meal detection by redundant continuous glucose monitors and the unscented Kalman filter, *Biomed Signal Process Control* **2017**, *38*, 86–99.

[14] Turksoy, K.; Hajizadeh, I.; Samadi, S. et al., Real-time insulin bolusing for unannounced meals with artificial pancreas, *Control Eng Pract* **2017**, *59*, 159–64.

[15] Cameron, F.; Ly, T.T.; Buckingham, B.A. et al., Closed-Loop Control Without Meal Announcement in Type 1 Diabetes., *Diabetes Technol Ther* **2017**, *19*, 527–32.

[16] Stenerson, N.; Cameron, F.; Wilson, D. et al., The impact of accelerometer and heart rate data on hypoglycemia mitigation in type 1 diabetes, *J Diabetes Sci Technol* **2014**, *9*, 64–9.

[17] Stenerson, N.; Cameron, F.; Payne, S. et al., The impact of accelerometer use in exercise-associated hypoglycemia prevention in type 1 diabetes, *J Diabetes Sci Technol* **2015**, *9*, 80–5.

[18] Turksoy, K.; Bayrak, E.; Quinn, L.; Littlejohn, E.; Cinar, A., Multivariable adaptive closed-loop control of an artificial pancreas without meal and activity announcement, *Diabetes Technol Ther* **2013**, *15*, 386–400.

[19] Dasanayake, I.; Bevier, W.; Castorino, k. et al., Early detection of physical activity for people with type 1 diabetes mellitus, *J Diabetes Sci Technol* **2015**, *9*, 506–11.

[20] Jacobs, P.; Resalar, N.; El Youssef, J. et al., Incorporating an exercise detection grading, and hormone dosing algorithm into the artificial pancreas using accelerometry and heart rate, *J Diabetes Sci Technol* **2015**, *9*, 1175–84.

[21] Breton, M.; Brown, S.; Karvetski, C. et al., Adding heart rate signal to a control-to-range artificial pancreas system improves the protection against hypoglycemia during exercise in type 1 diabetes, *Diabetes Technol Ther* **2014**, *16*, 506–11.

[22] Roder, P.V.; Wu, B.; Lui, Y.; Han, W., Pancreatic regulation of glucose homeostasis, *Ex Mol Med* **2016**, *3*, e219.

[23] Singh-Franco, D.; Robles, G.; Gazze, D. et al., Pramlintide Acetate Injection for the Treatment of Type 1 and Type 2 Diabetes Mellitus, *J Clin Ther* **2007**, *29*, 535–62.

[24] Galassetti, P.; Riddell, M.C., Exercise and type 1 diabetes (T1DM), *Compr Physiol* **2013**, *3*, 1309–36.

[25] Sonne, B.; Mikines, K.; Galbo, H., Glucose turnover in 48-hour-fasted running rats, *Am J Physiol* **1987**, *252*, R587–R593.

[26] McMahon, S.; Ferreira, L.; Ratnam, N. et al., Glucose requirements to maintain euglycemia after moderate-intensity afternoon exercise in adolescents with type 1 diabetes are increased in a biphasic manner, *J Clin Endocrinol Metab* **2007**, *92*, 963–968.

[27] Galassetti, P.; Tate, D.; Neill, R. et al., Effect of sex on counterregulatory responses to exercise after antecedent hypoglycemia in type 1 diabetes, *Am J Physiol Endocrinol Metab* **2003**, *287*, E16–E24.

[28] Olinder, A.; Kernell, A.; Smide, B., Missed bolus doses: devastating for metabolic control in CSII-treated adolescents with type 1 diabetes, *Pediatr Diabetes* **2009**, *10*, 142—-8.

[29] Jaser, S.; Datye, K., Frequency of missed insulin boluses in type 1 diabetes and its impact on diabetes control, *Diabetes Technol Ther* **2016**, *18*, 341—-2.

[30] Meade, L.; Rushton, W., Accuracy of carbohydrate counting in adults, *Clin Diabetes* **2016**, *34*, 142—-7.

[31] Burdick, J.; Chase, H.P.; Slover, R.H. et al., Missed insulin meal boluses and elevated hemoglobin A1c levels in children receiving insulin pump therapy, *Pediatr* **2004**, *113*, e221–4.

[32] O'Connell, M.; Donath, S.; Cameron, F., Poor adherence to integral daily tasks limits the efficacy of CSII in youth, *Pediatr Diabetes* **2011**, *12*, 556–9.

[33] Driscoll, K.a.; Johnson, S.B.; Hogan, J. et al., Insulin bolusing software: the potential to optimize health outcomes in type 1 diabetes mellitus., *J Diabetes Sci Technol* **2013**, *7*, 646–52.

[34] Riddell, M.C.; Gallen, I.W.; Smart, C.E. et al., Exercise management in type 1 diabetes: a consensus statement, *Lancet Diabetes Endocrinol* **2017**, *5*, 377–390.

[35] Bell, K.; Smart, C.; Steil, G. et al., Impact of Fat, Protein, and Glycemic Index on Postprandial Glucose Control in Type 1 Diabetes: Implications for Intensive Diabetes Management in the Continuous Glucose Monitoring Era, *Diabetes Care* **2015**, *38*, 1008—-15.

[36] Hause, E., Chronobiology in the endocrine system, *Adv Drug Deliv Rev* **2007**, *59*, 985–1014.

[37] Carroll, M.; Schade, D., The dawn phenomenon revisited: Implications for diabetes therapy, *Endocrine Pract* **2005**, *11*, 55–64.

[38] PLamper, M.; Gohlke, B.; Woelfle, J. et al., Interaction of Pubertal Development and Metabolic Control in Adolescents with Type 1 Diabetes Mellitus, *J Diabetes Res* **2017**, p. 8615759.

[39] Andrews, R.; Walker, B., Glucocorticoids and insulin resistance: Old hormones, new targets, *Clin Sci (Lond)* **1999**, *96*, 513–523.

[40] Andrews, R.; Walker, B., Invited review: Effects of acute exercise and exercise training on insulin resistance, *J Appl Physiol* **2002**, *93*, 788—796.

[41] Hovorka, R., Continuous glucose monitoring and closed-loop systems, *Diabetic Medicine* **2006**, *23*, 1—-12.

[42] Haidar, A.; Elleri, D.; Kumareswaran, K. et al., Pharmacokinetics of Insulin Aspart in Pump-Treated Subjects With Type 1 Diabetes: Reproducibility and Effect of Age, Weight, and Duration of Diabetes, *Diabetes Care* **2013**, *36*, e173–e174.

[43] Biagi, L.; Ramkissoon, C.M.; Facchinetti, A.; Leal, Y.; Vehi, J., Modeling the error of the medtronic paradigm veo enlite sensor, *Sensors* **2017**, *17*, 1361.

[44] Basu, A.; Dube, S.; Veettil, S. et al., Time lag of glucose from intravascular to interstitial compartment in type 1 diabetes., *J Diabetes Sci Technol* **2015**, *9*, 63–8.

[45] Nakamura, K.; Balo, A., The accuracy and efficacy of the Dexcom G4 Platinum continuous glucose monitoring system, *J Diabetes Sci Technol* **2015**, *9*, 1021—-6.

[46] Bailey, T.; Bode, B.; Christiansen, M.; Klaff, L.; Alva, S., The performance and usability of a factory-calibrated flash glucose monitoring system, *Diabetes Technol Ther* **2015**, *17*, 787–794.

[47] Damiano, E.; McKeon, K.; El-Khatib, F. et al., A comparative effectiveness analysis of three continuous glucose monitors: the Navigator, G4 Platinum, and Enlite, *J Diabetes Sci Technol* **2014**, *8*, 699–708.

[48] Rodbard, D., Characterizing accuracy and precision of glucose sensors and meters, *J Diabetes Sci Technol* **2014**, *8*, 980–5.

[49] Pleus, S.; Schoemaker, M.; Morgenstern, K. et al., Rate-of-Change Dependence of the Performance of Two CGM Systems During Induced Glucose Swings, *J Diabetes Sci Technol* **2015**, *9*, 801–7.

[50] Biagi, L.; Bertachi, A.; Quirós, C. et al., Accuracy of Continuous Glucose Monitoring before, during, and after Aerobic and Anaerobic Exercise in Patients with Type 1 Diabetes Mellitus, *Biosensors* **2018**, *8*, E22.

[51] Taleb, N.; Emami, A.; Suppere, C. et al., Comparison of Two Continuous Glucose Monitoring Systems, Dexcom G4 Platinum and Medtronic Paradigm Veo Enlite System, at Rest and During Exercise, *Diabetes Technol Ther* **2016**, *18*, 561–7.

[52] Bally, L.; Zueger, T.; Pasi, N. et al., Accuracy of continuous glucose monitoring during differing exercise conditions, *Diabetes Res Clin Pract* **2016**, *112*, 1–5.

[53] Moser, O.; Mader, J.; Tschakert, G. et al., Accuracy of Continuous Glucose Monitoring (CGM) during Continuous and High-Intensity Interval Exercise in Patients with Type 1 Diabetes Mellitus, *Nutrients* **2016**, *8*, 489.

[54] Atkinson, M.; Eisenbarth, G.; Michels, A., Type 1 Diabetes, *Lancet* **2014**, *9911*, 69–82.

[55] Han, H.; Kang, G.; Kim, J.; Choi, B.; Koo, S., Regulation of glucose metabolism from a liver-centric perspective, *Exp Mol Med* **2016**, *48*, e218.

[56] James, D.; Brown, R.; Navarro, J.; Pilch, P., Insulin-regulatable tissues express a unique insulin-sensitive glucose transport protein, *Nature* **1988**, *333*, 183–5.

[57] Jeker, L.; Bour-Jordan, H.; Bluestone, J., Breakdown in peripheral tolerance in type 1 diabetes in mice and humans, *Cold Spring Harb Perspect Med* **2012**, *3*, a007807.

[58] Barnett, R., Type 1 Diabetes, *Lancet* **2017**, *396*, 1941.

[59] Lind, M.; Svensson, A.; Kosiborod, M. et al., Glycemic Control and Excess Mortality in Type 1 Diabetes, *N Engl J Med* **2014**, *3741*, 1972–82.

[60] Huxley, R.; Peters, S.; Mishra, G.; Woodward, M., Risk of all-cause mortality and vascular events in women versus men with type 1 diabetes: a systematic review and meta-analysis, *Lancet Diabetes Endocrinol* **2015**, *3*, 198–206.

[61] Tao, B.; Pietropaolo, M.; Atkinson, M.; Schatz, D.; Taylor, D., Estimating the Cost of Type 1 Diabetes in the U.S.: A Propensity Score Matching Method, *PLoS One* **2010**, *5*, e11501.

[62] Cobas, R.; Ferraz, M.; Matheus, A. et al., The cost of type 1 diabetes: a nationwide multicentre study in Brazil, *Bulletin of the World Health Organization* **2013**, *91*, 389–464.

[63] Hex, N.; Bartlett, C.; Wright, D.; Taylor, M.; Varley, D., Estimating the current and future costs of Type 1 and Type 2 diabetes in the UK, including direct health costs and indirect societal and productivity costs, *Diabetic Med* **2012**, *29*, 855–62.

[64] Lopez-Bastida, J.; JP, L.; Oliva-Moreno, J. et al., Social economic costs of type 1 diabetes mellitus in pediatric patients in Spain: CHRYSTAL observational study, *Diabetes Res Clin Prac* **2017**, *127*, 56–9.

[65] Agiostratidou, G.; Anhalt, H.; Ball, D. et al., Standardizing Clinically Meaningful Outcome Measures Beyond HbA1c for Type 1 Diabetes: A Consensus Report of the American Association of Clinical Endocrinologists, the American Association of Diabetes Educators, the American Diabetes Association, the Endocrine Society, JDRF International, The Leona M. and Harry B. Helmsley Charitable Trust, the Pediatric Endocrine Society, and the T1D Exchange, *Diabetes Care* **2017**, *40*, 1622–30.

[66] Leasher, J.; Bourne, R.; Flaxman, S. et al., Global estimated on the n umber of people blind or visually impaired by diabetic retinopathy: A meta-analysis from 1990 to 2010, *Diabetes Care* **2016**, *39*, 1643—9.

[67] Fong, D.; Aiello, L.; Gardner, T. et al., Retinopathy in diabetes, *Diabetes Care* **2004**, *27*, s84–s87.

[68] Woodcock, A.; Bradley, C.; Plowright, R. et al., The influence of diabetic retinopathy on quality of life: interviews to guide the design of a condition-specific, individualised questionnaire: the RetDQoL, *Patient Educ Couns* **2004**, *53*, 365–83.

[69] Sloan, F.; Belsky, D.; Ruiz Jr, D.; Lee, P., Changes in incidence of diabetes mellitus-related eye disease among US elderly persons, *Arch Ophthalmol* **2008**, *126*, 1548–53.

[70] Vinik, E.; Hayes, R.; Oglesby, A. et al., The development and validation of the Norfolk QOL-DN, a new measure of patients' perception of the effects of diabetes and diabetic neuropathy, *Diabetes Technol Ther* **2005**, *7*, 497–508.

[71] Nicolucci, A.; Carinci, F.; Cavaliere, D. et al., A meta-analysis of trials on aldose reductase inhibitors in diabetic peripheral neuropathy, *Diabet Med* **1996**, *13*, 1017—-26.

[72] Jaiswal, M.; Divers, J.; Dabelea, D. et al., Prevalence of and Risk Factors for Diabetic Peripheral Neuropathy in Youth With Type 1 and Type 2 Diabetes: SEARCH for Diabetes in Youth Study, *Diabetes Care* **2017**, *40*, 1226–32.

[73] Gordois, A.; Scuffham, P.; Shearer, A.; Oglesby, A.; Tobian, J., The Health Care Costs of Diabetic Peripheral Neuropathy in the U.S., *Diabetes Care* **2003**, *26*, 1790–5.

[74] Maahs, D.; Rewers, M., Editorial: Mortality and renal disease in type 1 diabetes mellitus–progress made, more to be done, *J Clin Endocrinol Metab* **2006**, *91*, 3757–9.

[75] Orchard, T.; Secrest, A.; Miller, R.; Costacou, T., In the absence of renal disease, 20 year mortality risk in type 1 diabetes is comparable to that of the general population: a report from the Pittsburgh Epidemiology of Diabetes Complications Study, *Diabetologia* **2010**, *53*, 2312—9.

[76] Collins, A.; Foley, R.; Chavers, B. et al., United States Renal Data System 2011 Annual Data Report: Atlas of chronic kidney disease & end-stage renal disease in the United States, *Am J Kidney Dis* **2011**, *59*, e1–420.

[77] Ahola, A.; Saraheimo, M.; Forsblom, C. et al., Health-related quality of life in patients with type 1 diabetes–association with diabetic complications (the FinnDiane Study), *Nephrol Dial Transplant* **2010**, *25*, 1903–8.

[78] Molitch, M.; DeFronzo, R.; Franz, M. et al., Nephropathy in diabetes, *Diabetes Care* **2004**, *27*, S79–83.

[79] Miller, R.; Secrest, A.; Sharma, R.; Songer, T.; Orchard, T., Improvements in the life expectancy of type 1 diabetes: the Pittsburgh Epidemiology of Diabetes Complications study cohort, *Diabetes* **2012**, *61*, 2987–92.

[80] Schnell, O.; Standl, E., Diabetes and cardiovascular disease. Current status of trials, *Clin Res Cardiol* **2010**, *Suppl*, 27—34.

[81] Van Cauter, E.; Polonsky, K.; Scheen, A., Roles of circadian rhythmicity and sleep in human glucose regulation, *Endocr Rev* **1997**, *18*, 716–38.

[82] Piché, M.; Arcand-Bossé, J.; Després, J. et al., What is a normal glucose value? Differences in indexes of plasma glucose homeostasis in subjects with normal fasting glucose, *Diabetes Care* **2004**, *27*, 2470–7.

[83] Vahl, T.; D'Alessio, D., Gut peptides in the treatment of diabetes mellitus, *Expert Opin Investig Drugs* **2004**, *13*, 177–88.

[84] Ludvik, B.; Thomaseth, K.; Nolan, J.J. et al., Inverse relation between amylin and glucagon secretion in healthy and diabetic human subjects, *Eur J Clin Invest* **2003**, *33*, 316–22.

[85] Raddatz, D.; Ramadori, G., Carbohydrate metabolism and the liver: actual aspects from physiology and disease, *Z Gastroenterol* **2007**, *45*, 51–62.

[86] Yamatani, K.; Shi, Z.; Giacca, A. et al., Role of FFA-glucose cycle in glucoregulation during exercise in total absence of insulin, *Am J Physiol* **1992**, *263*, E646–E653.

[87] Sprague, J.; Arbelaez, A., Glucose Counterregulatory Responses to Hypoglycemia, *Pediatr Endocrinol Rev* **2011**, *9*, 463—75.

[88] Bolli, G., Physiological insulin replacement in type 1 diabetes mellitus, *Exp Clin Endocrinol Diabetes* **2001**, *109*, S317—-S332.

[89] Diabetes Control and Complications Trial Research Group.; Nathan, D.; Genuth, S. et al., The effect of intensive treatment of diabetes on the development and progression of long-term complications in insulin dependent diabetes mellitus, *N Engl J Med* **1993**, *329*, 977—-86.

[90] Gomez-Perez, F.; JA, R., Insulin therapy: current alternatives, *Arch Med Res* **2005**, *36*, 258—-72.

[91] Boscari, F.; Galasso, S.; Facchinetti, A. et al., FreeStyle Libre and Dexcom G4 Platinum sensors: Accuracy comparisons during two weeks of home use and use during experimentally induced glucose excursions, *Diabetes Technol Ther* **2018**, *20*, 180–6.

[92] Juvenile Diabetes Research Foundation Continuous Glucose Monitoring Study Group.; Beck, R.; Hirsch, I. et al., The effect of continuous glucose monitoring in well-controlled type 1 diabetes, *Diabetes Care* **2009**, *32*, 1378–83.

[93] Juvenile Diabetes Research Foundation Continuous Glucose Monitoring Study Group., Effectiveness of continuous glucose monitoring in a clinical care environment: evidence from the Juvenile Diabetes Research Foundation continuous glucose monitoring (JDRF-CGM) trial, *Diabetes Care* **2010**, *33*, 17—22.

[94] Chase, H.; Beck, R.; Xing, D. et al., Continuous glucose monitoring in youth with type 1 diabetes: 12-month follow-up of the Juvenile Diabetes Research Foundation continuous glucose monitoring randomized trial, *Diabetes Technol Ther* **2010**, *12*, 507—15.

[95] Lawson, M.; Bradley, B.; McAssey, K. et al., The JDRF CCTN CGM TIME Trial: Timing of Initiation of continuous glucose Monitoring in Established pediatric type 1 diabetes: study protocol, recruitment and baseline characteristics, *BMC Pediatr* **2014**, *14*, 183.

[96] Vigersky, R., The benefits, limitations, and cost-effectiveness of advanced technologies in the management of patients with diabetes mellitus, *J Diabetes Sci Technol* **2015**, *9*, 320–30.

[97] Ehrhardt, N.; Chellappa, M.; Walker, M.; Fonda, S.; Vigersky, R., The effect of real-time continuous glucose monitoring on glycemic control in patients with type 2 diabetes mellitus, *J Diabetes Sci Technol* **2011**, *9*, 668—-75.

[98] Edelman, S.V., Regulation Catches Up to Reality: Nonadjunctive Use of Continuous Glucose Monitoring Data., *J. Diabetes Sci. Technol.* **2016**, pp. 1–5.

[99] Food and Drug Administration.
FDA expands indication for continuous glucose monitoring system, first to replace fingerstick testing for diabetes treatment decisions, 2016.

[100] Clinical Chemistry and Clinical Toxicology Devices Panel of the U.S. Food and Drug Administration's Medical Device Advisory Committee., FDA Advisory Panel Votes to Recommend Non-Adjunctive Use of Dexcom G5 Mobile CGM, *Diabetes Technol. Ther.* **2016**, *18*, 512–516.

[101] Howey, D.; Bowsher, R.; Brunelle, R.; Woodworth, J., [Lys(B28), Pro(B29)]-Human Insulin: A Rapidly Absorbed Analogue of Human Insulin, *Diabetes* **1994**, *43*, 396—-402.

[102] Melki, V.; Renard, E.; Lassmann-Vague, V. et al., Improvement of HbA1c and blood glucose stability in IDDM patients treated with lispro insulin analog in external pumps, *Diabetes Care* **1998**, *21*, 977—82.

[103] Pickup, J.; Keen, H.; Parsons, J.; Alberti, K., Continuous subcutaneous insulin infusion: An approach to achieving normoglycaemia, *BMJ* **1978**, *1*, 204—7.

[104] Steineck, I.; Cederholm, J.; Eliasson, B. et al., Insulin pump therapy, multiple daily injections, and cardiovascular mortality in 18,168 people with type 1 diabetes: observational study, *BMJ* **2015**, *350*, h3234.

[105] Thabit, H.; Hovorka, R., Continuous subcutaneous insulin infusion therapy and multiple daily insulin injections in type 1 diabetes mellitus: A comparative overview and future horizons, *Expert Opinion Drug Del* **2016**, *13*, 389—-400.

[106] Roze, S.; Smith-Palmer, J.; Valentine, W. et al., Cost-effectiveness of continuous subcutaneous insulin infusion versus multiple daily injections of insulin in Type 1 diabetes: A systematic review, *Diabet Med* **2015**, *32*, 1415—24.

[107] Pickup, J.; Keen, H., Continuous subcutaneous insulin infusion at 25 years: evidence base for the expanding use of insulin pump therapy in type 1 diabetes, *Diabetes Care* **2002**, *25*, 593–8.

[108] Walsh, J.; Roberts, R.; Bailey, T., Guidelines for optimal bolus calculator settings in adults, *J Diabetes Sci Technol* **2011**, *5*, 129—-35.

[109] Ly, T.; Nicholas, J.; Retterath, A. et al., Effect of sensor-augmented insulin pump therapy and automated insulin suspension vs standard insulin pump therapy on hypoglycemia

in patients with type 1 diabetes: a randomized clinical trial, *JAMA* **2013**, *310*, 1240—-47.

[110] Bergenstal, R.; Klonoff, D.; Garg, S. et al., Threshold-based insulin-pump interruption for reduction of hypoglycemia, *N Engl J Med* **2013**, *369*, 224—-32.

[111] Zhong, A.; Choudhary, P.; McMahon, C. et al., Effectiveness of automated insulin management features of the MiniMed 640G sensor-augmented insulin pump, *Diabetes Technol Ther* **2016**, *18*, 657—-63.

[112] Ly, T.; Weinzimer, S.; Maahs, D. et al., Automated hybrid closed-loop control with a proportional-integral-derivative based system in adolescents and adults with type 1 diabetes: individualizing settings for optimal performance, *Pediatr Diabetes* **2017**, *18*, 348–55.

[113] U. S. Food and Drug Administration., The content of investigational device exemption (IDE) and premarket approval (PMA) applications for artificial pancreas device systems, In *The content of investigational device exemption (IDE) and premarket approval (PMA) applications for artificial pancreas device systems*; Silver Spring, MD, 2012; chapter 2, pp. 1–3.

[114] Capel, I.; Rigla, M.; García-Sáez, G. et al., Artificial pancreas using a personalized rule-based controller achieves overnight normoglycemia in patients with type 1 diabetes, *Diabetes Technol Ther* **2014**, *16*, 172—9.

[115] Ly, T.; Keenan, D.; Roy, A. et al., Automated Overnight Closed-Loop Control Using a Proportional-Integral-Derivative Algorithm with Insulin Feedback in Children and Adolescents with Type 1 Diabetes at Diabetes Camp, *Diabetes Technol Ther* **2016**, *18*, 377–84.

[116] Doyle 3rd, F.J.; Huyett, L.M.; Lee, J.B.; Zisser, H.C.; Dassau, E., Closed-loop artificial pancreas systems: engineering the algorithms, *Diabetes Care* **2014**, *37*, 1191–7.

[117] Bequette, B., Challenges and Recent Progress in the Development of a Closed-loop Artificial Pancreas, *Annu Rev Control* **2012**, *36*, 255–66.

[118] Trevitt, S.; Simpson, S.; Wood, A., Artificial Pancreas Device Systems for the Closed-Loop Control of Type 1 Diabetes: What Systems Are in Development?, *J Diabetes Sci Technol* **2012**, *10*, 714–23.

[119] Turksoy, K.; Quinn, L.; Littlejohn, E.; Cinar, A., Multivariable adaptive identification and control for artificial pancreas systems, *IEEE Trans Biomed Eng* **2014**, *61*, 883–91.

[120] Rossetti, P.; Ampudia-Blasco, F.; Laguna, A. et al., Evaluation of a novel continuous glucose monitoring-based method for mealtime insulin dosing the ibolus in subjects with type 1 diabetes using continuous subcutaneous insulin infusion therapy: a randomized controlled trial, *Diabetes Sci Technol* **2012**, *14*, 1043—-52.

[121] Nimri, R.; Muller, I.; Atlas, E. et al., Night glucose control with MD-Logic artificial pancreas in home setting: a single blind, randomized crossover trial-interim analysis, *Pediatr Diabetes* **2014**, *15*, 91–9.

[122] de Bock, M.; McAuley, S.; Abraham, M. et al., Effect of 6 months hybrid closed-loop insulin delivery in young people with type 1 diabetes: a randomised controlled trial protocol, *BMJ Open* **2018**, *8*, e020275.

[123] Garg, S.; Weinzimer, S.; Tamborlane, W. et al., Glucose outcomes with the in-home use of a hybrid closed-loop insulin delivery system in adolescents and adults with type 1 diabetes, *Diabetes Technol Ther* **2017**, *19*, 155—63.

[124] Dassau, E.; Pinsker, J.; Kudva, Y. et al., 12-Week 24/7 ambulatory artificial pancreas with weekly adaptation of insulin delivery settings: effect on hemoglobin A1c and hypoglycemia, *Diabetes Care* **2017**, *40*, 1719—-26.

[125] Kovatchev, B.; Cheng, P.; Anderson, S. et al., Feasibility of long-term closed-loop control: a multicenter 6-month trial of 24/7 automated insulin delivery, *Diabetes Technol Ther* **2017**, *19*, 18—-24.

[126] Anderson, S.; Raghinaru, D.; Pinsker, J. et al., Multinational home use of closed-loop control is safe and effective, *Diabetes Care* **2016**, *39*, 1143—-50.

[127] Pinsker, J.; Laguna Sanz, A.; Lee, J. et al., Evaluation of an artificial pancreas with enhanced model predictive control (eMPC) and a glucose prediction trust index with unannounced exercise, *Diabetes Technol Ther* **2017**, *20*, 455—64.

[128] Moroder, L.; Musiol, H., Insulin-From its Discovery to the Industrial Synthesis of Modern Insulin Analogue, *Angew Chem Int Ed Engl* **2017**, *56*, 10656–69.

[129] Grunberger, G., The need for better insulin therapy, *Diabetes Obes Metab* **2013**, *15*, 1–5.

[130] Home, P., Plasma insulin profiles after subcutaneous injection: how close can we get to physiology in people with diabetes?, *Diabetes Obes Metab* **2015**, *17*, 1011–20.

[131] Homko, C.; Deluzio, A.; Jimenez, C.; Kolaczynski, J.; Boden, G., Comparison of insulin aspart and lispro: pharmacokinetic and metabolic effects, *Diabetes Care* **2003**, *26*, 2027–31.

[132] Slattery, D.; Ameil, S.; Choudhary, P., Optimal prandial timing of bolus insulin in diabetes management: a review, *Diabet Med* **2018**, *35*, 306–16.

[133] Heise, T.; Stender-Petersen, K.; Hövelmann, U. et al., Pharmacokinetic and Pharmacodynamic Properties of Faster-Acting Insulin Aspart versus Insulin Aspart Across a Clinically Relevant Dose Range in Subjects with Type 1 Diabetes Mellitus, *Clin Pharmacokinet* **2017**, *56*, 649–60.

[134] Heinemann, L.; Baughman, R.; Boss, A.; Hompesch, M., Pharmacokinetic and Pharmacodynamic Properties of a Novel Inhaled Insulin, *J Diabetes Sci Technol* **2017**, *11*, 148–56.

[135] Smart, C.E.; Ross, K.; Edge, J.A. et al., Can children with type 1 diabetes and their caregivers estimate the carbohydrate content of meals and snacks?, *Diabet Med* **2010**, *27*, 348–53.

[136] Mehta, S.; Quinn, N.; Volkening, L.; Laffel, L., Impact of carbohydrate counting on glycemic control in children with type 1 diabetes, *Diabetes Care* **2009**, *32*, 1014—6.

[137] Brazeau, A.; Mircescu, H.; Desjardins, K. et al., Carbohydrate counting accuracy and blood glucose variability in adults with type 1 diabetes, *Diabetes Res Clin Pract* **2013**, *99*, 19—23.

[138] Kawamura, T.; Takamura, C.; Hirose, M. et al., The factors affecting on estimation of carbohydrate content of meals in carbohydrate counting, *Clin Pediatr Endocrinol* **2015**, *24*, 153—65.

[139] Laurenzi, A.; Bolla, A.; Panigoni, G. et al., Effects of carbohydrate counting on glucose control and quality of life over 24 weeks in adult patients with type 1 diabetes on continuous subcutaneous insulin infusion: a randomized, prospective clinical trial (GIOCAR), *Diabetes Care* **2011**, *34*, 823—7.

[140] Lodefalk, M.; Aman, J.; Bang, P., Effects of fat supplementation on glycaemic response and gastric emptying in adolescents with type 1 diabetes, *Diabet Med* **2008**, *25*, 1030—-5.

[141] Garcia-Lopez, J.; Gonzalez-Rodriguez, M.; Pazos-Couselo, M. et al., Should the amounts of fat and protein be taken into consideration to calculate the lunch prandial insulin bolus? Results from a randomized crossover trial, *Diabetes Technol Ther* **2013**, *15*, 166—-71.

[142] Smart, C.; Evans, M.; O'Connell, S. et al., Both dietary protein and fat increase postprandial glucose excursions in children with type 1 diabetes, and the effect is additive, *Diabetes Care* **2013**, *36*, 3896—-902.

[143] Wolever, T.; Mullan, Y., Sugars and fat have different effects on postprandial glucose responses in normal and type 1 diabetic subjects, *Nutr Metab Cardiovasc Dis* **2011**, *21*, 719—-25.

[144] Wolpert, H.; Atakov-Castillo, A.; Smith, S.; Steil, G., Dietary fat acutely increases glucose concentrations and insulin requirements in patients with type 1 diabetes: implications for carbohydrate-based bolus dose calculation and intensive diabetes management, *Diabetes Care* **2013**, *36*, 810—6.

[145] Paterson, M.; Smart, C.; Lopez, P. et al., Influence of dietary protein on postprandial blood glucose levels in individuals with Type 1 diabetes mellitus using intensive insulin therapy, *Diabet Med* **2014**, *33*, 592—-8.

[146] Neu, A.; Behret, F.; Braun, R. et al., Higher glucose concentrations following protein- and fat-rich meals - the Tuebingen Grill Study: a pilot study in adolescents with type 1 diabetes, *Pediatr Diabetes* **2014**, *16*, 587—-91.

[147] Reddy, M.; Herrero, P.; El Sharkawy, M. et al., Metabolic Control With the Bio-inspired Artificial Pancreas in Adults With Type 1 Diabetes A 24-Hour Randomized Controlled Crossover Study, *J Diabetes Sci Technol* **2015**, pp. 405–13.

[148] Dassau, E.; Zisser, H.; Harvey, R.A. et al., Clinical evaluation of a personalized artificial pancreas., *Diabetes Care* **2013**, *36*, 801–9.

[149] Raynaud, L.; Drouet, L.; Martineaud, J. et al., Time course of plasma growth hormone during exercise in humans at altitude, *J Appl Physiol* **1981**, *50*, 229–233.

[150] Wallberg-Herinksson, H.; Gunnarsson, R.; Henriksson, J. et al., Increased peripheral insulin sensitivity and muscle mitochondrial enzymes but unchanged blood glucose control in type I diabetics after physical training, *Diabetes* **1982**, *31*, 1044–1050.

[151] Moy, C.; Songer, T.; LaPorte, R. et al., Insulin-dependent diabetes mellitus, physical activity, and death, *Am J Epidemiol* **1993**, *137*, 74–81.

[152] Schiavon, M.; Dalla Man, C.; Kudva, Y.; Basu, A.; Cobelli, C., In silico optimization of basal insulin infusion rate during exercise: implication for artificial pancreas, *J Diabetes Sci Technol* **2013**, *7*, 1461–9.

[153] Patton, S.; Clements, M.; Fridlington, A. et al., Frequency of Mealtime Insulin Bolus as a Proxy Measure of Adherence for Children and Youths with Type 1 Diabetes Mellitus, *Diabetes Technol Ther* **2013**, *15*, 124–8.

[154] Turksoy, K.; Paulino, T.; Zaharieva, D. et al., Classification of Physical Activity: Information to Artificial Pancreas Control Systems in Real Time, *J Diabetes Sci Technol* **2015**, *9*, 1200—7.

[155] Dalla Man, C.; Micheletto, F.; Lv, D. et al., The UVA/PADOVA Type 1 Diabetes Simulator: New Features, *Journal Diabetes Sci Technol* **2014**, *8*, 26–34.

[156] Kovatchev, B.; Breton, M.; Dalla Man, C.; Cobelli, C., In silico preclinical trials: a proof of concept in closed-loop control of type 1 diabetes, *J Diabetes Sci Technol* **2009**, *3*, 44–55.

[157] Herrero, P.; Palerm, C.; Dassau, E. et al., A glucose absorption model library of mixed meals for in silico evaluation of artificial beta-cell control algorithms, Diabetes Technology Meeting. DTM, 2007.

[158] Dassau, E.; Herrero, P.; Zisser, H. et al., Implications of Meal Library & Meal Detection to Glycemic Control of Type 1 Diabetes Mellitus through MPC Control, *IFAC-PapersOnLine* **2008**, *41*, 4228–33.

[159] Dalla Man, C.; Breton, M.; Cobelli, C., Physical activity into the meal glucose-insulin model of type 1 diabetes: in silico studies., *Diabetes Sci Technol* **2009**, *3*, 56–67.

[160] Bertachi, A.; Beneyto, A.; Ramkissoon, C.M.; Vehi, J., Assessment of Mitigation Methods to Reduce the Risk of Hypoglycemia for Announced Exercise in a Uni-hormonal Artificial Pancreas, *Diabetes Technol Ther* **2018**, *20*, 1–11.

[161] Rossetti, P.; Quiros, C.; Moscardo, V. et al., Closed-Loop Control of Postprandial Glycemia Using an Insulin-on-Board Limitation Through Continuous Action on Glucose Target, *Diabetes Technol Ther* **2017**, *19*, 3158–3172.

[162] León-Vargas, F.; Garelli, F.; De Battista, H.; Vehi, J., Postprandial blood glucose control using a hybrid adaptive PD controller with insulin-on-board limitation, *Biomed Signal Process Control* **2013**, *8*, 724–32.

[163] Sala-Mira, I.; Diez, J.; Bondia, J., Insulin limitation in the Artificial Pancreas by Sliding Mode Reference Conditioning and Insulin Feedback: an in silico comparison, *IFAC-PapersOnLine* **2017**, *50*, 7746–8.

[164] Bergman, R.N.; Phillips, L.S.; Cobelli, C., Physiologic evaluation of factors controlling glucose tolerance in man: measurement of insulin sensitivity and beta-cell glucose sensitivity from the response to intravenous glucose., *J Clin Invest* **1981**, *68*, 1456–67.

[165] Facchinetti, A.; Sparacino, G.; Cobelli, C., Enhanced Accuracy of Continuous Glucose Monitoring by Online Extended Kalman Filtering, *Diabetes Technol Ther* **2010**, *12*, 353–63.

[166] Hovorka, R.; Canonico, V.; Chassin, L.J. et al., Nonlinear model predictive control of glucose concentration in subjects with type 1 diabetes, *Physiol Meas* **2004**, *25*, 905–20.

[167] Herrero, P.; Calm, R.; Vehí, J. et al., Robust fault detection system for insulin pump therapy using continuous glucose monitoring., *J Diabetes Sci Technol* **2012**, *6*, 1131–41.

[168] Roy, A.; Parker, R.S., Dynamic modeling of exercise effects on plasma glucose and insulin levels, *J Diabetes Sci Technol* **2007**, *1*, 338–47.

[169] Julier, S.J.; Uhlmann, J.K., Unscented filtering and nonlinear estimation, *Proceedings of the IEEE* **2004**, *92*, 401–422.

[170] Uhlmann, J.K., Simultaneous map building and localization for real time applications, Technical report, University of Oxford, 1994, transfer thesis.

[171] Larsen, J., *Correlation Functions and Power Spectra, Section for Cognitive Systems, Informatics and Mathematical Modelling*; Technical University of Denmark, 2009.

[172] Dalla Man, C.; Camilleri, M.; Cobelli, C., A System Model of Oral Glucose Absorption: Validation on Gold Standard Data, *IEEE Trans Biomed Eng* **2006**, *53*, 2472–8.

[173] Schnell, O.; Barnard, K.; Bergenstal, R. et al., Role of Continuous Glucose Monitoring in Clinical Trials: Recommendations on Reporting, *Diabetes Technol Ther.* **2017**, *19*, 391–9.

[174] Samadi, S.; Rashid, M.; Turksoy, K. et al., Automatic Detection and Estimation of Unannounced Meals for Multivariable Artificial Pancreas System, *Diabetes Technol Ther* **2018**, *20*, 235–46.

[175] Weaver, K.; Hirsch, I., The hybrid closed-loop system: evolution and practical applications, *Diabetes Technol Ther* **2018**, *20*, S2–16–S2–23.

[176] Campbell, M.; Walker, M.; Bracken, R. et al., Insulin therapy and dietary adjustments to normalize glycemia and prevent nocturnal hypoglycemia after evening exercise in type 1 diabetes: a randomized controlled trial, *BMJ Open Diabetes Res Care* **2015**, *3*, e000085.

[177] Palerm, C.C., Physiologic insulin delivery with insulin feedback: a control systems perspective, *Comput Methods Programs Biomed* **2011**, *102*, 130–137.

[178] Revert, A.; Garelli, F.; Picó, J. et al., Safety auxiliary feedback element for the artificial pancreas in type 1 diabetes, *IEEE Transactions on Biomedical Engineering* **2013**, *60*, 2113–2122.

[179] Swain, D.; Leutholtz, B.; King, M.; Haas, L.; Branch, J., Relationship between % heart rate reserve and % VO2 reserve in treadmill exercise, *Med Sci Sports Exerc* **1998**, *30*, 318–21.

[180] Kapitza, C.; Hovelmann, U.; Nosek, L. et al., Continuous glucose monitoring during exercise in patients with type 1 diabetes on continuous subcutaneous insulin infusion, *J Diabetes Sci Technol* **2010**, *4*, 123–31.

[181] Steil, G.M.; Palerm, C.C.; Kurtz, N. et al., The effect of insulin feedback on closed loop glucose control, *J Clin Endocrinol Metab* **2011**, *96*, 1402–8.

[182] Wilinska, M.E.; Chassin, L.J.; Schaller, H.C. et al., Insulin kinetics in type-1 diabetes: continuous and bolus delivery of rapid acting insulin, *IEEE Transactions on Biomedical Engineering* **2005**, *52*, 3–12.

[183] Quirós, C.; Bertachi, A.; Giménez, M. et al., Blood glucose monitoring during aerobic and anaerobic physical exercise using a new artificial pancreas system, *Endocrinol Diabetes Nutr* **2018**, *65*, 342–7.

Universitat de Girona

MiceLab™

Modeling, Identification & Control Engineering